IEEE Access
Multidisciplinary | Rapid Review | Open Access Journal

Received 12 January 2024, accepted 22 January 2024, date of publication 30 January 2024, date of current version 28 February 2024.

Digital Object Identifier 10.1109/ACCESS.2024.3360267

SURVEY

A Comparative Study of Cutting-Edge Bi-Directional Power Converters and Intelligent Control Methodologies for Advanced Electric Mobility

PATTAN MUTHUKUMAR[1], MOHAN VENKATESHKUMAR[2], (Member, IEEE), AND CHENG SIONG CHIN[3], (Senior Member, IEEE)

[1]Department of Electrical and Electronics Engineering, Amrita School of Engineering, Amrita Vishwa Vidyapeetham, Chennai 601103, India
[2]Department of Electrical and Electronics Engineering, Amrita School of Engineering, Amrita Vishwa Vidyapeetham, Coimbatore 641112, India
[3]Faculty of Science, Agriculture and Engineering, Newcastle University in Singapore, Singapore 599493

Corresponding author: Mohan Venkateshkumar (m_venkateshkumar@cb.amrita.edu)

ABSTRACT Bidirectional converters (BDCs) are important in electric vehicles (EVs). This study investigated different bidirectional power converters and their efficiencies, energy densities, and cost parameters. Control methods such as pulse width modulation (PWM) and hysteresis control are also examined. Comparisons on how well they regulate the output voltage and current in converters are performed. This paper also provides an overview of the types of BDCs used in EVs, including flyback, forward, and push-pull converters. The efficiency, energy density, and cost of each converter are assessed to identify the most appropriate model for EVs. The control methods including the advantages and disadvantages of PWM and hysteresis control and how they influence converter performance are examined. Suggestions for applying bidirectional power converters and control approaches in electric vehicles are also proposed. In summary, the paper consolidates the existing research, findings, and current gaps leading to advancements in the field and provide resources for emerging methodologies and concepts for advanced electric mobility.

INDEX TERMS Energy storage, E-vehicle, bidirectional DC converters, DAB, multilevel converter, Z-source, PWM control, hysteresis control, sliding mode control, dual-loop control, MPC, ANN.

NOMENCLATURE

BDC	Bidirectional DC Converter.
EV	Electric Vehicle.
SEPIC	Single-ended primary-inductor converter.
ZVS	Zero Voltage Switching.
PI	Proportional Integral.
PID	Proportional Integral De.
DAB	Dual Active Bridge.
FB	Full Bridge.
ANN	Artificial Neural Network.
CCM	Continuous Conduction Mode.
DCM	Discontinuous Conduction Mode.
RDS	Drain – to – Source Resistance.
VSI	Voltage Source Inverter.
ZVS	Zero Voltage Switching.
PFC	Power Factor Correction.
PV	Photovoltaic.
MPPT	Maximum Power Point Tracking.
QRF	Quasi Resonant Flyback.
SMPS	Switched Mode Power Supply.
THD	Total Harmonic Distortion.
PWM	Pulse Width Modulation.
MPC	Multi-Port Control.
SMC	Sliding Mode Control.
RL	Resistance and Inductance.
PPO	Proximal Policy Optimization.
TSBB	Two-Switch Buck-Boost.
CC	Constant Current.

The associate editor coordinating the review of this manuscript and approving it for publication was Vitor Monteiro.

CV	Constant Voltage.
IM	Induction Motor.
DAB	Dual Active Bridge.
SRM	Switched Reluctance Motor.
MF	Member Function.
TPS	Triple Phase Shifted.
PSR	Primary Side Regulation.
ANN	Artificial Neural Network.
ADC	Analog to Digital Converter.
MLI	Multi-Level Inverter.
ZVT	Zero Voltage Transition.
BTB	Back-to-Back.
TPC	Time – to – Peak Current.
ISM	Interleaved Switching Mode.
NN	Neural Network.
PFM	Pulse Frequency Modulation.
ACF	Active Clamp Flyback.
RES	Renewable Energy Source.
LCDD	Lumped Capacitance Distributed Diode.
AQSL	Adaptive Quadratic Synchronous Learning.
CLLC	Capacitor Inductor-Inductor Capacitor.
RMS	Root Mean Square.
DAHB	Dual Active Half Bridge.
TDR	Time Domain Reflectometry.
FBLLC	Full Bridge LLC.
PS-FB	Phase Shifted Full Bridge.
D3ABC	Dual Three-Phase AC/DC Converter.
CFMDAB	Cascaded Full Bridge Modular Dual Active Bridge.
HFL- PCS	High Frequency Link Power Conditioning System.
MVDC	Medium Voltage DC.
ANPC	Active Neutral Point Clamped.
Z-NDC-MLI	Zero Neural Clamped Multi Level Inverter.
3L-NPC	Three Level Neural Point Clamped.
HSVM	High Speed Vector Modulation.
HVDC	High Voltage Direct Current.
DSMC	Direct Sliding Mode Control.
CSMC	Current Source Model Predictive Control.
DI-SMC	Direct Input Sliding Mode Control.
MRAC	Model Reference Adaptive Control.
DMPC	Decentralized Model Predictive Control.
DO	Differential Operator.
MOSFET	Metal Oxide Semiconductor Field Effect Transistor.
IGBT	Insulated-Gate Bipolar Transistor.
BBC	Buck Boost Converter.
DDMPC	Distributed Dual-Model Predictive Control.
SVPWM	Space Vector Pulse Width Modulation.
DONMPC	Distributed Optimal Neural Model Predictive Control.
DOLMMPC	Distributed Optimal Linear Matrix Model Predictive Control.
DSBBC	Dual Stage Buck Boost Converter.
RWFNN	Radial Basis Function Wavelet Neural Network.
SVM	Space Vector Modulation.
SVPWM	Space Vector Pulse Width Modulation.
LPF	Low Pass Filter.
DTC	Direct Torque Control.
MPDTC	Model Predictive Direct Torque Control.
CTPS	Co-Operative Triple Phase Shifted Modulation.
ASTSMC	Adaptive Super-Twisting Sliding Mode Control.
STSMC	Super-Twisting Sliding Mode Control.
MATLAB	Matrix Laboratory.

I. INTRODUCTION

Bidirectional converters play a crucial role in electric vehicles, facilitating the seamless power conversion between motors and battery modules. As observed in regenerative braking systems, these converters also enable the battery to charge and discharge. This study examined various model predictive control structures designed for hydrogen fuel cells and other fuel-cell-based variable power setups. Their suitability for vehicular applications was also assessed based on cost-effectiveness, environmental friendliness, the absence of emissions, and the ability to handle substantial power loads. The different types of non-isolated DC-DC converters [1] also identify the obstacles faced by fuel cell technology and outline its potential uses. Furthermore, it also provides a comprehensive categorization of DC-DC converters.

Electric vehicles (EVs) frequently use diverse Bidirectional DC Converters (BDCs), including buck-boost, single-ended primary inductors, and boost converters. A specific iteration of the DC Converter, namely the boost converter, raises the voltage level from a lower input voltage to a noticeably higher output voltage. This component finds widespread application in EVs owing to its capacity to efficiently transform the battery energy for electric motors. Conventionally, the modulation of the pulse width (PWM) governs the boost converter, enabling adept efficiency and steadfast output voltage.

The buck–boost converter, categorized as a DC converter, empowers meticulous adjustment of voltage levels, offering versatility in achieving both voltage amplification and reduction. It is a common fixture in EVs because of its proficiency in converting battery energy for electric motors and facilitating battery charging and discharging. Typically, the PWM technique steers the control of the buck–boost converter, facilitating high-efficiency functionality and consistent output voltage.

The structure of bidirectional power converters (BDCs) plays a crucial role in the overall energy-management system of electric vehicles. A bidirectional converter is a power electronics device that can transfer electrical energy between two ports in both directions. It allows for efficient energy flow from a source to a load and returning energy to the source.

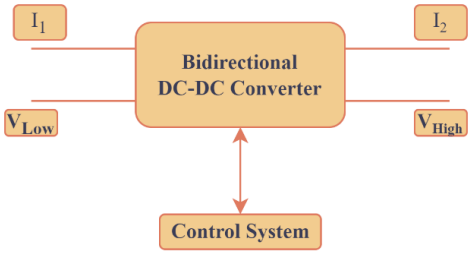

FIGURE 1. Structure of BDC.

A Bidirectional DC Converter is a device that efficiently converts electrical energy between two voltage sources, V_{Low} (low voltage) and V_{High} (high voltage), in either a stepping up (boost) or stepping down (buck) mode. It utilizes power electronic switches and a control system to manage bidirectional energy flow, making it essential in applications like energy storage, electric vehicles, and renewable energy systems as shown in Fig 1. This versatility is crucial in applications like electric vehicles, renewable energy systems, and battery storage, enabling energy management, grid integration, and improved overall system efficiency. Bidirectional converters play a pivotal role in modern energy systems by facilitating bi-directional power transfer and control. This extensive review and comparative analysis examined various BDC types and evaluated their efficiencies, energy densities, and cost metrics. In addition, various control techniques, such as PWM and hysteresis control, are reviewed to assess their effectiveness in regulating the output voltage and current of the converter. This study aims to identify the most suitable converter model for EV usage by providing an overview of the BDC types used in EVs and evaluating their performance. Furthermore, it highlights the significance of control strategies. This finding suggests areas for further research aimed at enhancing the efficiency of BDCs in EVs (Fig. 2).

The SEPIC adjusts the voltage levels, accommodating both the increases and decreases. This converter finds frequent application in Electric Vehicles (EVs) owing to its capacity to convert energy between the battery and the electric motor effectively. This in turn facilitates battery discharge and charging. Control of SEPIC Converters commonly employs a pulse-width modulation (PWM) technique, enabling the converter to operate efficiently and produce a stable output voltage.

The development of control strategies for bidirectional DC converters that encompass hysteresis, sliding mode, and Proportional Integral (PI) approaches is contingent on specific requirements of the EV system. Hysteresis control, characterized by its simplicity and robustness, is a fundamental approach that does not require an intricate mathematical model of the converter. Nonetheless, it falls short of the efficiency achieved by alternative control methods, potentially leading to a pronounced harmonic distortion.

On the other hand, Sliding Mode Control (SMC) has emerged as a pivotal method owing to its resilience to constraint variations and ability to deliver rapid transient responses. However, implementing the method is intricate and may result in a phenomenon known as chattering. PI control is a widely adopted technique that is easy to implement and has favorable outcomes. However, it may not possess the same level of robustness as other control strategies that may require a precise mathematical representation of the converter.

Bidirectional DC converters play an important role in EV functioning. The selection of converter type and control methodology depends on the precise requirements of the EV system. This study accurately analyzed bidirectional DC converters from both the topological and regulatory perspectives. The topologies were neatly categorized into isolated and non-isolated types and each was further divided into eight distinct classes. For clarity, a summary of the tabulation has been provided. The exploration of methodologies, such as single/dual/triple phase shifts, contributes to optimizing the overall outcomes. [1], [2], [3], [4]. The most prevalent control paradigms, including PID, Fuzzy logic, model predictive, Sliding Mode, and Digital Control, were also analyzed.

The main contribution of this review paper lies in its in-depth analysis and comparative study of various converter topologies and control strategies, aimed at identifying the most suitable converter topology and its corresponding control strategies for the application in electric vehicles (EVs). This extensive investigation offers valuable insights into the selection of optimal bidirectional power converter solutions and control approaches for EVs, ultimately enhancing their performance, efficiency, range, and cost-effectiveness.

II. VARIOUS CATEGORIES OF BI-DIRECTIONAL DC CONVERTERS

A. BUCK-BOOST CONVERTER

A modified two-switch buck-boost (TSBB) converter is proposed, which reduces the number of components and semiconductors compared to conventional TSBB, thereby reducing power loss. The source terminals of metal oxide semiconductor field-effect transistors (MOSFETs) connected to the ground allow simpler gate driver IC selection, as high-side gate signals are no longer required [5], as shown in Fig.3. Vin can be adjusted to align it with V_{out}. The buck–boost converter can transform voltage levels, whether surpassing or falling below the target output voltage. Its operation involves the adaptation of the input voltage to a DC level, and is subsequently employed to steer a switching converter. This converter adjusts the voltage upwards or downward, as required, to attain the intended output voltage. Buck–boost converters are widely used in scenarios where the input voltage displays notable variations or when isolation between the input and output is required.

To counteract the destabilizing effects stemming from the active load of the DC-to-DC Buck-Boost Converter (BBC), the Distributed Dual-Model Predictive Control (DDMPC) scheme aims to achieve a rapid reference convergence. In this

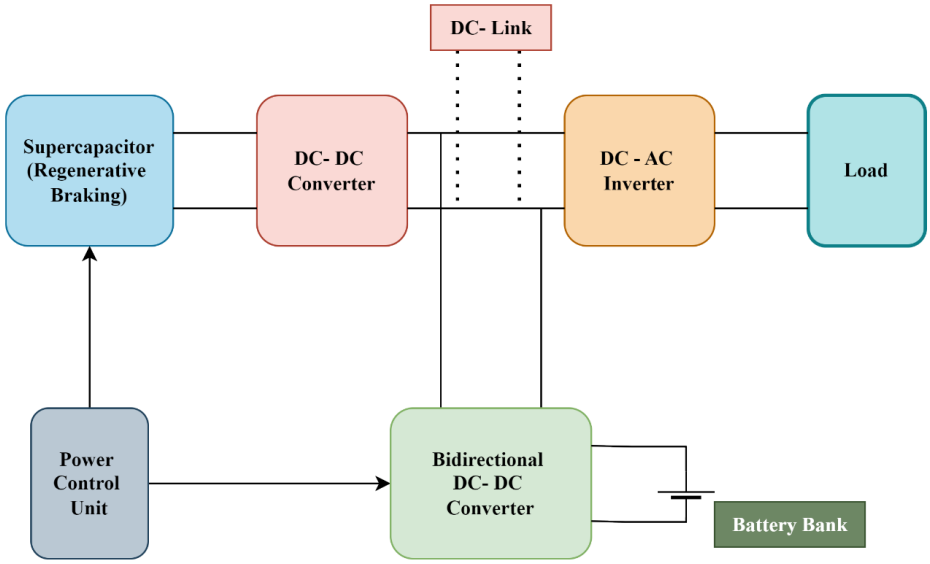

FIGURE 2. Block diagram of E-vehicle system.

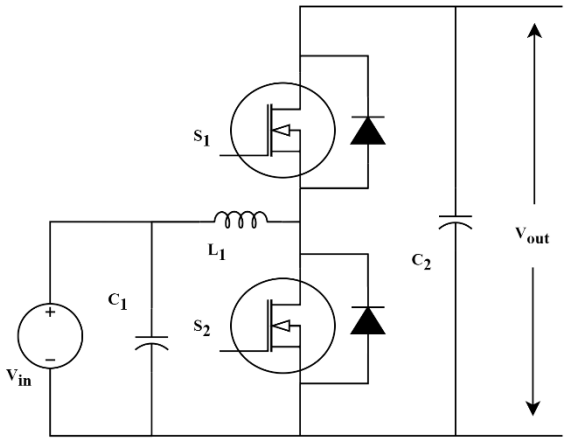

FIGURE 3. Buck-boost converter.

strategy, the ((RL) algorithm scrutinizes the system state and devises the optimal control policy. The Proximal Policy Optimization (PPO) algorithm is harnessed and juxtaposed with a proportional-integral (PI) controller for comparison [6].

The Dual-Stage Buck-Boost Converter (DSBBC) holds a prominent position as the preferred direct-current/direct-current (dc/dc) converter for applications such as photovoltaic systems, power factor correction, and low-voltage portable devices. This preference arises from its broad input-voltage compatibility and consistent output voltage polarity. However, when configured in a constant-current (CC) setup, the DSBBC encounters notable output voltage oscillations during transitions between modes. Employing an interleaved modulator (IM) technique with uniform duty cycles can alleviate inductor ripple current, although it can sustain a higher average inductor current. However, the application of an interleaved modulator with duty offset has demonstrated its potential to curtail conventional inductor current, thereby augmenting the overall efficiency of the converter [7]. The planned lossless snubber cell for the BBC system offers soft switching aimed at all power switches in both power-flow directions. The absence of a significant circulating current at various load levels resolves the reverse-recovery problem typically encountered in synchronous rectifiers.

The expression for the output voltage (V_{out}) of the buck–boost converter c is formulated as follows:

$$V_{out} = \left(\frac{D}{1-D}\right) V_{in} \tag{1}$$

where:

- V_{out} is the output voltage,
- D represents the duty cycle (the proportion of time the switch is ON during one switching cycle), and
- V_{in} denotes the input voltage.

This allows high-frequency switching (60 kHz) across all power switches, thereby enhancing the efficiency and power density. This design eliminates the need for auxiliary switches and is characterized by a straightforward structure, high reliability, and a lack of complex auxiliary circuits or driving algorithms [8]. The Buck-Boost converter, a versatile power electronic device, offers valuable insights and possesses notable merits and demerits for applications in electric vehicle (EV) systems. This enables efficient voltage regulation, accommodates diverse input voltage ranges, and facilitates bidirectional operations for energy management. With a high-power conversion efficiency and compact form factor, it is cost-effective while maintaining performance. However, controlling the buck-boost converter can be complex, necessitating careful handling of load variations and

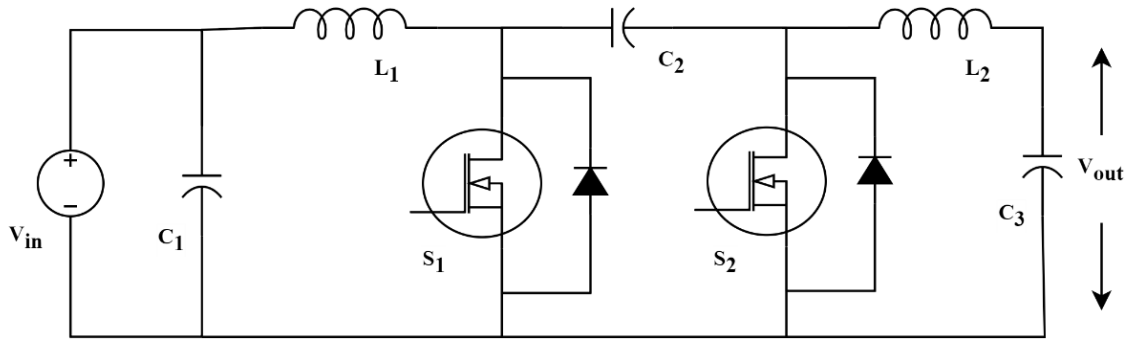

FIGURE 4. Cuk converter.

input voltage changes. Electromagnetic interference poses a challenge and requires additional compliance. Furthermore, the converter has limitations in its voltage conversion range. Nonetheless, buck-boost converters remain a favored choice owing to their versatility, efficiency, and ability to handle diverse input voltages, contributing to the progression and integration of EV systems.

B. CUK CONVERTER

The capacitive voltage divider within this converter precisely handles the required voltage conversion. The Cuk converter ingeniously combines the benefits of both Buck and Boost converters, resulting in superior power conversion efficiency that remains strong across a wide range of input and output voltage conditions. By strategically using capacitors and inductors, the Cuk converter enhances the power conversion efficiency and reduces the switching losses. Owing to these exceptional qualities, the Cuk converter has become a popular choice in various power electronics applications, such as battery charging, solar power systems, and electric vehicles, further solidifying its reputation in the field.

The flow-graph modeling technique was utilized to explore the one-cycle control method, which is a nonlinear approach that leads to a comprehensive understanding of the behaviors of both large and small signals in switching converters. A systematic design method was formulated for such control systems with a Cuk converter serving as an example. Additionally, a description grounded in practical insights is presented to clarify how one-cycle control achieves immediate regulation without requiring an infinitely high loop gain [9], as shown in Fig. 4.

The Cuk converter is a type of DC-DC converter that can step up or step-down voltage levels. Its operation is based on the Cuk topology, which incorporates a coupled inductor. The Cuk converter's exact equations for voltage and current relationships can be derived from circuit analysis. Here's the general equation for the Cuk converter:

$$V_{out} = \left(\frac{1-D}{D}\right) V_{in} \tag{2}$$

where:

- V_{out} is the output voltage.
- V_{in} is the input voltage.
- D is the duty cycle of the switching transistor (ratio of on-time to total switching period).

Cuk converters generate evenly spaced voltage levels, which are suitable for driving a four-phase switched reluctance motor (SRM) using a split capacitor converter. The proposed PWM AC-DC converter functions in Discontinuous Conduction Mode, yielding benefits such as smaller size, reduced costs, and reduced reliance on sensor components. An advanced voltage control loop was employed to proficiently manage the DC-link voltage and achieve power factor correction (PFC) at the AC mains. This control methodology and its associated analysis and discussion can be found in [11].

C. SEPIC CONVERTER

This DC-DC converter converts voltage levels using inductors and capacitors. Specifically, SEPIC transforms the voltage from one level to another. The SEPIC Converter constitutes a variation of the Conventional Buck and Boost Operation and is accomplished with high and low voltage levels, as required. SEPIC converters are widely used in applications that require a stable Vout, even when Vin fluctuates. Furthermore, it is applicable in scenarios where the source voltage exceeds the load voltage, or, conversely, as exemplified in the circuit diagram presented in Fig. 5.

An innovative SEPIC was proposed to address the shortcomings of the inadequate step-up ratio and voltage stress often observed in traditional boost converters. This solution employs a shared-boost inductor switch and harnesses a SEPIC converter to enhance step-up capability. The leakage inductor of the transformer eliminates the need for a current snubber, thus alleviating the reverse recovery issues. This valuable insight can be incorporated into a PhD research survey [12]. The modified coupled-inductor SEPIC converter provides a new approach for attaining a significant voltage increase within the range of 2–10. By adding an extra diode, a low-voltage MOSFET with a low RDS-ON can be chosen, cutting costs and lessening switch-related losses. In contrast to similar setups with comparable voltage gain potential, this suggested design stands out for its simplicity and requirement

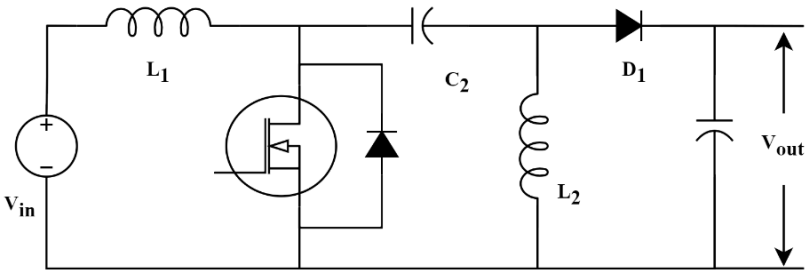

FIGURE 5. SEPIC converter.

for fewer components. The expression for the output voltage (V_{out}) of the SEPIC.

$$V_{out} = \left(\frac{D}{1-D}\right)\left(V_{in} + \frac{V_{in}}{1-D}\right) \tag{3}$$

where:

- V_{out} is the output voltage.
- D represents the duty cycle (the ratio of time the switch is ON to the switching cycle time).
- V_{in} denotes input voltage.

The SEPIC converter is a highly adaptable DC-DC converter that can perform both step-up and step-down voltage conversions, making it a suitable option for numerous applications in power management and energy conversion systems. This streamlined design approach leads to a more compact and lightweight converter that enhances power density and ensures improved reliability in various applications.

In addition, the optimized topology enables advanced energy conversion systems, allowing efficient power resource utilization while maintaining cost-effectiveness and performance. Specifically, the innovative SEPIC achieves significant gains without the need for a transformer or coupled inductor, reducing switch-voltage stress and conduction losses. Its continuous input current is well suited for sustainable power sources such as fuel cells. Furthermore, the control system is straightforward, permitting regulation in the CCM by maintaining equal gating pulses for both switches. Therefore, an additional clamping circuit was unnecessary. The SEPIC converter demonstrates remarkable advantages, such as non-inverting output, exceptional efficiency, and significant amplification. The modified SEPIC with its maximum voltage gain outperformed the conventional SEPIC and other single-switch converters, making it ideal for harnessing renewable-energy sources. The analysis of its voltage gain considers both continuous and discontinuous conduction modes while considering nonideal components [15].

D. ZETA CONVERTER

A Zeta Converter (Z-Source Inverter) is a power electronic converter that combines inductors, capacitors, and diodes for voltage isolation. Its voltage source inverter (VSI) topology enables various input voltages and quality output voltages that are suitable for renewable energy systems, electric vehicles, and industrial drives. The Z-source network boosts the input voltage, filters the harmonic content, and provides clean output voltage. Its high-power density, efficiency, low cost, compact size, and bidirectional power flow make it ideal for grid-tied inverters, electric vehicles, and microgrids, as shown in Fig.6.

The expression for Zeta Converter,

$$D = \frac{\frac{V_{out}}{V_{in}}}{1 + \frac{V_{out}}{V_{in}}} \tag{4}$$

where:

- D is the duty cycle (the fraction of time the switch is ON during one switching cycle)
- V_{in} is the input voltage

A comprehensive analysis and experimental investigation were conducted on a two-switch Isolated Zeta DC-DC converter to assess its steady-state performance. The primary concern revolved around the high-voltage stress experienced by the transistors, which was attributed to the resonance between the leakage inductance of the transformer and output capacitance. To mitigate this issue, an additional transistor and two clamping diodes were introduced on the primary side of the transformer to effectively reduce the voltage stress to the level of the input DC voltage [16]. A zeta-flyback converter with soft-switching capabilities is proposed to achieve zero-voltage switching (ZVS).

This inventive design brought together the Zeta and Flyback configurations, making use of shared power components on the primary side of the transformer, partial magnetizing flux reset, and power distribution for the output. To achieve zero-voltage switching (ZVS) during switch turn-on, a buck-boost-type active clamp circuit was integrated in parallel with the primary side of the Isolated Transformer. This circuit helps recycle energy from the leakage inductor while maintaining the peak voltage stress on the switches during the turn-off of the main switch. A new hybrid circuit, founded on an active-quad-switched-inductor (AQSL), was proposed, harmoniously blending Zeta and Boost converters. Unlike traditional zeta circuits with intermittent input currents, this hybrid zeta-boost converter ensures uninterrupted input and output currents without depending on high-frequency

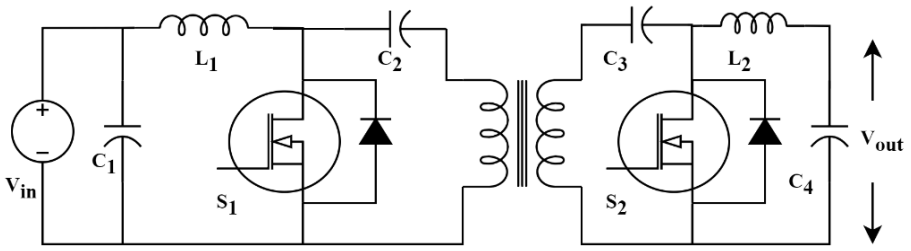

FIGURE 6. Zeta converter.

transformers or multiple diode and capacitor stages. As a result, it yields a higher voltage gain while reducing input source consumption [17], [18]. For Electric Vehicle (EV) applications, a Bridgeless Isolated Power Factor Correction (PFC) Zeta-Luo converter featuring an integrated power factor pre-regulator was previous designs owing to the shared output inductors between the PFC and Zeta-Luo conversions. Wide-range testing under steady-state conditions, varying main voltages, and different load scenarios validated satisfactory power factor-based charging in Constant Current (CC) and Constant Voltage (CV) modes [19].

A novel design based on the Zeta topology was proposed to address the need for a transformerless buck–boost converter. This converter preserves the advantages of Zeta, including its buck-boost capability, DC insulation, and continuous output current. Moreover, it offers a higher voltage gain while employing only a single switch, thereby reducing the voltage stress and minimizing the on-state resistance, thereby leading to lower losses [20]. In the domain of solar photovoltaic (PV)-fed water-pumping systems, a cost-efficient and effective Brushless DC Motor Drive was introduced. The Zeta Converter was harnessed to maximize power extraction from the solar array, eliminating the need for phase-current sensors using a control algorithm. A Variable Voltage Source Inverter (VSI) facilitates motor speed control by adjusting the DC-link voltage, without requiring additional circuitry. The Zeta Converter, controlled via an Incremental Conductance MPPT algorithm, enabled a soft start for the motor, ensuring smooth operation [21].

By conducting a careful analysis and employing creative design strategies, several converters based on the zeta topology have been suggested to tackle specific challenges in power electronics. These challenges include decreasing the voltage stress, increasing the efficiency, achieving greater voltage gain, and enhancing the control capabilities. These improvements lay the groundwork for more effective and dependable power conversion across various applications ranging from electric vehicles to solar-powered systems. This converter integrates a BOOST circuit for solar panel energy optimization and three SEPIC/ZETA circuits for efficient energy management between the photovoltaic panels, battery, and supercapacitor [121]. It ensures stable voltage and power during mode switching, demonstrating the ability to manage multiple operating modes effectively. This converter contributes to extended driving range and battery life of SEVs by utilizing solar energy, thereby promoting environmentally friendly operation.

E. FLYBACK CONVERTER

A flyback converter is a type of switched-mode power supply (SMPS) that employs a single switch to transfer energy to a load. This method achieved both voltage isolation and conversion. An inductor is used to store energy in a flyback bidirectional DC converter (BDC). It boasts a high efficiency and operates at a specific frequency. However, this solution requires an intricate design, owing to the high-voltage stress exerted on the switch. A review of active clamped flyback control Integrated Circuits highlighted only two suitable vendors. Suggestions for component selection and the incorporation of novel features are provided.

The study emphasizes that an extremely high switching frequency is not obligatory; the ''maximum efficiency vs. magnetizing inductance'' graph reaches its extremes at 400μH. The circulating power losses were scrutinized and observed to increase with input voltage. Analysis of the short-circuit characteristics necessitates the inclusion of a hybrid clamp in conjunction with multimode control [25], as illustrated in Fig.7.

This study conveys information about the power-supply architecture, Integrated Circuit design aspects, over-power protection, and key comparison options. The experiments yielded findings including a peak efficiency of 87.1% at 620V and a rated load. The investigation delved into Quasi-Resonant Flyback (QRF) losses sans load, their reliance on input voltage, and the connection between the switching frequency and load. Bode plots were used to analyze the bandwidth, phase margin, and gain margin. A comparison of the simulation and measurement results indicated that Type-2 compensation can ensure stable operation. The study determined that compensation and regulated output selection influence the Quasi-Resonant Flyback (QRF) converter efficiency at varying switching frequencies [26].

Hybrid topology of forward and flyback conversion with series and parallel connections on primary and secondary sides, respectively. It is free from start-up issues and high-voltage spikes on the switches. Controlled and designed for soft-switching and built-in flyback transformers as filter inductors, reducing the current ripple voltage flyback

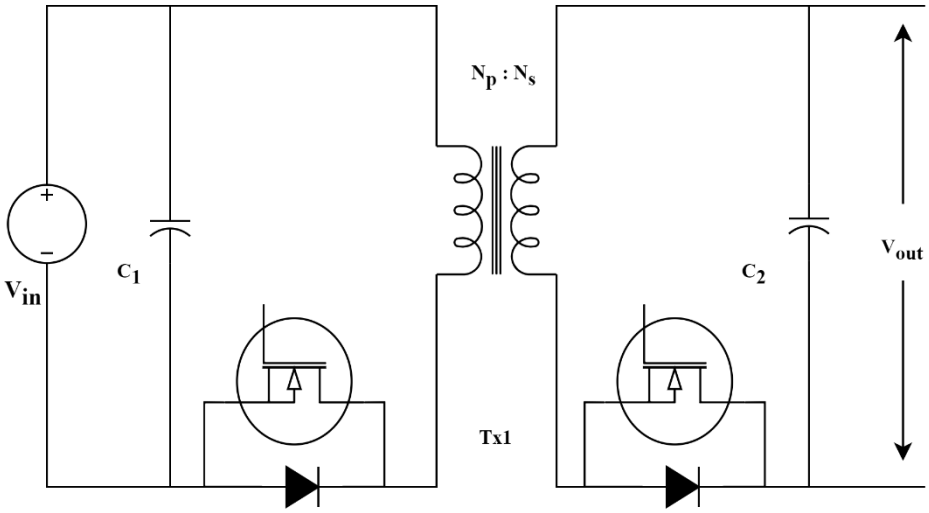

FIGURE 7. Flyback converter.

BDC [22]. The proposed flyback push–pull DC converter presents benefits compared to typical converters, including reduced output diodes and consistent output features for both buck and boost modes under continuous conduction conditions. [23].

The basic formula for the output voltage (V_{out}) of a flyback converter is as follows:

$$V_{out} = \left(\frac{D}{1-D}\right)\left(\frac{N_s}{N_p}\right) V_{in} \tag{5}$$

where:

- V_{out} is the output voltage,
- D represents the duty cycle (the ratio of time the switch is ON to the switching cycle time),
- N_s is the number of turns in the secondary winding of the transformer,
- N_p is the number of turns in the primary winding of the transformer, and V_{in} denotes the input voltage.

The active-clamp converter has several beneficial qualities, including zero-voltage switching (ZVS), reduction of reverse-recovery effects, a broad range of conversion, and minimal fluctuation in the input current. Incorporating two interconnected coils enhances the power density in both the flyback and forward modes, while the full-bridge inverter and LC filter ensure that the load receives a low-voltage signal with minimal Total Harmonic Distortion (THD). This, in turn, increases the overall efficiency and power density across different input-voltage ranges [24]. The Primary-side Regulation (PSR) Flyback Converter, widely used in low-power applications, mainly functions in Discontinuous Conduction Modulation (DCM).

However, a shift to Continuous Conduction Modulation (CCM) is necessary to increase output power. Unfortunately, CCM requires a costly Analog-to-Digital Converter (ADC). To overcome this problem and uphold the output current control in both DCM and CCM modes, an innovative Digital Peak Current Control method is introduced. However, an inadvertent calculation error during mode transition can lower the output current, straying from the intended level. To counter this, a Hysteretic Multimode Control strategy comprising two Pulse-Width Modulation (PWM) modes and two pulse-frequency modulation (PFM) modes was employed. This ensures precise current regulation, eliminates calculation errors, and enhances performance and stability under various conditions. Digital control techniques decrease circuit complexity and elevate the overall reliability of the converter [27].

F. FORWARD CONVERTER

The forward BDC converter operates both forward and bidirectional. In forward mode, it increases the input voltage, and in bidirectional mode, it reduces the higher DC voltage, serving as both an up-and-down converter. It is composed of two power switches, MOSFETs or IGBTs, and two energy storage devices, such as inductors or capacitors. Switching these parts and using control circuits changes the converter mode and adjusts the voltage [24]. Its advantages include high efficiency, especially when operating in two directions, and impressive power compactness, making it suitable for small, portable applications such as battery management, electric vehicles, and eco-friendly power sources. However, challenges arise in managing complex switching and vulnerability to shifts in input voltage and load conditions, demanding careful timing and a particular design for optimal performance, as shown in Fig. 8. The forward converter is a type of DC-DC converter commonly used in power electronics. Its operation involves a transformer and a diode bridge.

A 2-SW Active Clamped Forward converter was used to address the issue of high-voltage stress on the switches in an Active Clamped Forward (ACF) converter. This solution is

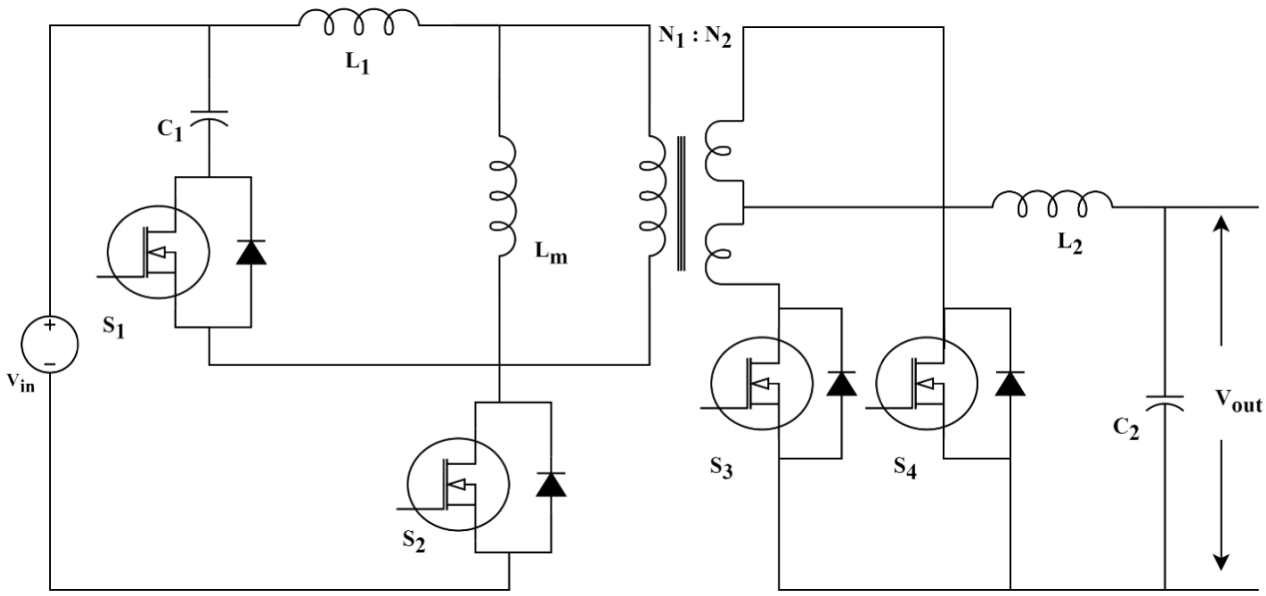

FIGURE 8. Forward converter.

particularly suitable for low-power to medium-power applications. A clamping diode, in conjunction with a gate signal that turns off after a delay, was employed to cap the voltage stress at the input level or reset the capacitor voltage. This approach provides a simple and effective solution for this problem. By combining a clamping diode and a precisely timed gate signal, the converter directly controls the voltage stress, effectively managing the potential challenges. Using a gate signal that turns off after a delay, along with a clamping diode, offers a practical and efficient method to confine the voltage stress to the input level or reset the capacitor voltage. This technique not only simplifies the voltage stress management but also guarantees peak converter performance. The integration of a clamping diode and a delayed turn-off gate signal provides a direct and dependable method for alleviating voltage stress, demonstrating the viability and efficiency of this solution. [28]. Newly introduced forward converter incorporates zero-voltage switching (ZVS) and Resonant Capacitor resistance (RC-R) pulse-width modulation (PWM), introducing a simplified auxiliary circuit. This auxiliary circuit is compatible with both single-switch and two-switch forward converters, ensuring smooth switching of the main and auxiliary MOSFETs, regardless of variations in the line and load conditions. The output voltage equation for the forward converter is as follows:

$$V_{out} = D\left(\frac{N_2}{N_1}\right) V_{in} \tag{6}$$

where:

- V_{out} is the output voltage.
- V_{in} is the input voltage.
- D is the duty cycle of the switching transistor (ratio of on-time to total switching period).
- N_1 is the number of primary windings turns on the transformer.
- N_2 is the number of secondary windings turns on the transformer.

Innovative converters provide additional flexibility by allowing duty cycles above 0.5 that is suitable for diverse applications with a wide input voltage range. In addition to the aforementioned benefits, the proposed forward converter with ZVS and RC-R PWM features an optimized auxiliary circuit. This aids in the smooth switching of both the main and auxiliary MOSFETs, while maintaining resilience to line and load variations. The integration of the ZVS and RC-R PWM techniques in the novel forward converter design ensures the efficient and seamless switching of MOSFETs, offering dependable performance across changing conditions.

Through a refined auxiliary circuit, the newly developed forward converter achieved gentle MOSFET switching, ensuring reliability across different input voltages. The increased versatility of converters, functioning beyond 0.5, suits diverse industries with varying voltage requirements. Without a magnetic element, the streamlined auxiliary circuit enhances the power density compared with existing Zero-Voltage Transition (ZVT) forward converters. A comparison with ZVT forward converters evaluates the planned converter performance and analyzes the operational stability and various operating modes [30].

These modes encompass an active switch, diode, transformer, and balanced compensated demagnetization voltage source. Different subcircuits harmonize compensated demagnetization voltage sources, leading to the development of diverse forward-switching cells. These include the Resonant Capacitor-Diode (RCD), active-clamping, lossless current–doubler (LCDD), Flyback-Integrated, and

Independent-Circuit configurations achieved through topology derivation rules [31].

G. PUSH-PULL CONVERTER

The DC converter employs a pair of switching transistors, with one set up in a Common-Emitter arrangement (known as the 'pusher') and the other in a Common-Collector setup (known as the 'puller'). This arrangement increases the voltages and decreases the DC input power. It is relatively straightforward to design and adept at handling high power loads. It has various advantages over other DC-DC converters, such as a reduced ripple voltage at the output owing to double sampling in each switching cycle, improved efficiency stemming from the complementary action of the two transistors, and elevated current delivery to the load. This setup typically comprises two switching transistors, a diode, a transformer, and a control circuitry, making it versatile for applications in power supplies for electronic devices, DC motor drives, and renewable energy systems, as illustrated in Fig.9.

A two-stage structure emerges from the coexistence of the current source and non-isolated DC converter through a shared inductor arrangement. This eliminates the need for a capacitor by using the same inductors as in the single-stage setup. Additionally, a high-frequency transformer guarantees the attainment of the rated output, even in challenging fuel-cell output scenarios. Moreover, the switching frequency of the push–pull converter is adjusted to double that of the buck converter, effectively curtailing the current peaks [32]. Despite its simplicity and the absence of complex multi-resonant tuning, the converter configuration shows exceptional stability in maintaining a consistent current output over a broad voltage range during unrestricted operation. This accomplishment is attributed to the use of analytical methods that establish normalized connections, forming the basis for overarching design principles [33].

Within the domain of control strategies, an enhanced approach tailored for push-pull Dual Active Bridge converters is introduced. The aim is to broaden the zero-voltage switching (ZVS) range and alleviate the effects of the current stress. In contrast to conventional modulation techniques that primarily manipulate power through adjustments in the primary duty cycle and phase-shift angle, the proposed modulation incorporates the duty cycle on the secondary side in the pulse-width modulation (PWM). This inventive approach, driven by modified PWM modulation, provides a control law that directly reduces the root-mean-square (RMS) current while simultaneously upholding an extensive ZVS range [34].

To counter the voltage spikes and reclaim the energy stored in the leakage inductors, a sophisticated integration of auxiliary switches, resonant inductors, and clamping capacitors was executed on the transformer's primary side. This novel integration, implemented within the advanced active-clamp push-pull converter, leads to substantial enhancements in converter efficiency. Specifically, it addresses zero-voltage switching losses linked to the main and auxiliary switches [35]. A switching control strategy designed explicitly for a current feed push-pull converter featuring an active voltage doubler rectifier or an active rectifier on the secondary side of the isolation transformer is proposed.

The expression for the output voltage (V_{out}) of the push-pull converter can be given as

$$V_{out} = \frac{2N_2}{N_1}\left(V_{in} - V_f - V_{ce}\right) D \tag{7}$$

Let:

- V_{out} is the output voltage,
- N_1 represents the number of turns in the primary winding of the center-tapped transformer,
- N_2 denotes the number of turns in each half of the secondary winding of the center-tapped transformer,
- D be the duty cycle (the ratio of time the switches are ON to the switching cycle time),
- V_{in} represents the input voltage,
- V_f denotes the voltage drop across the diodes, and
- V_{ce} represents the voltage drop across transistors when switched ON.

The push–pull converter employs a center-tapped transformer and switching transistors to achieve both voltage conversion and isolation. The duty cycle (D) manages the ON time of the transistor, thereby influencing the output voltage. The transformer turn ratio ($2N_2/N_1$) enables a voltage step-up or step-down. The diode and transistor voltage drops (V_f and V_{ce}) were factored into for loss consideration. This approach offers a key benefit by facilitating soft switching and ensuring the seamless operation of single- and dual-inductor push-pull converters, regardless of the active rectifier type utilized [36].

To attain optimal performance, a pioneering design that combines a push-pull circuit, an active voltage doubler circuit, and a bidirectional switch is proposed. This inventive converter functions in two modes, effectively achieving zero-voltage switching and remarkable efficiency even at high frequencies. Importantly, it avoids the flow of an instant reactive current. Notably, the converter achieves a high conversion ratio without the need for a high-turn-ratio transformer [37]. These converters epitomize a synergistic blend of innovative designs and advanced control strategies, resulting in substantial advancements in efficiency, stability, and power delivery. Consequently, they have emerged as highly viable options for a wide array of applications in power electronics

H. HALF-BRIDGE CONVERTER

An adaptable solution for altering the voltage levels in a DC power source was introduced, which enabled changes in energy direction. By comparing two switching transistors, two diode, inductor, and capacitor, this converter handles high power and facilitates bidirectional energy flow. The control circuit for this converter is more complex owing to its bidirectional energy-flow capability. The Circuit shown

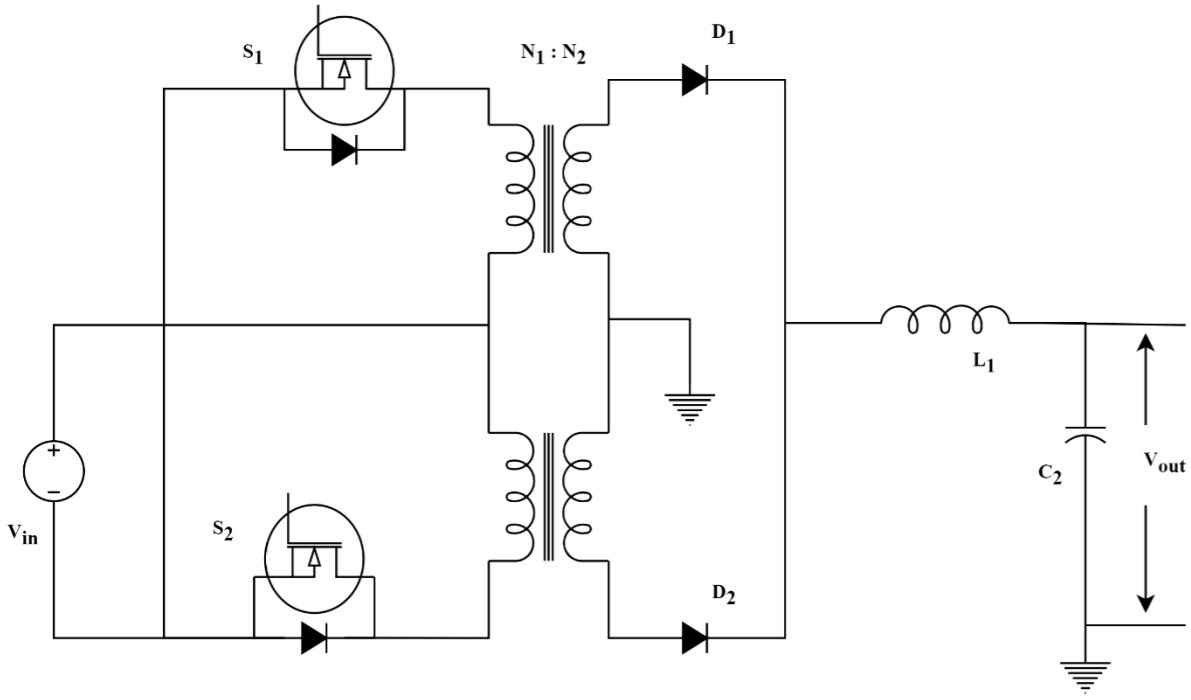

FIGURE 9. Push-pull converter.

in Fig.10 incorporates a half-bridge capacitor–inductor–inductor–capacitor–capacitor (CLLC) resonant circuit and buck/boost circuit, leveraging synchronous pulse-width modulation to achieve higher voltage gain. The CLLC resonant circuit enables soft switching for MOSFETs, and thorough simulations confirm the converter's ability to achieve zero-voltage or zero-current switching [38]. Reducing the root-mean-square (RMS) current in a dual-active-half-bridge (DAHB) converter involves adjusting the duty ratio and phase shift control. This approach employs mathematical optimization and simulations to determine the optimal circuit conditions. Through the integration of a 3D-modulation strategy with closed-loop control, the converter achieves its lowest RMS current, facilitating zero-voltage switching. [39]. These approaches improve the efficiency of EV applications by reducing power losses and optimizing power transfer. Control strategies are devised to minimize the RMS current while maintaining the power output with or without a zero-voltage switching (ZVS) operation. Validation through simulations and experiments demonstrated the potential for higher efficiency gains [40]. These strategies are particularly beneficial for EVs and for optimizing power conversion, utilization, and power flow management.

A prominent advantage of the newly devised DC converter for fuel-cell vehicles is its ability to achieve zero-current and zero-voltage switching. This was made possible using a secondary modulation clamp that effectively regulated the voltage. This converter boasts attributes such as a compact design and reduced cost, which are attributed to the utilization of low-voltage-rated components with minimal on-state resistance. These factors contribute to reduced conduction losses and heightened overall efficiency [41]. These features make it highly suitable for EV applications, improving power conversion and utilization in fuel-cell vehicles. Designing a push-pull forward half-bridge BDC with a variable input voltage requires careful component selection and topology considerations to minimize power loss and maximize efficiency. Optimization methods include simulations, analytical equations, and experimental testing. The input voltage range and load power are essential for efficient operation within a specified range of the converter [42]. This tailored approach ensures optimal performance in EV applications by prioritizing the power efficiency and precise control.

The mathematical equation for the output voltage (V_{out}) of the half-bridge converter can be written as follows.

$$V_{out} = \left(V_{in} - V_{f1} - V_{f2} - V_{ce1} - V_{ce2} - V_d\right) \times D \quad (8)$$

where:

- V_{out} is the output voltage.
- V_{in} is the input voltage.
- V_{f1} and V_{f2} are the voltage drops across the two diodes.
- V_{ce1} and V_{ce2} are the voltage drops across the two switching transistors (usually MOSFETs).
- V_d is the voltage drop across the freewheeling diode
- D is the duty cycle of the switching signal, representing the fraction of the switching period during which the transistor is ON.

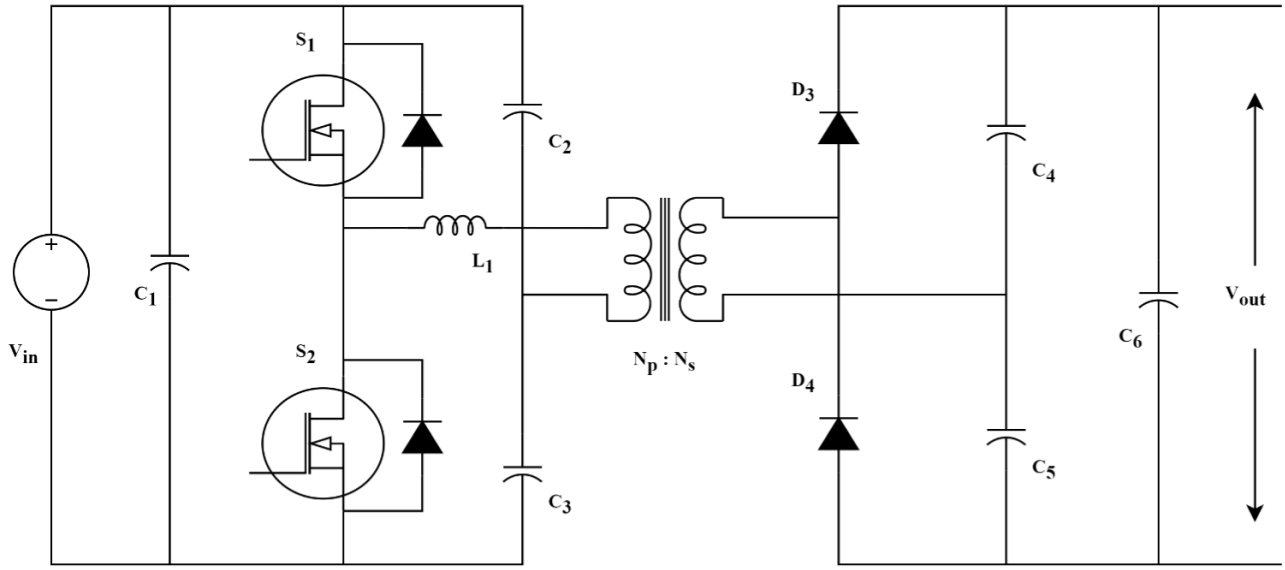

FIGURE 10. Half-bridge converter.

The latest DC converters have a wide range of applications including low-power to high-power scenarios, fuel-cell vehicles, and power generation. Its advanced design has several benefits, such as a straightforward circuit layout without any drawbacks to the total device rating (TDR), soft-switching capabilities without any additional devices, high efficiency, and simple control [43]. This knowledge highlights the versatility and advantages of DC converters in various power applications, particularly in the field of electric vehicle technology.

This highlights the converter's proficiency in effectively managing diverse power levels and its unique advantages for fuel-cell vehicles. However, it is essential to consider specific requirements and constraints of each application when selecting the most suitable converter topology. The presented converters provide flexible and efficient solutions for voltage conversion in EV vehicles, enabling the precise control of power flow and bidirectional energy transfer.

The integration of innovative circuit topologies, resonant circuits, and optimized control strategies in these converters leads to improved efficiency, reduced power losses, and better performance in electric vehicle (EV) environments. However, the complexity of the control circuit and challenges associated with specialized modulation techniques must be considered when comparing them with other converter types. Nonetheless, these converters have significant potential for advancing the power electronics in EV vehicles.

I. FULL-BRIDGE CONVERTER

Voltage conversion was achieved using four MOSFETs, allowing for voltage stepping-up or stepping-down, and bidirectional energy flow. The converter comprises four transistors, two diodes, an inductor, and a capacitor, arranged in a full-bridge configuration, as shown in Fig.11. It can handle higher voltage and power ratings as well as higher frequency switching, making it suitable for renewable energy systems. However, bidirectional energy flow capability adds complexity to the control circuit. A novel onboard battery charger design based on a full-bridge-inductor inductor converter (FB–LLC) with series-parallel transformers was proposed for electric vehicles.

This design enables zero-voltage switching (ZVS) for power switches and zero-current switching (ZCS) for rectifier diodes, leading to improved efficiency [44]. A modern controller was designed and evaluated for a zero-voltage-switching PS-FB Converter. The controller aims to regulate the output voltage and widen the input voltage range, thereby enhancing overall performance [45].

Experimental validation of the design parameters, including a wide output voltage range, high-power output, and versatile switching frequency, was conducted using a laboratory prototype [46]. A conversion ratio of approximately nine is recommended to facilitate the battery refill and depletion processes.

The mathematical equation for the output voltage (V_{out}) of the full-bridge converter is as follows:

$$V_{out} = (V_{in} - 2V_{ce} - V_d) \times D \tag{9}$$

where:

- V_{out} is the output voltage.
- V_{in} is the input voltage.
- V_{ce} is the voltage drop across each of the four switching transistors (usually MOSFETs).
- V_d is the voltage drop across the freewheeling diode.

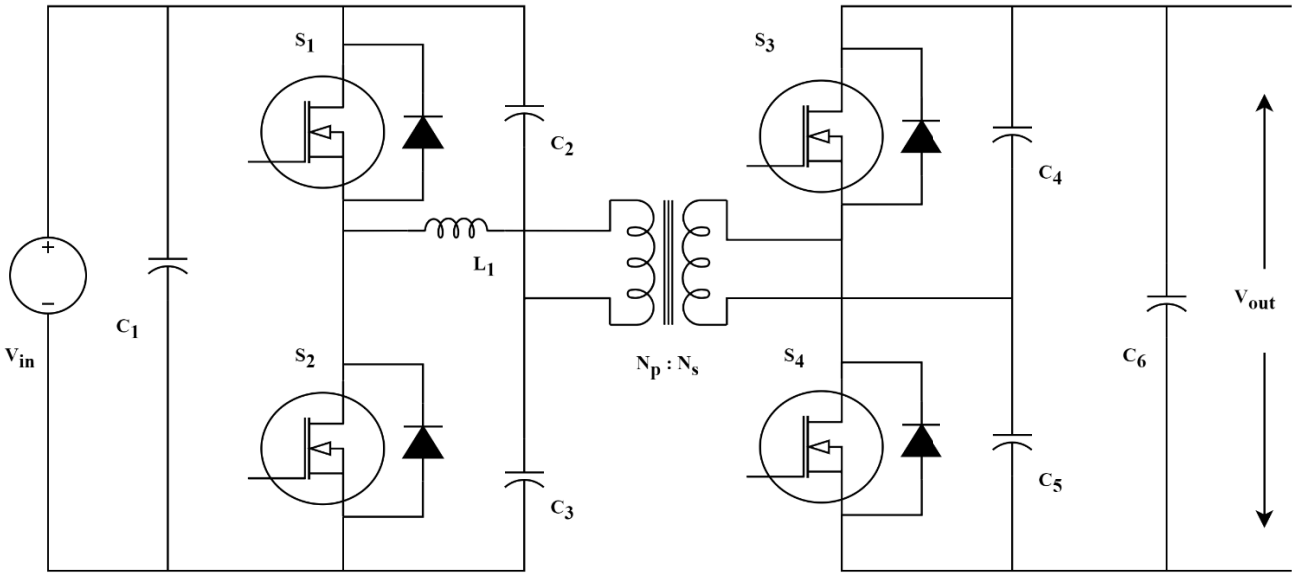

FIGURE 11. Full-bridge converter.

- *D* is the duty cycle of the switching signal, representing the fraction of the switching period during which the transistors are ON.

The converter incorporates active flyback and passive capacitor-diode snubbers, providing soft-start-up and soft-switching capabilities to reduce voltage and current spikes [47]. TPC (Total Phase Control) is a new method that enables control of phase angle and duty cycle while achieving ZVS and ZCS. This paper outlines the principles and design considerations [48].

In addition, a PWM-based ISM Controller was proposed for the PSFB Converter, which surpasses the limitations of the linear compensator. The dynamic state-space model was analyzed to assess its sliding motion, steady-state conditions, and indirect PWM control [49]. These converter design and control strategy advancements offer benefits such as efficient voltage conversion and bidirectional energy flow power delivery, and improved system performance for electric vehicles. However, bidirectional energy flow adds complexity to the control circuit, potentially affecting the cost and size of the converter. However, these innovations have advanced EV technology by providing efficient and reliable power electronics solutions.

J. DUAL-ACTIVE-BRIDGE CONVERTER

The DC-DC converter is efficient and adjustable and can regulate the voltage and reverse energy flow. It has two full-bridge circuits, each with four transistors, allowing it to handle high powers and voltages. This makes them a good option for use in renewable energy systems. Fig.12 shows the Conventional Dual Active Bridge Converter. However, Bidirectional DC-DC converters have been difficult to use in industrial settings owing to circulating current and ZVS issues (56). Researchers have achieved success with high-power Bidirectional DC-DC Converters.

This converter could deliver 100 kW of power at 750 V DC and 20 kHz. It uses SiC MOSFET dual modules and Schottky barrier diodes, achieving 98.8% efficiency at 41 kW and a rated power of 98 % [52]. The BDC can be connected in series or parallel by increasing the voltage or current ratings. An innovative bi-directional switch using silicon carbide (SiC) MOSFETs, designed for high-temperature applications in motor drives. It utilizes Power Overlay (POL) technology for enhanced integration, reducing parasitic inductance and improving high-temperature characteristics [122]. This makes it suitable for ''solid-state transformers'' and ''power electronic transformers.'' The dual active bridge (DAB) converter is more complex owing to it bidirectional energy flow and two parallel full-bridge circuits. Extensive investigations have been conducted to address the challenges arising from semiconducting switches and driver signals. These investigations have provided valuable insights for accurately predicting the DC Bias magnetizing current in DAB converters and for developing calculation methods.

The Dual Active Bridge (DAB) converter is a complex and versatile topology commonly used in applications like DC microgrids and renewable energy systems. The equations for the output voltage of a Dual Active Bridge converter are more involved than those for simpler converters like the half-bridge or full-bridge converters. The DAB converter operates with multiple switches and control schemes.

Below, I'll provide a simplified version of the equations for the output voltage, but it's important to note that the actual analysis of a DAB converter can be quite complex and may

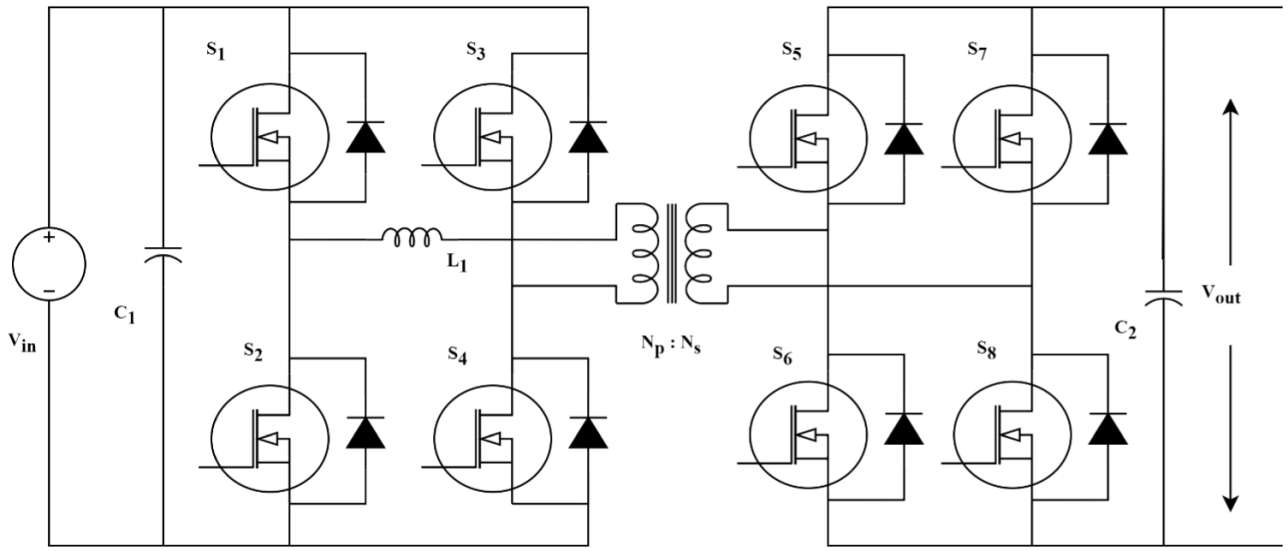

FIGURE 12. Dual active bridge converter.

involve state-space modeling and control algorithms.

$$V_{out} = V_{in} * D * \frac{Ns}{Np} \tag{10}$$

where:

- V_{out} is the output voltage.
- V_{in} is the input voltage.
- D is the duty cycle of the switching signal, representing the fraction of the switching period during which the transistors are ON.
- N_p is number of turns in Primary winding
- N_s is number of turns in Secondary winding

Again, please note that this is a simplified representation, and the actual analysis and control of a Dual Active Bridge converter involve more complex mathematics, including considerations for control strategies, phase-shift angles, and additional factors specific to the application. Design and analysis of DAB converters often require simulation software or specialized tools to obtain accurate results. This understanding has been active in controlling the selection of suitable semiconductor devices and optimizing transformer designs, contributing to cost reduction and compactness of the overall system [50]. In addition, a new modulation scheme has been proposed for the (D3ABC) Dual Three-Phase Active. Bridge Converter features two three-phase ac ports, two dc ports, and an Isolated Transformer. This modulation scheme addresses the challenges arising from different line frequencies at AC ports, such as low-frequency power pulsations, fluctuating DC link voltages, and distorted phase currents. The proposed modulation scheme enhances converter performance by eliminating low-frequency power pulsations and increasing the theoretical maximum transmittable power between the primary and secondary sides. The effectiveness of the proposed modulation scheme was verified using circuit simulation results [51]. Furthermore, an MPC-based (Model Predictive Control) approach utilizing Total Phase Shift (TPS) modulation and a current stress-optimized scheme has been proposed to enhance the dynamic performance of DAB.

This paper comprehensively covers various aspects, including historical research, significance of high-frequency link power conversion systems (HFL PCSs), control policies, soft-switching solutions, hardware design, optimization, and typical application schemes. Design recommendations and future trends for dual-active bridge-isolated bidirectional DC–DC converters (DAB-IBDCs) are also discussed [53], [54], [55]. These advancements in DC-DC converter technologies offer significant advantages for electric vehicles. These devices enable efficient voltage conversion, bidirectional energy flow, improved power delivery, and enhanced system performances. However, the complex control circuitry and challenges related to circulating current and zero-voltage switching (ZVS) pose limitations that require careful consideration during design and implementation. Nonetheless, these innovations have contributed to progress in EV technology, providing more efficient and reliable power electronics solutions.

K. MULTI-LEVEL CONVERTER

A multilevel bidirectional DC converter offers a distinct advantage by utilizing multiple voltage levels instead of a single level, effectively reducing harmonic distortion in the load voltage. These converters can function in the forward and bidirectional modes, serving as step-up and step-down converters. The implementation of multilevel bidirectional DC converters involves multiple power electronic switches [as metal-oxide-semiconductor field-effect

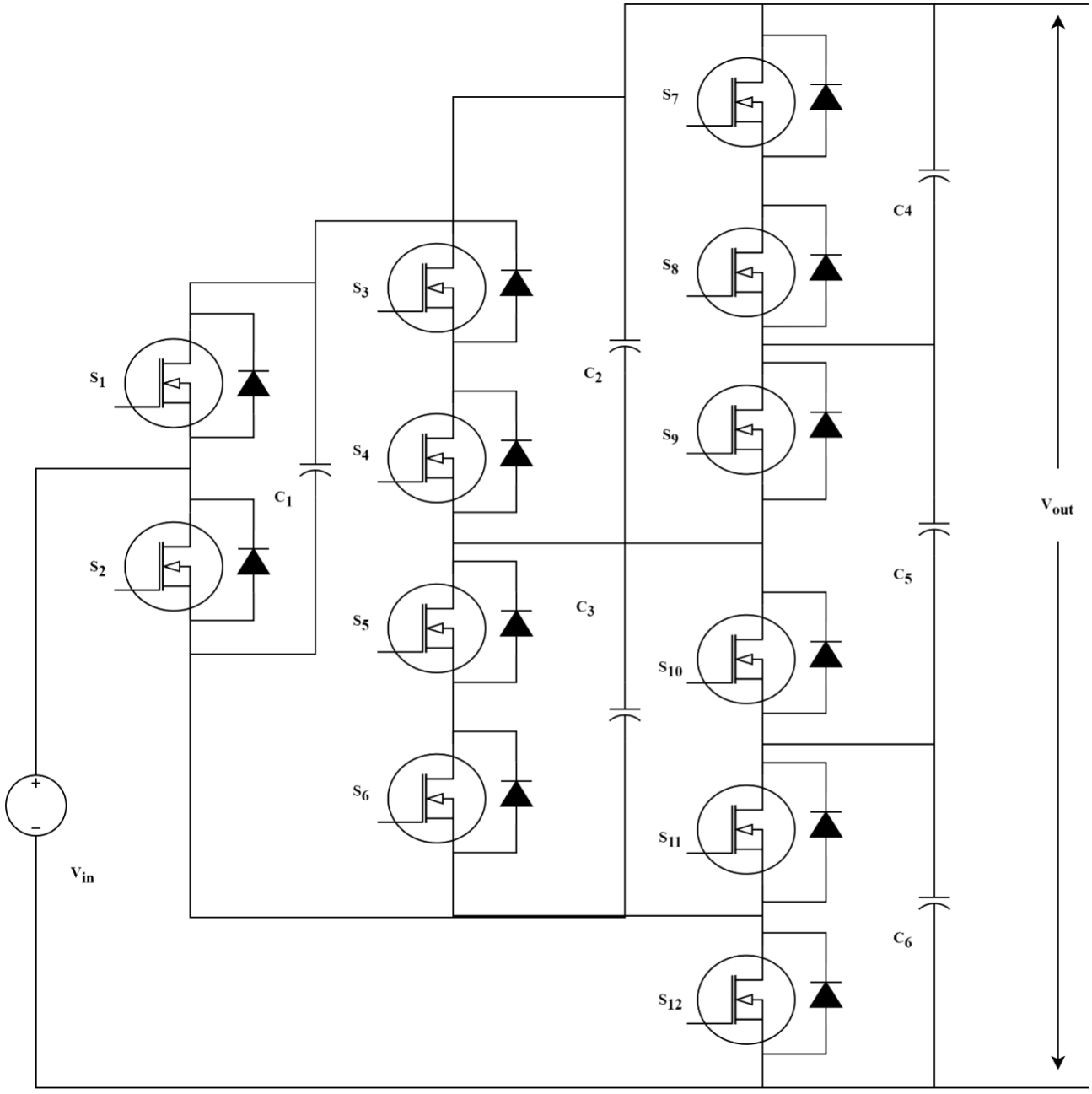

FIGURE 13. Multi-level converter.

transistors (MOSFETs) or insulated-gate bipolar transistors (e.g., inductors or capacitors)]. The converter can change its operating mode and adjust its output voltage by appropriately controlling these components.

The conventional dual-active bridge converter is illustrated in Fig.13. One significant advantage of multilevel converters is their capacity to reduce waveform irregularities, which leads to better voltage quality by producing smoother sinusoidal voltage waveforms and minimizing the harmonic content in V_{out}. The CF-MDAB converter, a multilevel bidirectional DC converter family member, incorporates favorable traits from DAB circuits, including gentle switching and compact passive components. Another prevalent type of inverter is the multilevel inverter (MLI), which converts DC voltage to AC voltage at multiple levels. Multi-level DC-DC converters are a class of power converters designed to provide multiple voltage levels at the output by combining several voltage sources or switches. The specific equations for a multi-level DC-DC converter can vary widely depending on the topology and control strategy used. One common

type of multi-level converter is the Multi-Level Neutral Point Clamped (NPC) converter, which has three voltage levels at the output.

A simplified equation for the output voltage (V_{out}) of a three-level Neutral Point Clamped (NPC) converter can be written as follows.

$$V_{out} = \left(\frac{V_{in}}{2}\right)(M + N) \tag{11}$$

where:

- V_{out} is the output voltage.
- V_{in} is the DC input voltage.
- M is the modulation index of the upper arm of the converter.
- N is the modulation index of the lower arm of the converter.

The modulation indices (M and N) typically range from -1 to 1, where -1 corresponds to full negative voltage, 0 corresponds to zero voltage, and 1 corresponds to full positive voltage. The sum of M and N should always be zero in a three-level NPC converter to maintain the neutral point at the desired voltage level.

The actual calculation of M and N, as well as the control strategy used to generate the switching signals for the converter, depends on the specific application, design requirements, and control scheme. Multi-level converters can have more complex equations and control algorithms when additional levels or features are involved. These converters are often designed and analyzed using simulation software or dedicated hardware control platforms.

The output voltage equations vary owing to their distinct configurations and modulation methods for different multilevel converters, such as cascaded H-bridge or diode-clamped converters. It is important to acknowledge that multi-level converters' intricacy might necessitate computer simulations or specialized software for precise analysis and design. Moreover, converter datasheets and relevant research articles can offer specific formulas for specific applications. These qualities contribute to the impressive efficiency and compactness. Additionally, the current feed-multilevel dual active bridge (CF-MDAB) converter is purpose-built for breaker less MVDC systems to ensure seamless operation during DC faults. The direct-current control capabilities at the input and output suit these applications. Recent studies have successfully integrated battery energy storage into MVDC grids using a CF-MDAB converter, showcasing its adeptness in managing operations and fault currents. This converter provides an efficient solution for high-power-density MVDC systems, particularly for enduring DC faults. It is crucial for EV charging to minimize energy losses during charging, owing to its high efficiency and power density. Soft switching of the converter reduces switching losses and improves overall efficiency. These compact passive components enable lightweight and space-efficient EV chargers.

The CF-MDAB converter's battery energy storage integration aligns with the trend of using EVs as energy reservoirs, enabling a two-way energy flow. However, similar to other multilevel converters, the drawback lies in the control complexity. Advanced algorithms and hardware add system intricacy and cost. In addition, the limited multilevel converter availability for EV chargers might hinder accessibility and procurement. Nonetheless, CF-MDAB's benefits of CF-MDAB —efficiency, density, and fault ride-through— make it a promising solution for dependable EV charging infrastructure [58]. In the context of electric vehicle chargers, multilevel converters provide several benefits. They improve the power quality by reducing harmonics and producing smoother output waveforms. Furthermore, their remarkable efficiency curtails energy wastage during the charging. Multilevel converters play a role in shrinking the charger dimensions and weight owing to their enhanced power density, thereby enabling compact solutions. Another strength is their adaptability to diverse voltage levels, which ensures harmony with the various EV battery systems.

These converters are easily scalable, with different power requirements and charger configurations. However, the use of multilevel converters in electric vehicle (EV) chargers is problematic. One key challenge is intricate control, demanding advanced algorithms and hardware, elevating system intricacy and costs. Implementing these converters can be more expensive than traditional options, thereby influencing overall charger expenses. They may also be sensitive to input voltage changes, thus demanding additional voltage regulation mechanisms for steady operation. Additionally, increased switching frequencies in multilevel converters may trigger electromagnetic interference, thereby requiring additional electromagnetic compatibility (EMC) steps. Finally, it is noteworthy that the market availability of multilevel converters, particularly for EV chargers, might be limited compared with widely accepted converter technologies.

L. THREE-LEVEL NPC CONVERTER

An electronic device bidirectionally converts DC power while maintaining a constant neutral-point voltage. The Three Level – Neural Point Clamped Converter(3L-NPC) has three voltage levels: high, low, and neutral as shown in fig.14. Power semiconductor devices are regulated by a converter control algorithm using a pulse-width modulation (PWM) scheme to control switching. The Three-Level NPC Converter has several advantages over other DC-DC converters. It can manage high-power levels efficiently, reducing voltage-related issues and the impact on switching devices.

A Three-Level Neutral Point Clamped (NPC) converter is a type of multi-level DC-DC converter commonly used in medium-voltage power conversion applications. It provides three voltage levels at the output.

The voltage across the load in a three-level NPC converter can be expressed as follows:

$$V_{out} = \frac{2}{3}V_{in}(D_1 - D_2) \tag{12}$$

where:

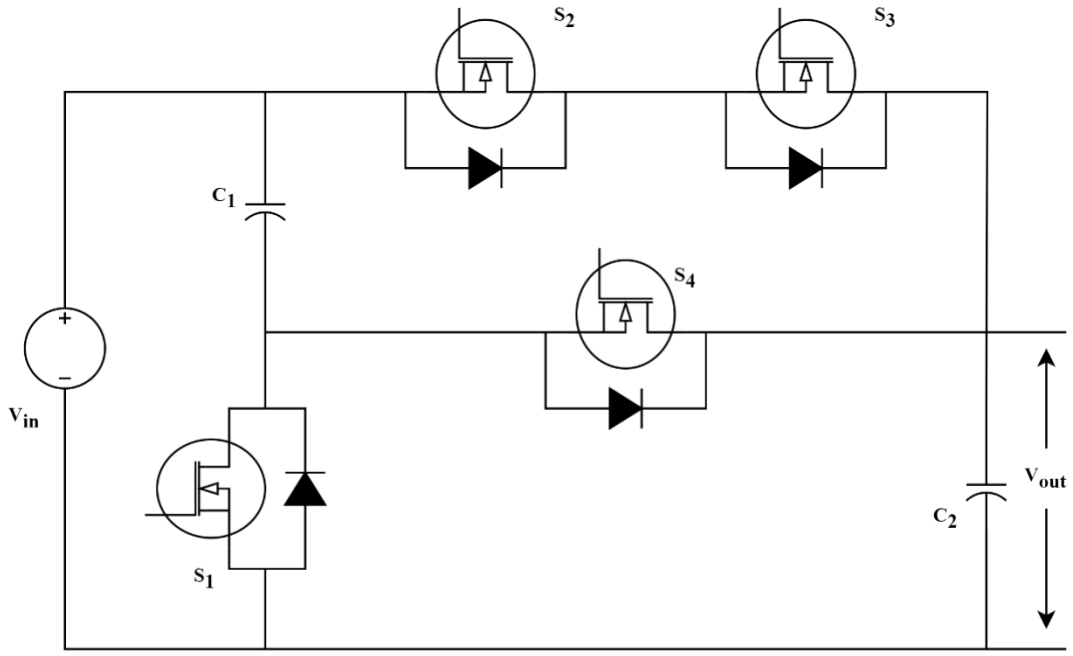

FIGURE 14. Three-level neural point clamped conver.

- V_{out} is the output voltage.
- V_{in} is the DC input voltage.
- D_1 is the duty cycle of the upper switching devices.
- D_2 is the duty cycle of the lower switching devices.

In a three-level NPC converter, the upper and lower switching devices work together to create three voltage levels across the load: $-V_{dc}/2$, 0, and $+V_{dc}/2$. The duty cycles D_1 and D_2 determine how the voltage levels are distributed. Typically, the duty cycles D_1 and D_2 are controlled based on the desired output voltage and the modulation strategy used. The sum of D_1 and D_2 should always be less than or equal to 1. This equation provides a simplified representation of the output voltage of a three-level NPC converter. In practical applications, control algorithms and modulation techniques are employed to generate the appropriate switching signals for the upper and lower switching devices to achieve the desired output voltage and maintain proper operation. The ''neutral-point-clamping'' mechanism reduces total harmonic distortion of the input current, improving power quality. It maintains a constant neutral-point voltage level and uses a three-level voltage structure for efficient power distribution. This converter has great potential for high-power bidirectional DC-DC conversion applications. It has several benefits compared to other converters, such as fewer components, higher efficiency, and simpler circuit design [57]. The system uses a cascaded approach and proportional-resonant compensator to regulate a new active neutral-point clamped (ANPC) five-level converter [60].

This study introduces HSVM, a new technique with neutral-point balancing and direct-current control of the inverter input. This enables Z-NPC-MLI in solar grid-connected operations to produce high-quality voltage and current waveforms, making it suitable for grid-connected inverter systems [80]. Simulations and experiments showed that the proposed method reduces harmonics and improves grid power quality. It is also efficient and cost effective.

The proposed system, which utilizes hysteresis current control Space Vector Pulse Width Modulation (HSVM) and neutral point balancing control, presents several advantages over alternative approaches, such as higher efficiency, cost-effectiveness, and improved power quality [105]. Precise voltage regulation and optimal current flow of the system make it a reliable solution for grid-linked solar activities. Simulation and experimental evaluations of the system demonstrated its ability to effectively suppress harmonics, leading to improved grid power quality and reliable operation. With its cost-efficient design and impressive performance in active filtering, the proposed system holds great promise for widespread adoption in diverse applications that require high-power quality and efficient grid-connected operations.

M. CASCADED H-BRIDGE CONVERTER

It was composed of multiple H-bridge cells connected in series. It uses a series of power semiconductor devices to switch between high- and low-voltage levels to achieve bidirectional power flow. The CHB converter offers high efficiency, power density, and reduced input–current harmonic distortion. It was composed of multiple series-connected H-bridge cells. Power semiconductor devices enable bidirectional power flow and converter circuits, as shown in Fig.15.

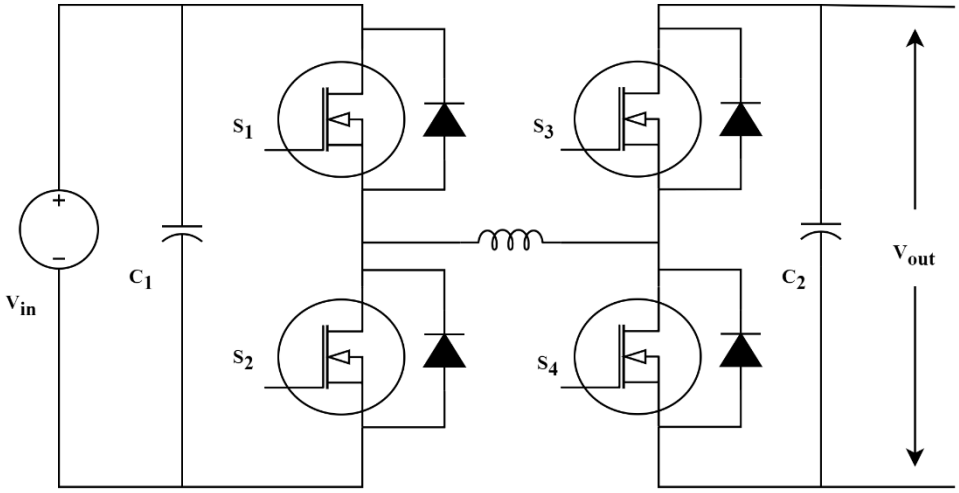

FIGURE 15. Cascaded H-bridge converter.

CHB converters are particularly suitable for renewable energy systems and electric vehicles, demonstrating their advantages for various applications [90]. Multilevel cascaded H-bridge converters offer a promising solution for large-scale photovoltaic power plants by facilitating direct connections to medium-voltage distribution networks without high-power transformers. However, the stochastic variability of the environmental factors results in power imbalances among the three phases, resulting in unanticipated problems. To mitigate these concerns, this study introduces three innovative zero-sequence injection methods to complement the traditional method [91]. A novel approach was devised to design and control a 6.6-kV back-to-back (BTB) setup incorporating bidirectional isolated DC/DC converters and modular multilevel cascade pulse-width modulation (PWM) converters. This system effectively reduces harmonic distortions using a cascade connection of multiple converter cells per phase and the implementation of low-voltage steps. This mitigates electromagnetic interference emissions [92].

A Cascaded H-Bridge DC-DC converter is a multi-level converter topology that combines multiple H-Bridge cells in series to achieve a high number of voltage levels at the output. The output voltage equation for a Cascaded H-Bridge DC-DC converter can be quite complex and depends on the number of H-Bridge cells and their modulation strategies.

The output voltage equation for a two-level Cascaded H-Bridge converter can be written as follows.

$$V_{out} = \left(\frac{V_{in}}{2}\right)[(D_1 - D_2) + (D_3 - D_4) + \cdots] \quad (13)$$

where:

- V_{out} is the output voltage.
- V_{in} is the DC input voltage.
- $D_1, D_2, D_3, D_4, \ldots$ are the duty cycles of the individual H-Bridge cells in the cascaded structure.

In a Cascaded H-Bridge converter, each H-Bridge cell can provide two voltage levels: $+V_{dc}/2$ and $-V_{dc}/2$. The duty cycles (D_1, D_2, D_3, D_4, ...) determine how these voltage levels are combined to create the desired output voltage. The actual control and modulation strategy for a Cascaded H-Bridge converter can be more complex, especially in configurations with more than two H-Bridge cells. Pulse-width modulation (PWM) techniques and control algorithms are typically employed to achieve multi-level output voltages. The number of H-Bridge cells in the cascaded structure and the specific modulation scheme used will determine the complexity of the equations and control algorithms required for accurate voltage control. Simulation software and control platforms are often used to implement and analyze Cascaded H-Bridge converters for practical designs and analysis.

Integrating bidirectional isolated DC/DC converters and modular multilevel cascade PWM converters in a 6.6-kV back-to-back (BTB) configuration demonstrates remarkable advancements in the regulation and functionality of power conversion systems. By adopting a cascade connection approach and incorporating low-voltage steps, the developed system shows notable improvements in harmonic suppression and reduction of electromagnetic interference, ensuring optimal performance and compatibility with stringent emission standards. The innovative combination of bidirectional isolated DC/DC converters and modular multilevel cascade PWM converters paves the way for enhanced power quality and electromagnetic compatibility in high-voltage applications, making them promising solutions for various industrial and grid-connected systems. A novel approach was proposed to address grid current imbalances in large-scale solar power systems by utilizing interconnected H-bridge multilevel converters.

The method uses a common DC bus created by low-voltage-side ports, enabling independent operation of each inverter and equal load sharing. An innovative H-bridge multilevel boost inverter was designed specifically for electric and hybrid vehicles, which offers a groundbreaking solution

that eliminates the need for large inductors. The fault-tolerant technique improves the performance and reliability of cascaded H-bridge converters [95].

The cascaded H-bridge DC converter combines multiple modules to achieve precise voltage control and high efficiency. It offers enhanced voltage resolution and improved fault tolerance but introduces complexity and a larger physical footprint. The converter reduces harmonic distortions, accommodates different voltage levels, and facilitates modular maintenance. However, it requires a careful circuit layout and presents challenges during load variations and electromagnetic interference. Commercial adoption may be limited because of its specialized nature and compatibility requirements. In conclusion, the converter provides benefits such as voltage control and efficiency but requires consideration of its complexities and limitations.

N. MULTI-PORT DAB CONVERTER

Two bridge circuits were used for the galvanic isolation and high-frequency power conversion. The converter has multiple ports that can be configured for various applications such as renewable energy, battery storage, and EV charging. It operates by switching the power between the input and output sides at a high frequency for an efficient transfer with reduced losses. Bidirectional switches enable energy flow in both directions, providing flexibility in controlling power flow and energy storage. This is a versatile and efficient device for improving DC-based power systems. Modular multilevel converter and cascaded H-bridge-based DC transformer structure for low-voltage DC distribution networks. The circuit is illustrated in Fig.16.

The transformer utilizes different carrier-phase-shift pulse-width modulation control methods to produce equal and unequal five-level voltage waveforms and quasi-square-wave modulation for easy insulation design. Extended-phase-shift control is used for a 3-port DC Converter with the proposed voltage equalization strategy for grouped capacitors [87]. A multi-port DC-DC converter is a complex converter topology that typically includes multiple input and output ports, allowing energy to flow between several sources and loads. The equations for a multi-port DC-DC converter can be highly dependent on the specific configuration and control strategy used. There isn't a single standard equation that applies to all multi-port converters.

However, I can provide a simplified representation of a dual-input, dual-output multi-port DC-DC converter as an example:

Let's consider a dual-input, dual-output converter with two input voltage sources (V_{dc1} and V_{dc2}) and two output voltage ports (V_{out1} and V_{out2}). The equations for such a converter are as follow.

1. Output Voltage at Port 1 (V_{out1}):

$$V_{out1} = \left(V_{dc1} - V_{f1} - V_{f2} - V_{ce1} - V_{ce2} - V_d\right) \times D_1 \tag{14}$$

2. Output Voltage at Port 2 (V_{out2}):

$$V_{out2} = \left(V_{dc2} - V_{f3} - V_{f4} - V_{ce3} - V_{ce4} - V_d\right) \times D_2 \tag{15}$$

where:

- V_{out1} and V_{out2} are the output voltages at ports 1 and 2, respectively.
- V_{dc1} and V_{dc2} are the input voltages from sources Vin.
- V_{f1}, V_{f2}, V_{f3}, and V_{f4} are voltage drops across diodes in the converter.
- V_{ce1}, V_{ce2}, V_{ce3}, and V_{ce4} are voltage drops across switching transistors.
- V_d represents the voltage drop across any freewheeling diodes (if used).
- D_1 and D_2 are the duty cycles of the switching signals controlling the converter.

The actual equations for a multi-port converter can become significantly more complex as you add more ports, incorporate bidirectional power flow, and use different control strategies. Additionally, you may need to consider factors such as inductance, capacitance, and control logic specific to your converter configuration. In practice, designing and analyzing multi-port DC-DC converters often involves simulation software, modeling, and control algorithms tailored to the specific requirements of the application. A multiport dual-active-bridge (DAB) converter is a versatile power conversion device tailored for EV chargers that delivers numerous advantages, addresses specific needs, and offers avenues for future enhancement.

This satisfies the increasing demand for efficient EV charging through multiple ports for simultaneous charging, improving convenience, and reducing time. Bidirectional power flow enables V2G and V2H applications, allowing EV batteries to supply power during peak demands or emergencies. In addition, the converter boasts high power density, facilitating a compact and lightweight charger design. This satisfies the increasing demand for efficient EV charging through multiple ports for simultaneous charging, improving convenience, and reducing time. Bidirectional power flow enables V2G and V2H applications, allowing EV batteries to supply power during peak demands or emergencies. In addition, the converter boasts high power density, facilitating a compact and lightweight charger design. This ensures high efficiency, minimizes energy losses, and enhances the power quality by reducing harmonics and voltage fluctuations. However, several challenges remain. Multiport operation of the converter requires sophisticated control algorithms and hardware implementation, necessitating advanced techniques. Coordinating multiple ports and managing power-sharing require careful consideration. Cost is another concern owing to the increased number of components and control systems; however, integration and cost-reduction strategies can address this issue. Future improvements can focus on optimizing power management algorithms, enhancing charging efficiency, and advancing fault detection and diagnostic techniques to improve reliability and safety. Beyond EV charging,

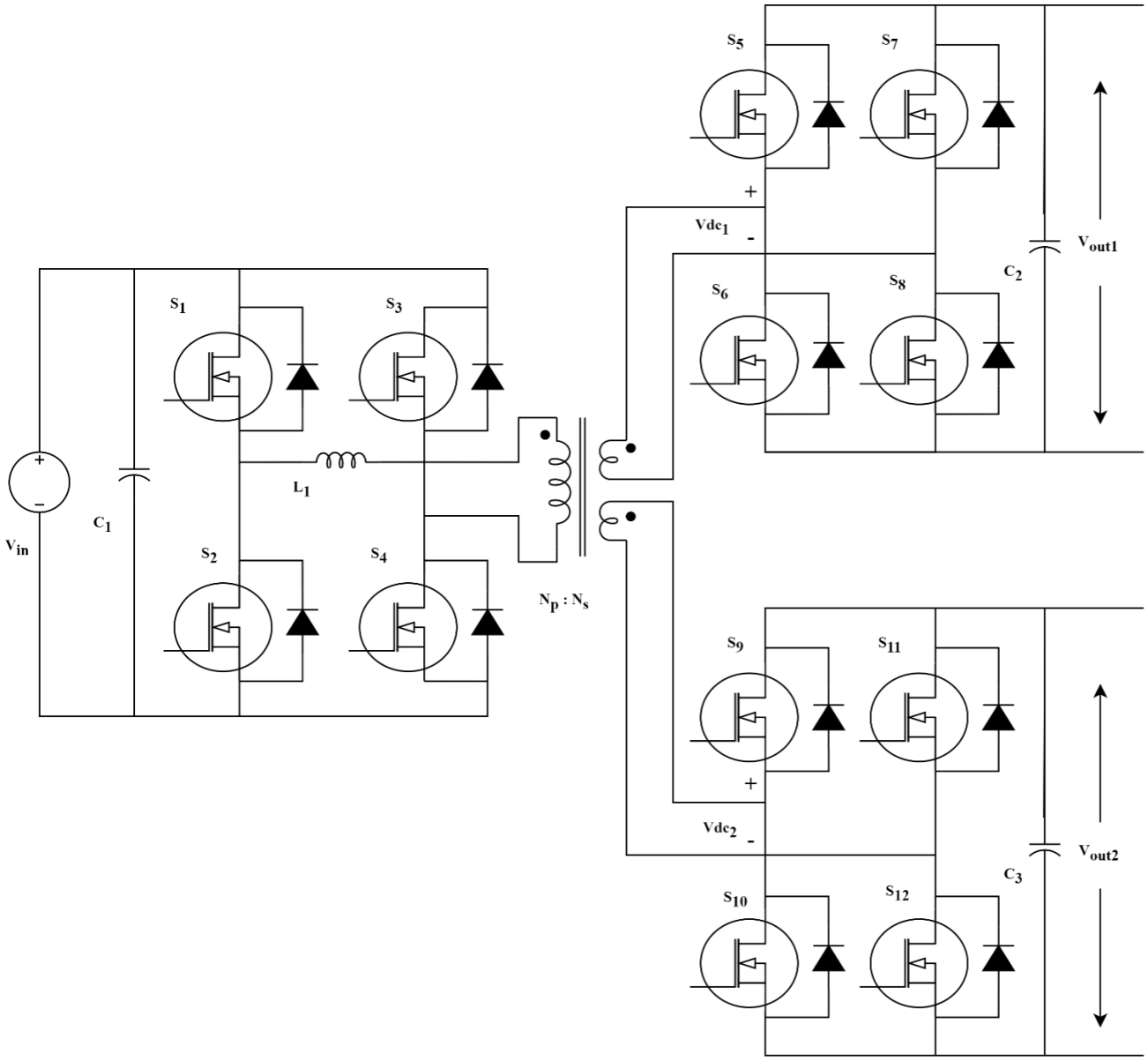

FIGURE 16. Multiport DAB bidirectional DC converter.

the multiport DAB converter has broader applicability in renewable energy systems such as solar and wind power integration, enabling efficient power conversion and grid integration. This presents opportunities for broader adoption across diverse energy applications. A multiport DAB converter offers substantial benefits in terms of simultaneous charging, bidirectional power flow, power density, and power quality. Advancing control algorithms, mitigating cost challenges, and exploring new applications will unlock their full potential for EV charging and renewable energy systems. A novel multiport converter (MPC) with an induction heating capability for electric vehicles (EVs) can reduce the system cost by eliminating the need for external heaters. MPC integrates a DAB and an interleaved PWM converter to manage multiple rechargeable batteries. Through a thorough operational analysis, it was discovered that the output power of the induction heating inverter can be autonomously adjusted using phase-shift control techniques [88]. MPC, a multiport converter based on supercapacitors, has been specifically developed to safeguard hybrid energy storage systems against sustainable energy sources (RES) and various loads. The proposed MPC architecture was configured to be highly efficient, reducing losses and switches, thus making it an economical solution [89].

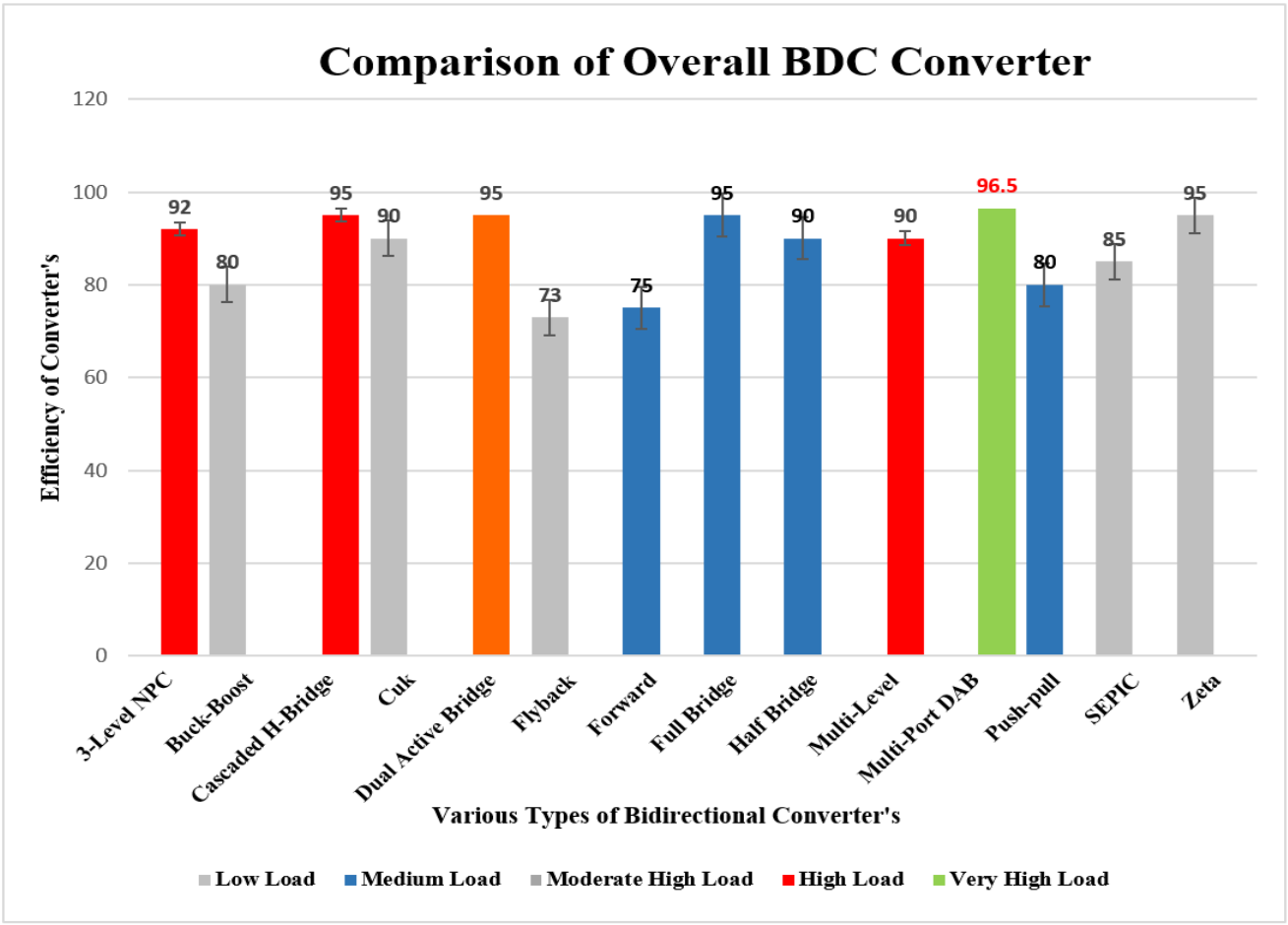

FIGURE 17. Comparison of overall BDC converter.

III. OVERVIEW: TYPES OF BIDIRECTIONAL DC CONVERTER

A. COMPARISON OF OVERALL BDC

Figure 17 shows the performance of various Bidirectional DC Converters (BDCs) in a visual format. They show their efficiency variation corresponding to the load range with different topologies allowing easy comparison. The chart helps in selecting the most suitable BDC for a given application based on the desired outcomes and requirements.

A comprehensive overview of various Bidirectional DC Converters (BDCs) based on parameters such as the voltage range, efficiency, number of switches, diodes, and capacitors. The chart also includes a formula for calculating the duty cycle, enabling a comparative analysis of the converters and the selection of the most appropriate BDC for specific applications. The visual representation of the chart allows for quick identification of high-efficiency converters and those suitable for low-to medium-voltage ranges. The outcome chart serves as a valuable tool for understanding the strengths and weaknesses of each converter type, facilitating decision-making for optimal BDC selection. It provides a concise and informative summary, helping researchers and practitioners to choose the most suitable BDC for their specific needs for electric vehicle (EV) systems. These charts provide information on their characteristics, performance, and efficiency, which ranges from 90% to 95%. EV system designers can use this information to select converters, such as full bridge, dual active bridge, or multilevel converters, which enable fast charging, high-power handling, and bidirectional power flow. The charts also highlight the complexity and cost-effectiveness of certain converters, such as the Multiport DAB Converter. Overall, these resources are valuable for making informed decisions regarding converter selection, optimizing charging infrastructure, and ensuring sustainable transportation.

The comprehensive study in Table 1 provides an extensive overview of various bidirectional DC converters, offering a comprehensive panorama of diverse converters distinguished by their unique voltage range, efficiency characteristics, and constituent components, such as switches, diodes, capacitors, and governing duty-cycle formulas. The best fitting converter for a specific application depends on the demands at hand, and the study thoroughly examines notable converters like Buck-Boost, Cuk, SEPIC, Zeta, Flyback, Forward,

Push-Pull, Half Bridge, Full Bridge, DAB, Multi-Level, 3L-NPC, Cascaded H-Bridge, and Multiport DAB converters. These converters serve as versatile workhorses, suitable for a wide range of DC-DC power supplies, battery chargers, LED drivers, AC-DC power supplies, motor drives, lighting systems, renewable energy systems, HVDC systems, and various industrial applications. One of their shared attributes is a high efficiency rating, consistently surpassing 90% to 95%, making them an ideal choice for managing electrical energy efficiently. To enhance the understanding of each converter type, this paper includes detailed citations and references.

In Table 1, the various DC-DC converter topologies exhibit high efficiency, typically above 90%, making them suitable for a wide range of applications. The number of switches, diodes, and capacitors varies based on the specific converter topology, with control strategies often based on duty cycle modulation. These converters find applications in diverse fields, including power supplies, motor drives, LED drivers, and renewable energy systems. The Buck-Boost, Cuk, SEPIC, and Zeta converters operate efficiently with low to medium voltage ranges, making them ideal for DC-DC power supplies and battery chargers. Flyback and Forward converters, suitable for low to high voltage applications, excel in AC-DC power supplies and motor drives.

Push-Pull, Half Bridge, and Full Bridge converters, known for their high efficiency, serve power supplies, motor drives, and lighting systems effectively. Dual-Active Bridge (DAB) and Multi-Level converters cater to high voltage and power requirements, benefiting renewable energy systems and motor drives. The 3-Level NPC and Cascaded H-Bridge converters offer robust solutions for industrial applications and renewable energy systems. Overall, the comprehensive review underscores the efficiency and versatility of various converter topologies while highlighting their suitability for a wide array of practical applications, enabling enhanced energy management and power conversion in today's diverse technological landscape.

IV. REVOLUTIONIZING EV CHARGING

The integration of BDC technology, combined with advanced control strategies, is transforming the EV charging landscape and revolutionizing the industry. This groundbreaking method ensures faster, more reliable, and more efficient charging for electric vehicles, thereby contributing to sustainable transportation demands. By optimizing the charging infrastructure through the BDC technology, the growing EV charging needs can be effectively met. Intelligent power management and seamless integration with smart grids further enhances the charging process, thereby advancing a greener and more efficient future. Selecting suitable BDCs for EV chargers involves evaluating factors such as the power rating, voltage levels, efficiency, and cost. Full-bridge converters and dual-active bridge converters are common choices, offering bidirectional operation and high-power handling. The choice of BDCs depends on application-specific requirements, necessitating a comprehensive analysis of converter topologies to determine optimal solutions. EV charging topologies include AC, DC, and wireless tailored for diverse settings. AC chargers, which are prevalent in homes, convert AC power into DC power for battery charging. DC chargers, found in commercial areas, directly power batteries and offer higher outputs. Wireless inductive charging, which wirelessly transfers energy, has emerged. The distinction between EV chargers for cars and bikes lies in their power output and charging capabilities, particularly for DC fast charging needs.

A. TOP RECOMMENDED DC CONVERTERS FOR EV CHARGER APPLICATIONS

Based on the survey, Table 2 shows that DAB and full-bridge converters are highly suitable for electric vehicle charging owing to their high efficiency and reliability. The half-bridge converter also shows good outcomes but is less efficient than DAB and full-bridge converters. Multiport converters are versatile but have limitations in terms of complexity and cost-effectiveness.

Each converter type has its own advantages and disadvantages, making it difficult to determine the most effective. However, converters such as buck-boost and full-bridge converters have a wide voltage range and are efficient, making them suitable for various applications. Multilevel and Cascaded H-Bridge converters offer benefits such as handling higher power levels, reducing harmonic content in motor drives, and compatibility with modern grid integration techniques. The converter choice depends on the specific application requirements and a thorough analysis of trade-offs.

V. TYPES OF CONTROL TECHNIQUES USED IN BDC CONVERTERS

Several control techniques are commonly used in bidirectional DC-DC converters,

A. HYSTERESIS CONTROL

Hysteresis control, a prominent method employed in BDCs, allows the accurate regulation of the output voltage or current without requiring a complex scientific model of the converter. Hysteresis control is a valuable method for effectively regulating bidirectional DC-DC converters, commonly used in applications like battery energy storage systems and electric vehicles. This control approach begins with an initialization phase where initial parameters and a hysteresis band (H) are set. The output, whether it's voltage or current, is continuously measured and compared to a desired reference value. If the output falls within the hysteresis band, no immediate action is taken to prevent rapid, continuous switching. However, if the output goes below the lower band limit, the converter is turned on, and its performance is closely monitored until it rises above the lower boundary. Conversely, if the output exceeds the upper limit, the converter is turned off and monitored until it falls below the upper limit. This process repeats to maintain the output within the desired

TABLE 1. Performance metrics of various bidirectional DC converters.

Parameter	Voltage Stress on Diodes	Voltage Stress on Switches	Voltage Range	Exact Efficiency	No of Switches	No of Diodes	No of Capacitors	Duty Cycle Formula	Features & Application
Buck-Boost Converter	$V_{in} + V_{out}$	V_{in} - V_{out}	Low to medium voltage	High efficiency (>90%)	2	2	1 to 2	Vout/Vin = 1/(1-D)	DC-DC power supplies, battery chargers, and LED drivers
Cuk Converter	$V_{in} + V_{out}$	V_{in} - V_{out}	Low voltage	High efficiency (>90%)	2	2	2	Vout/Vin = -D/(1-D)	DC-DC power supplies and battery chargers
SEPIC Converter	$V_{in} + V_{out}$	V_{in} - V_{out}	Low to medium voltage	High efficiency (>90%)	2	2	2	Vout/Vin = 1+D	DC-DC power supplies and LED drivers
Zeta Converter	$V_{in} + V_{out}$	V_{in} - V_{out}	Low to medium voltage	High efficiency (>90%)	2	2	1 to 2	Vout/Vin = 1/(1-D)	DC-DC power supplies and LED drivers
Flyback Converter	$V_{in} + V_{out}$	V_{out}	Low to medium voltage	High efficiency (>90%)	1 to 2	1 to 2	1 to 2	Vout/Vin = Np/Ns	AC-DC power supplies and low-power applications
Forward Converter	V_{in}	V_{out}	Low to high voltage	High efficiency (>90%)	1 to 2	1 to 2	1 to 2	Vout/Vin = 1/(1-D)	AC-DC power supplies and motor drives
Push-Pull Converter	(1 - Duty Cycle) V_{out}	$V_{in} + V_{out}$	Low to medium voltage	High efficiency (>95%)	2	2	1	It depends on the load	Power supplies, motor drives, and lighting systems
Half Bridge Converter	V_{in}	V_{in}	Low to medium voltage	High efficiency (>95%)	2	4	1	It depends on the load	Power supplies, motor drives, and lighting systems
Full Bridge Converter	V_{in}	V_{in}	Low to medium voltage	High efficiency (>95%)	4	8	2	It depends on the load	Power supplies, motor drives, and lighting systems
DAB Converter	$V_{in} + V_{out}$	$V_{in} + V_{out}$	Low - high voltage and Current	High efficiency (>95%)	4	8	2	Depends on the load	Renewable energy systems and motor drives

TABLE 1. *(Continued.)* **Performance metrics of various bidirectional DC converters.**

Multi-Level Converter	Depends on the topology and no. of levels.	Depends on the topology and no. of levels.	High voltage and power	High efficiency (>95%)	Based on the specific Level	Based on the specific Level	Based on the specific Level	Based on the specific Level	Renewable energy systems, motor drives, HVDC systems, etc.
3 L - NPC Converter	$V_{in} + V_{out}$	$V_{in} + V_{out}$	Medium voltage	High efficiency (>95%)	2N	3(N-1)	3(N-1)	Based on the specific Level	Industrial applications, renewable energy systems
Cascaded H-Bridge Converter	Depends on the topology and no. of levels.	Depends on the topology and no. of levels.	High voltage and power	High efficiency (>95%)	N(N-1)	2N+2	2N+2	Based on the specific Level	Renewable energy systems, motor drives, HVDC systems, etc.
Multiport DAB Converter	Depends on the topology and no. of levels.	Depends on the topology and no. of levels.	Low to medium voltage	High efficiency (>95%)	2N	2N	2N	Based on the specific Level	Renewable energy systems, motor drives, HVDC systems, etc.

TABLE 2. **Comparison chart for BDC converters suitable for electric vehicle charge.**

Criteria	Full Bridge Converter	Dual Active Bridge Converter	Multi-port DAB Converter
Topology	FB	DAB	N - DAB
Voltage Range	Wide range	Wide range	Wide range
Efficiency	High efficiency	High efficiency	High efficiency
Power Handling	High power levels	High power levels	Highest power levels
Bidirectional Operation	Both Direction	Both Direction	Both Direction
Suitability for Electric Vehicle Chargers	Maximum power apps necessitate dependable and smooth performance.	Maximum power apps necessitate dependable and smooth performance.	Maximum power apps necessitate dependable and smooth performance.
Cost	Moderate cost	Higher cost compared to full bridge converter	Extremely High Cost

range, offering stability while reducing excessive switching. Hysteresis control provides a practical means to balance output precision and switching frequency, serving the specific needs of various applications. The process flow of hysteresis control is shown in Fig.18.

Hysteresis control, that is commonly used in BDCs, offers several benefits owing to its simplicity and effectiveness. This method does not require a feedback loop, thereby simplifying the control circuit. Hysteresis control can work with other techniques, such as PWM or pulse-frequency modulation, to improve regulation. However, the width of the hysteresis band affects the ripple and the response. A narrow band reduces the ripple, but slows the response, whereas a wide band has the opposite effect. For steady-state operation, hysteresis control is good; however, for fast changes, advanced methods such as PI or PID should be used.

In Class E DC Converters, MPL hysteresis control generates load power by selecting nearby input powers. This reduces the transition and conduction losses, thus boosting efficiency. A nonlinear strategy that controls the output capacitor current ensures a quick reaction to changes, although it is influenced by switching frequency factors. Hysteresis is robust but causes losses and distortion. Combining it with PWM and predictive control improves efficiency and

TABLE 3. Suitability and efficiency of BDC's for E-vehicles.

Bidirectional DC-DC Converter Configuration	Efficiency (% of maximum)	Tentative Cost Range	Reason Why Individual Bidirectional Topologies are Suitable/Not Suitable for E-Vehicle?
Buck-Boost Converter	80	Low	Limited power handling capability; may not meet high-power EV requirements.
Cuk Converter	90	Low	Typically used in low-voltage applications and may not provide the power levels required for EVs.
SEPIC Converter	85	Low	Primarily used for low to medium power; may not scale up to the power range of 30 kW - 440 kW.
Zeta Converter	95	Low	Primarily designed for low to medium voltage ranges, making it unsuitable for high-voltage EVs.
Flyback Converter	70	Low	Typically used in low-power applications and may not meet the high-power demands of EVs.
Forward Converter	75	Medium	Limited power handling capability; may not meet high-power EV requirements.
Push-pull Converter	80	Medium	Generally used for lower power levels; may not provide the required power output for high-power EVs.
Half Bridge Converter	90	Medium	Suitable for medium to high-power applications, making it a potential choice for high-power EVs.
Full Bridge Converter	95	Medium	Suitable for high-power applications, making it a viable option for high-power EVs.
Dual Active Bridge Converter	95	Moderate High	Designed for high-power applications and can be suitable for high-power EVs.
Multi-Level Converter	90	High	Offers scalability and high-power handling, making it suitable for high-power EV applications.
3-level Neutral Point Clamped Converter	95	High	Suitable for medium to high-power applications, potentially meeting the requirements of high-power EVs.
Cascaded H-Bridge Converter	95	High	Suitable for high-power applications, making it a viable option for high-power EVs.
Multi-Port DAB Converter	95	Very High	Suitable for high-power applications, offering versatility for high-power EVs.

accuracy. PWM adapts frequency for efficiency, whereas the predictive control refines voltage regulation. Incorporating these refines of BDC converters enhances efficiency and precision.

Introducing a unified controller design methodology that enables the derivation of switching laws for both clock-driven and event-driven control of stationary converters. The computation of the switching planes is performed systematically, ensuring the desired loop properties are in the vicinity of a nominal set point for a wide range of switching converters. This approach provides a robust framework for controller design that accommodates various converter topologies and operating conditions [84], [85], [86], [87].

The focus is on enhancing efficiency and battery life in fast-switching applications by adopting hysteresis current control in DC-DC buck converters. The paper conducts a mathematical modeling and performance analysis of a buck converter with this control scheme, evaluating its performance under varying duty ratios and load/supply transients. The results demonstrate that the hysteresis current control method outperforms fixed and variable frequency control techniques, providing superior dynamic performance and reduced voltage ripples [115].

B. SLIDING MODE CONTROL

This is an advanced control technique that can regulate the output voltage or current in BDC's. The SMC adjusts the switching pattern of the converter such that the output voltage or current of the converter follows a reference value, regardless of changes in the load or input voltage. The controller generated a control signal designed to drive the error to zero by utilizing a sliding surface to track the reference voltage. The two types of sliding-mode control are discontinuous sliding-mode control (DSMC) and continuous sliding-mode control (CSMC), as shown in Fig.19.

The DSMC uses a discontinuous control signal, whereas the CSMC uses a continuous one. The SMC provides good regulation outcomes and is relatively insensitive to changes in load or input voltage. However, it requires careful design of the sliding-mode controller and appropriate selection of

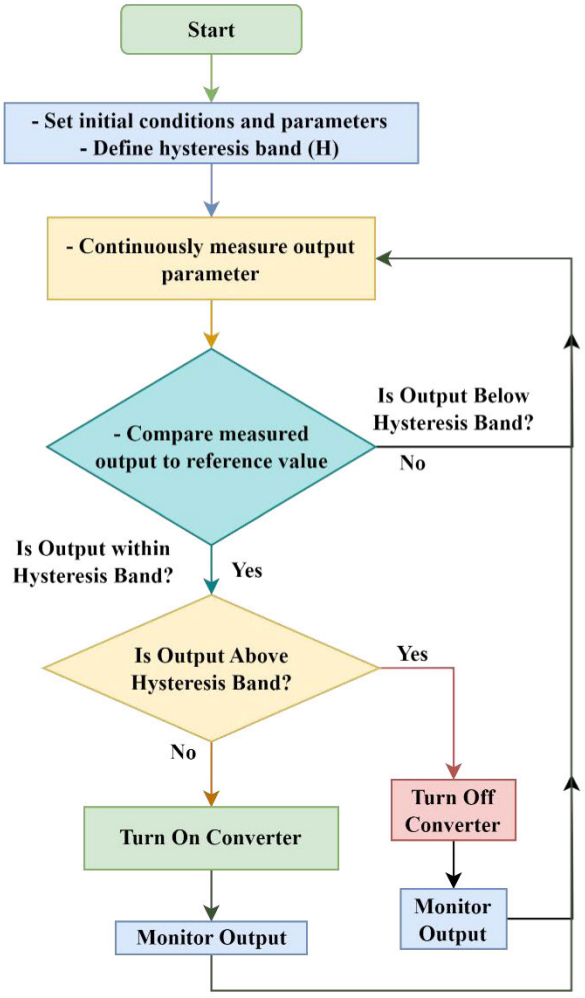

FIGURE 18. Flow chart of hysteresis control.

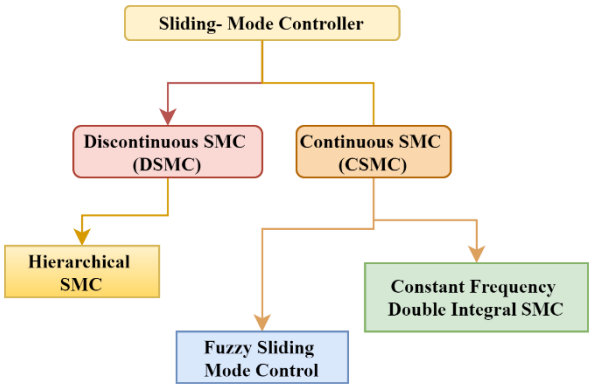

FIGURE 19. Classification of sliding-mode control.

control parameters such as the sliding surface, initial conditions, and switching function. Owing to the potential impact of measurement noise and variations in system parameters, sliding-mode control may require adjustment of the control parameters to maintain stability [64]. Calculation of the surfaces for ideal line regulation, ideal load regulation, and hysteretic current control can be achieved by combining the errors in the four state variables of the converter. This can be computed using a generic switching surface that assists in determining the equilibrium point of the control surface. This approach enables the precise control and regulation of the converter, ensuring optimal performance in terms of line regulation, load regulation, and current control. Three papers presented innovative control methods for regulating the voltage and power flow in various types of DC-DC converters. The proposed methodologies employ cutting-edge approaches, including the hierarchical sliding-mode control theory, F-SMC, and constant-frequency DI-SMC [81], to address the complex challenges in power flow regulation for renewable energy and motor drive applications. Through simulations and experimental validation [82], these control methods demonstrated exceptional feasibility and effectiveness in ensuring precise regulation while eliminating any remaining steady-state errors. Moreover, the proposed controllers exhibit remarkable robustness across a broad operating range, making them highly suitable for diverse practical applications [83].

Sliding mode control is an effective control strategy employed in BDC (buck-boost) converters used for EVs. This control method aims to tolerate the load voltage within a chosen range by creating a sliding surface that guides system dynamics. The sliding mode control algorithm dynamically adjusts the duty cycle of the power switches in the converter and continuously monitors the variance between the desired and actual output voltages. The objective was to guide the system state towards the sliding surface, ensuring a stable output voltage. One of the notable benefits of sliding mode control is its capacity to deliver reliable performance, even in the face of uncertainties and disturbances within the system. Real-time adaptation enhanced the robustness and stability of the control process.

The Sliding Mode Control process begins by setting the desired voltage and configuring system parameters like the switching frequency. This ensures the system operates at a pre-determined, high frequency for faster response and smoother control. Continuously, the voltage error is calculated as the difference between reference voltage and the actual voltage. Based on this error voltage, a specific algorithm within the reduced state controller generates a control signal. This control signal is then applied to the system through actuators, like MOSFETs in buck converters, to adjust its behavior and drive error voltage towards zero. Finally, the actual voltage is constantly measured to update the error voltage calculation and maintain the control loop. This process iterates continuously until the desired voltage error is achieved, ensuring accurate and efficient control of the system. The process flow shown in Fig.20. It ensures rapid responses, precise tracking, and accurate management of the output voltage. However, sliding-mode control can lead to

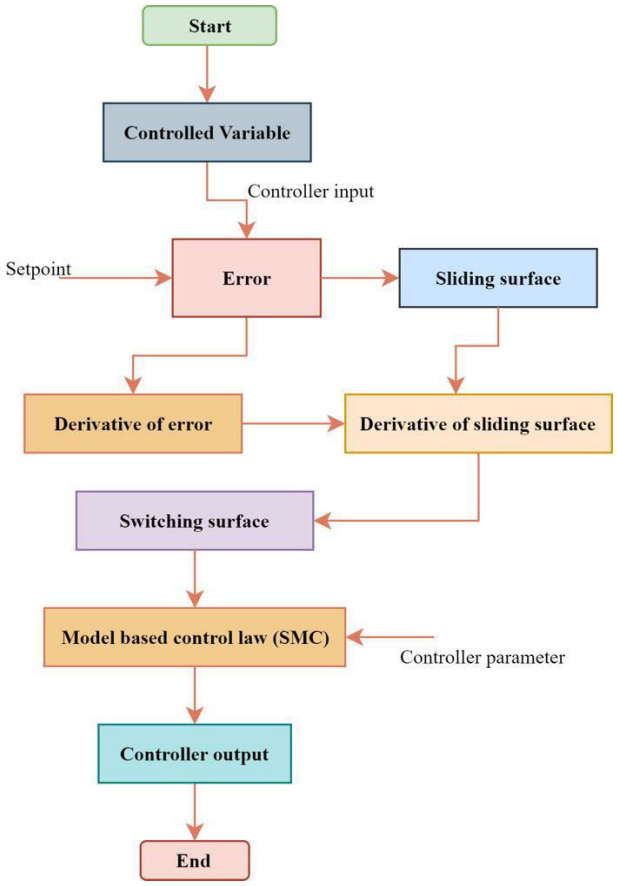

FIGURE 20. Flow chart of sliding mode control.

chattering of high-frequency switching, causing extra losses and electromagnetic interference. Tackling requires careful parameter tuning and design. Overall, sliding mode control is potent for BDC converters in EVs, offering robustness and accuracy. Addressing the chattering and loss requires careful implementation.

C. PI CONTROLLER

The Proportional-Integral (PI) controller combines proportional and integral control actions, offering a more efficient solution by addressing the disadvantages of each. Proportional controllers show output proportionality to the error signal, while integral controllers respond to the integral of the error signal. Combining both in a PI controller provides stability by reducing steady-state error. The PI controller's mathematical representation involves the sum of proportional and integral terms, contributing to the reduction of system instability associated with integral controllers. The controller's transfer function, expressed in Laplace transforms, demonstrates its effectiveness in significantly reducing steady-state error without compromising system stability. The ubiquitous use of proportional-integral (PI) control methodology exemplifies an advanced control technique embraced within bidirectional DC-DC converters, enabling the precise regulation of the output voltage or current. Employing a PI controller, this method dynamically modulates the converter's switching pattern by evaluating the discrepancy among the prevailing voltage level and the desired reference voltage and the block diagram illustrated in Fig.21. The proposed control scheme excels in managing the nonlinear dynamics and unique characteristics of boost converters, thereby ensuring a stable and precise control. The complexities of the CCM operation are effectively managed by combining cascade PI control and MRAC properties. The MATLAB/Simulink simulations validated the accuracy and robustness of the control system, showing a rapid response, minimal overshoot, and precise tracking. This validated the practical efficacy of the proposed method. Cascade control and MRAC techniques offer a promising solution for enhancing and boosting converter system performance and stability [73], [74], [75], [76]. In a DC-DC converter with a modified PI controller for electric vehicle (EV) battery charging. The system aims to achieve stable output voltage, high current density, and minimal overshoot for lithium-ion batteries, reducing charging time and improving converter lifespan. The proposed converter demonstrates effectiveness in minimizing power loss, maintaining a power factor of around 90%, and low total harmonic distortion, making it suitable for high-density load currents in EV applications [123].

D. FUZZY LOGIC CONTROL

In DC converters, fuzzy logic control is used to regulate the duty cycle of the converter by assessing input variables, such as the current voltage level and reference voltage. This was accomplished by using fuzzy logic. A flowchart illustrating this method is shown in Fig. 22. To determine the proper course of control for DC converters, the controller consults a predefined set of rules produced through the application of specialized knowledge and practical experience. Fuzzy logic controllers (FLCs) are useful tools for managing uncertain and nonlinear dynamics in complex systems such as those that utilize renewable or variable sources of electricity. Additionally, FLCs are neither complicated nor economical.

Processing information using fuzzy sets is one of the ways in which FLC helps improve decision-making. Owing to its ability to properly manage uncertainties and fluctuations in the input data, this results in decisions that are both more exact and adaptable. The FLC is a potent instrument that can be used for both decision making and control. In fuzzy logic control, imprecise terminology and membership degrees are used to analyze and assess data, which allows it to overcome the restrictions of traditional logic control of the precise mathematical models associated with a degree of membership that corresponds to a membership function (MF) that maps the elements of the universe to numerical values between 0 and 1. The selection and number of MFs employed significantly impact controller output, memory utilization, and computational efficiency.

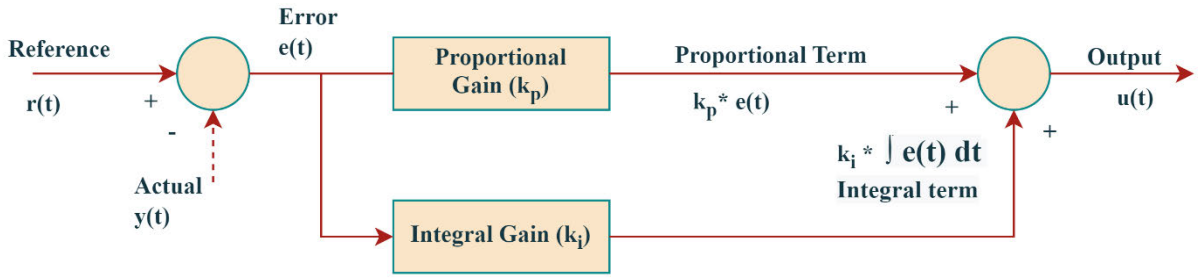

FIGURE 21. Block diagram for PI controller.

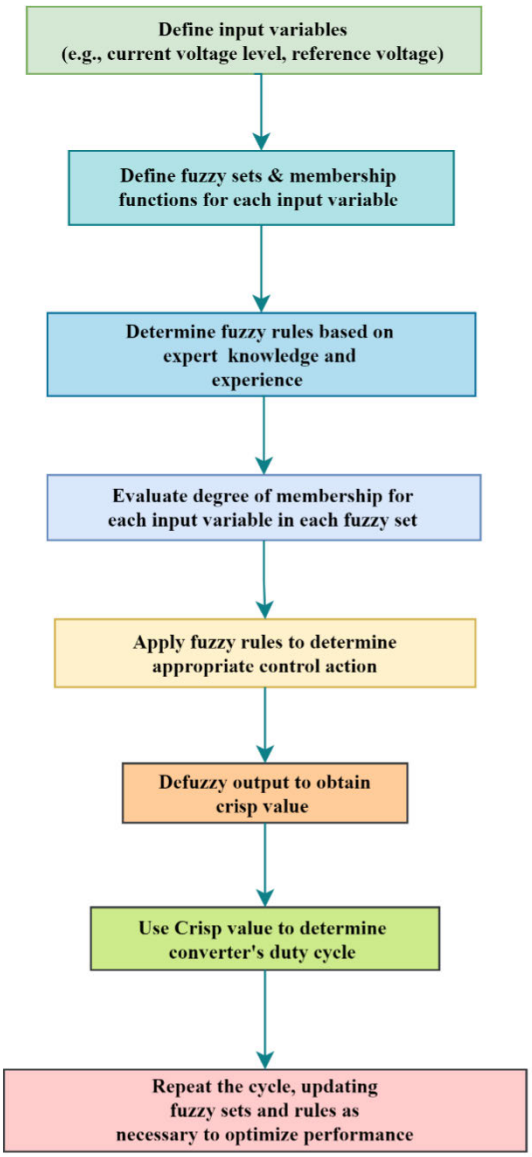

FIGURE 22. Process flow chart for fuzzy logic control.

As the membership degree value approached unity, the affiliation of the element with the fuzzy set increased. The construction of the fuzzy set and its associated MF is based on expert insights, and the common MF shapes include Trapezoidal, Gaussian, and bell shapes. This control method employs fuzzy logic, which is a mathematical approach to represent the uncertainty of human reasoning.

This paper describes a new method for controlling BDCs that uses a set of fuzzy rules to determine the duty cycle of the converter based on current–voltage and reference voltage levels. This method, called fuzzy-logic control, is used in systems that use fuzzy logic, which is a way of thinking about math that allows the representation of uncertain or vague information. Using fuzzy logic control in BDCs, it is possible to control the power flows between different sources, such as when a renewable energy source interacts with a grid. In a Bidirectional DC-DC converter (BDC), the fuzzy logic controller uses input variables, such as power flow and voltage level, to determine the correct control action. A set of fuzzy rules was used to process these input variables and determine the output control action. The system designer uses his or her knowledge and experience to develop these fuzzy rules, allowing the designer to tweak them to achieve the best converter performance. One of the best ways to use fuzzy-logic control in BDCs is to handle the complicated interactions of uncertain and nonlinear system dynamics. Therefore, they can be used to control systems that use renewable energy sources, that can change significantly and are difficult to predict. In addition, fuzzy logic control is easy and inexpensive to implement, making it a good choice for controlling BDCs, which is also beneficial for the budget.

A Bidirectional DC-DC converter (BDC) uses a fuzzy logic controller to determine the control action based on input variables such as the power flow and voltage level. The output control action was based on a set of fuzzy rules applied to these variables. The system designer uses his or her knowledge and experience to create these fuzzy rules, which gives the designer the freedom to work best for the performance of the converter.

One of the benefits of using fuzzy logic control in BDCs is that it can address the complicated and uncertain behavior of the system. Therefore, it can be used to control systems that use renewable energy sources, which can change significantly and are difficult to predict. Fuzzy logic control is also easy and inexpensive to set up, which makes it a good choice for controlling BDCs, which is also good for your budget.

E. MODEL PREDICTIVE CONTROL

The control method uses a mathematical model to predict future behavior. It can be used to control BDCs, such as those between renewable energy sources and the grid, by predicting the future state of the system based on the current control action and current state of the system. MPC can handle constraints on the system, such as voltage and power limits, multiple inputs and outputs, and multiple objectives, such as maximizing the power flow while minimizing losses. It is a powerful tool for controlling BDC because it can handle system constraints and systems with multiple objectives. The viability of the suggested regulating method for battery applications and Model Predictive Control was demonstrated through simulation results. A mode-activation control method was proposed as an optimal approach to govern and regulate the various operating modes of the battery, including the charge, discharge, and idle modes. As the converters are constructed, each of the three categories functions independently [66]. Neural networks simplify and implement predictive controllers in power electronics in a cost-effective manner, and the resulting process flow chart is used to visualize and better understand the control of BDCs, as shown in Fig.23. A wide analysis was conducted on the neural network architecture, illuminating the details of the training and validation procedures [68]. Model predictive control (MPC) and current stress-enhanced scheme (TPS) modulation were used to achieve a swift dynamic response and sustain the required load voltage level while satisfying the minimum current stress constraint. The current stress-optimized TPS scheme was employed to sustain the required load voltage level while minimizing the current stress on the system [54]. We considered a BDC with only the tabulated parameters when designing the controller when operating in boost mode. In this case, Model Predictive Control (MPC) is utilized to function in boost mode, but the same approach can also be used to operate in buck mode [67]. The dynamic and output equations that relate the output, input, and states of the converter are examined. Model predictive control (MPC) strategies were used to optimize the control of the converter by solving an optimization problem at each sampling time. The tuning parameters for the MPC were calculated using tuning rules from previous studies. The essential parameters encompassed in this context are sample time, prediction horizon, control horizon, move suppression coefficients, weighted factors for the controlled variable, and weight factor for the process variable. The sample time was carefully chosen to balance the computational load and dynamic behavior tracking. Ensure that the prediction horizon is sufficiently long to ensure nominal stability and that the control horizon is sufficiently long to show the effects of control actions clearly. Employ weighted factors for the controlled variable to accomplish a delicate degree of precision in regulating particular measured variables of the converter or establish a prioritized hierarchy for controller intervention across multiple output channels.

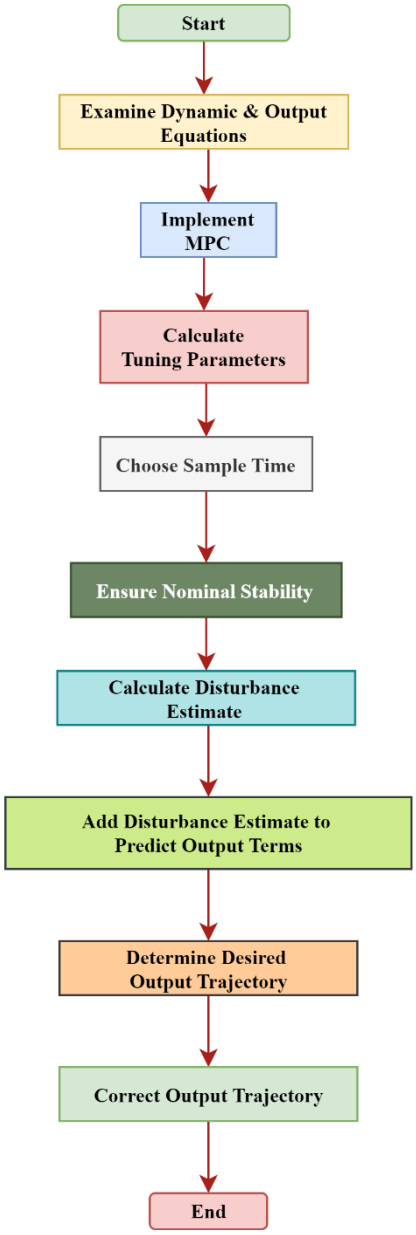

FIGURE 23. Flow chart for precise model predictive control of BDC's.

Compute disturbance estimation by deducting the current measured value of the process variable from the anticipated value of the process variable at the current sampling instance.

We present a constant disturbance estimation throughout the prediction horizon and incorporate it into the future projected output terms to augment the efficacy of the algorithm. The intended output trajectory is determined by subjecting the set point to a first-order filtering mechanism. The output trajectory was corrected by adding estimates of the disturbance to account for unmolded effects. A decentralized model predictive control (DMPC) algorithm for systems with multiple independent actuators and a central plant, relevant for

modular and highly dynamic systems. It divides the centralized controller's objective function into local objectives for each agent, ensuring the same performance as a centralized controller. Analytical proof of optimality and stability in unconstrained operation is provided, along with a region of attraction analysis for control input-constrained operation. Numerical studies involving a battery emulator system compare DMPC performance with the global optimum [118]. The study focuses on applying a Model Predictive Control (MPC) algorithm to regulate marine diesel engine speed, considering model mismatch and external disturbances. They address steady-state error by converting the nonlinear model to incremental form and introduce a discrete disturbance observer for feedback correction. Two controller variations, DONMPC and DOLMMPC, are proposed. Experimental verification shows that both models outperform the traditional PID controller. The DOLMMPC controller, with reduced online computation, is particularly suitable for practical engineering, meeting microprocessor computational limits [119].

F. NEURAL NETWORK CONTROL

This control method employs artificial neural networks to learn the behavior of the converter and optimize the control inputs based on the system constraints and outcome criteria. Neural Network (NN) control is a technique for controlling systems that utilizes artificial neural networks inspired by the structure and function of the human brain. By utilizing Neural Network (NN) control in Bidirectional DC-DC converters (BDCs), it is possible to effectively manage the power flow between diverse sources, including renewable energy and the grid. In NN control, a neural network is trained to recognize the complex relationship between the system inputs, such as power and voltage levels, and the desired output, which is the optimal control action. This process can be illustrated in Fig.24. The training process utilizes a vast dataset containing numerous input-output pairs, enabling the neural network to acquire precise learning, and forecasting abilities. Following the training, an NN can be employed to predict the control action for a given set of inputs. A neural network-predicted control action was sed to regulate the system. Neural network control can be implemented in BDCs by using feedforward, recurrent, or combined neural networks. The feedforward neural network output is directly based on the input. Recurrent neural networks store past inputs and outputs, and can process time-series data. Neural network control in BDCs is advantageous as it can manage the nonlinear dynamics and uncertainty. Neural networks can learn complex input-output relationships. (73).

NN control is suitable for BDC regulation owing to its capability to manage nonlinear behaviors and uncertainties, and its proficiency in multi-input and multi-output systems. NNs can be feed-forward, recurrent, or a combination of both.

A model-free adaptive method using an Artificial Neural Network (ANN) for real-time weight adjustments was developed for the Single-phase DAB technology. This approach combines a Proportional Integral controller with an ANN controller to improve the stability and offset disturbances from load and source fluctuations. The proposed Artificial Neural Network-Proportional-Integral (ANN-PI) controller exhibits a simplified design while maintaining the robustness of the alternative nonlinear control methods. Implementation occurred on the TI Launchpad platform, incorporating a 50 Watts laboratory-scale dual active bridge (DAB) test bench. This suggests that the ANN-PI controller provides an uncomplicated framework while retaining resilience, similar to the alternative nonlinear control techniques. The controller utilizes the TI Launchpad platform to effectively integrate into a laboratory-scale DAB test bench with a 50 Watts power rating [62]. The RWFNN controller uses a dual input system, including tracking error 'e' and its derivative 'eẏ'. The Membership Layer processes the input signals, whereas the Wavelet Layer processes signals based on these characteristics. The rule and recurrent layers play crucial roles in the functionality of the controller, with the output from the Rule Layer multiplied by the wavelet and recurrent signals. [108]. The fuzzy logic system consists of five layers, each of which performs distinct functions to extract valuable insights from input data. The input layer collects subjective language phrases, whereas the membership layer links the input terms to fuzzy sets using membership functions. The wavelet layer analyzes the output using wavelet transforms, capturing significant features and minimizing noise. The rule layer interprets the wavelet results using ''if-then'' regulations to derive final conclusions.

Finally, the output layer aggregates with the rule layer, resulting in a definitive outcome. The typical mechanism of this layer for producing precise outputs involves defuzzification, which transforms the fuzzy output into a crisp value that can be applied for decision-making purposes. The process flow of the neural network controller is shown in Fig.25.

The key aspect of the study is the integration of an Adaptive-Neuro Fuzzy Inference System (ANFIS) for enhanced battery performance during charge and discharge cycles. The system aims to improve the stability and efficiency of EV charging/discharging while reducing the load demand on the conventional AC grid [120]. Fuzzy logic controllers offer several advantages over traditional controllers, including robustness to input and system dynamics, flexibility in describing input variables, and efficiency in nonlinear systems, such as DC converters. The wavelet layer reduces the noise sensitivity, resulting in more stable and accurate control. Defuzzification in the output layer converts the fuzzy output into crisp values, thereby improving energy efficiency and cost savings.

G. SPACE VECTOR MODULATION CONTROL

SVM is a sophisticated control technique used in BDCs to manage power exchange between two DC voltage sources effectively. SVM involves breaking down the desired output voltage into three perpendicular vectors called spatial

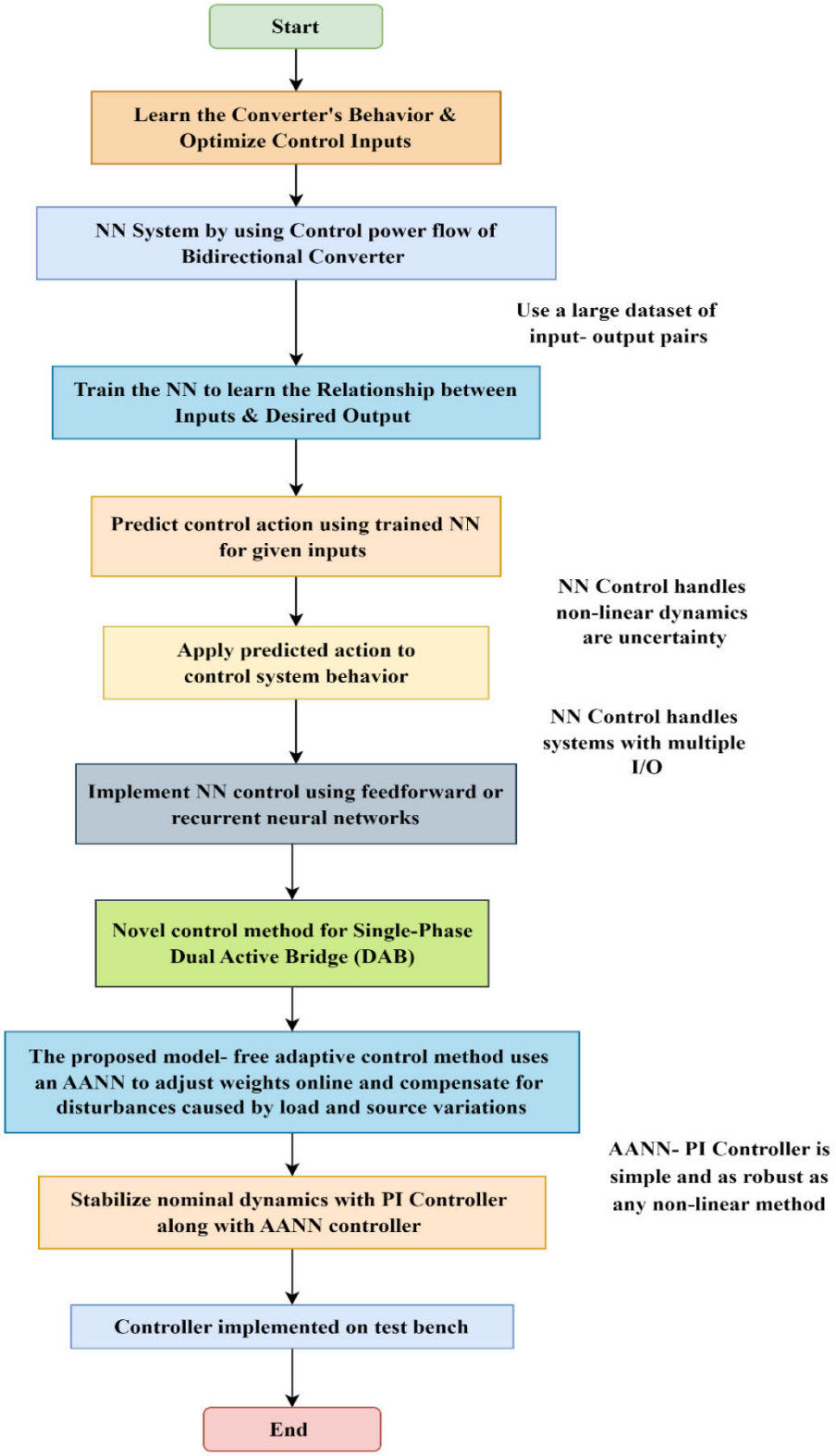

FIGURE 24. Process flow chart for neural network controller with BDC's.

vectors. Spatial vectors play a vital role in governing the converter switching, enabling precise power control. BDCs are electronic devices that facilitate bidirectional power transfer between DC sources. authors were proposed for EV charging, energy storage, and microgrid management. The SVM technique empowers the power control in BDCs by

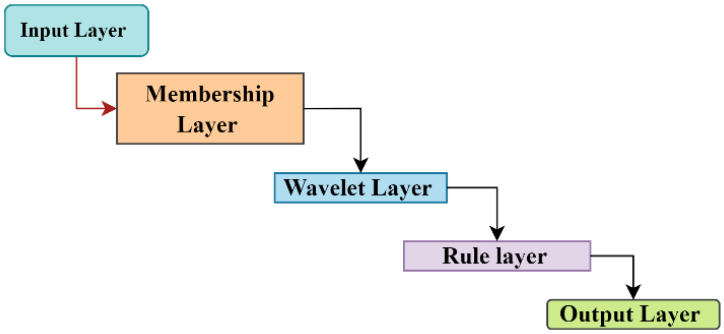

FIGURE 25. Process flow chart for neural network controller.

segmenting the output voltage into spatial vectors. This ensures efficient power regulation and minimal distortion. The SVM algorithm was integrated within the BDC control loops to compute the desired spatial vectors by adjusting the converter switches for smooth power flow. SVM, an advanced strategy, was explored for grid-connected Photovoltaic systems using Z-NPC-MLI. SVM overcomes challenges such as shoot-through and harmonic reduction and improves the performance of the grid-connected inverter. The study introduced SVM as a solution to current-controller-based SVPWM, enhancing the voltage and current waveforms for superior grid connections [80]. Despite the unbalanced input voltage conditions, the converter maintains a superior input current quality and a perfect sinusoidal output voltage [102]. i This paper introduces a creative control approach for a compact DC capacitor in a diode rectifier AC/DC converter to a DC/AC converter. This converter uses AC power, converts it to DC, and returns it to AC. A voltage sensor measures the DC voltage, which is filtered using a low-pass filter (LPF) to remove oscillations. An RC network forms the LPF. The LPF output was directed to an SVPWM controller to compute the modulation index. This index determines the output voltage amplitude adjustment, which is calculated by using the input DC voltage. However, as the DC voltage changes, the space-vector amplitude fluctuates. A novel SVPWM [102] strategy incorporating a changing modulation index was proposed to address this. This strategy effectively accounts for the dynamic nature of the DC voltage, ensuring that the amplitudes of the space vectors consistently generate sinusoidal output voltages, as shown in the process flowchart in Fig. 26.

Additionally, this paper introduces a distinctive approach for controlling the neutral-point voltage in a three-phase × 3 L-NPC converter using straightforward phase duty-ratio expressions in d-q-0 coordinates. This modulation technique facilitates voltage balance across all output levels and power factors, minimizing the distortion at the switching frequency [103]. These control strategies have notable advantages for EVs. They enhance the power conversion efficiency and optimize EV grid integration and battery charge/discharge.

These strategies elevate EV charging and ensure reliability by utilizing advanced modulation and voltage controls. However, compared to other methods, they introduce complexity owing to the time-varying modulation indexes. Determining and adjusting these indices considering DC voltage dynamics, poses computational and real-time challenges. Further research is crucial to address this issue by optimizing EV control. Scalability, robustness, and adaptability to diverse conditions are vital in real-world EV charging along with cost-effectiveness.

Modulation reduces the transformer current per switching period, enhancing the efficiency, as supported by experiments [104]. The proposed method is an enhanced SVM and VBC technique to address the voltage imbalances in the T-type 5 L-NNPP converter. This method effectively balances the capacitor voltages and has been validated through simulations and experiments [105].

H. DIRECT TORQUE CONTROL

DTC is a control technique used in BDCs to regulate the torque and speed in AC motor drives. It allows bidirectional power flow control and ensures smooth transitions between the operating states. DTC compares the actual and reference values using a lookup table to optimize the switching pattern of the converter and minimize the errors. The converter control algorithm selects switching patterns for the motor and generator drives, ensuring torque, speed, power generation, and voltage regulation. DTC has several advantages over other control methods, such as high dynamic outcome, fast response, and high efficiency.

DTC is a reliable and cost-effective solution as it does not require position or speed sensors. It compares the actual values with the reference values and selects switching patterns to reduce errors. The converter provides a high dynamic performance, fast response, and efficiency. A 10-horsepower motor drive system was used to evaluate the performance of the frame-angle-based direct-torque controller by focusing on voltage components [96]. Comparison of DTC techniques for DFI DC Generators, focusing on decreasing torque oscillations caused by nonlinear diode rectifiers and regulating the DC bus voltage and stator frequency [97]. The 5D-DTC

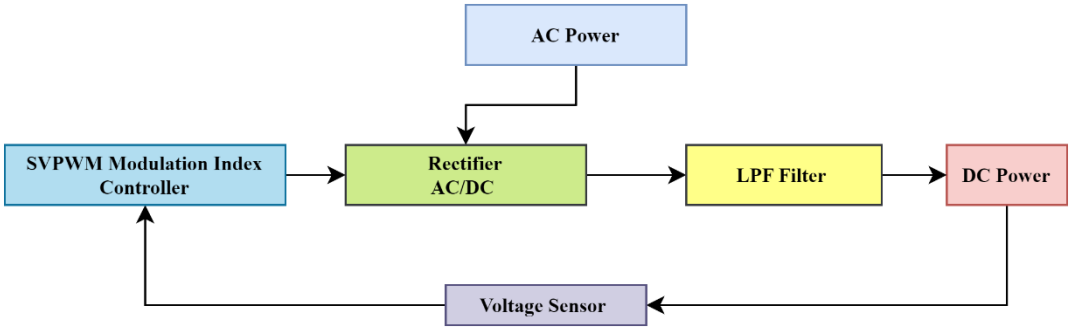

FIGURE 26. Block diagram of AC – DC conversion with SVPWM controller.

method for six-phase induction machines uses hysteresis regulators and clustering to suppress the current and address harmonics [98]. Lookup Table-based Model Predictive Direct Torque Control (LUT-MPDTC) enhances the performance of a synchronous generator with a Vienna rectifier by reducing torque and flux ripples and minimizing computational problems compared with traditional DTC [99]. As a novel approach based on current minimization, this study aims to determine the optimum values of the reference flux linkage in a vehicle control strategy, thereby improving its drivetrain efficiency. Experimental validation has confirmed the effectiveness and superiority of this method over other approaches [100].

Direct torque control (DTC) is a control strategy for BDC converters in EVs that provides precise torque control by directly adjusting the switching states and duty cycle. DTC eliminates the need for traditional modulation techniques, making it a fast and effective method for achieving high dynamic performance and accurate control. However, this may result in a higher switching frequency and associated losses, requiring careful parameter selection and control tuning to optimize performance and minimize torque ripples. Overall, DTC is a powerful technique for BDC converters that enables precise torque control and high performance, with careful consideration of the switching frequency and control parameters.

I. DYNAMIC EVOLUTION CONTROLLER

A dynamic evolution controller is a type of control system that utilizes a dynamic evolution algorithm to control the behavior of a system. The basic structure of the dynamic evolution controller is shown in Fig.27.

Dynamic evolution controllers (DECs) are essential in modern engineering applications. They take system inputs such as state or outcome measurements, and the evolution algorithm adjusts the control inputs in response to system behavior changes. State error function and optimization techniques enable the evolution algorithm to adjust the control inputs in real time. The output of the controller is used to control the system, which must be precise and responsive. The feedback mechanism allows the controller to receive information regarding the behavior of the system, which is used to adjust the control inputs accordingly. This crucial component enables the controller to respond to changes in system behavior and ensure stability and control. The evaluation function, which is a mathematical function, evaluates the outcome of the controller and provides feedback to the evolutionary algorithm. This function is essential because it ensures the effectiveness of the controller in controlling the behavior of the system.

The overall effectiveness of the dynamic evolution controller depends on factors such as the accuracy of the input measurements, the evolution algorithm design, and the real-time response capability of the controller. The key to managing complex systems is effective control of their dynamic evolution. The components of the controller, including the inputs, evolution algorithm, outputs, feedback, and evaluation, are crucial for maintaining system stability. The dynamic evolution controller adapts inputs based on system changes to achieve the desired outcomes depending on the accuracy, algorithm, and real-time response. This approach was used to establish a converter system controller for an FC electric car with an ultracapacitor energy storage through a Bidirectional DC-DC converter [65].

J. PHASE SHIFT CONTROL

Phase-shift control in DC Converters adjusts the phase relationship between the input voltage and inductor current to regulate the output voltage. This process involves three main steps. Single-phase shift (SPS) control involves aligning the phase shift between the input voltage and the inductor current. This approach maintains a constant switching frequency and duty cycle, simplifying the implementation but restricting output voltage control. The proposed setup adopts a cascaded method that incorporates a proportional-resonant compensator for the 5-level converter (5LC) and a single-phase shift approach for the dual active half-bridge converter (DAHBC). The comparative analysis demonstrated the superiority of the proposed topology over existing topologies in terms of higher efficiency, diminished switch stress, balanced power losses,

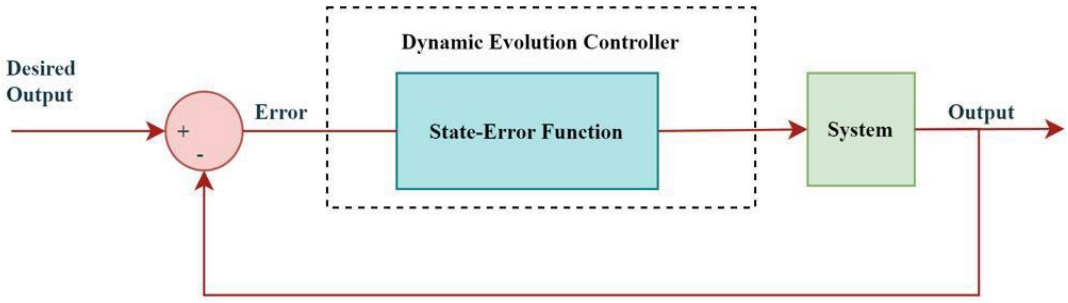

FIGURE 27. Block diagram of dynamic evolution controller.

and enhanced power quality across the operation modes [60]. A dual-phase shift (DPS) involves adding two distinct phase changes to the input voltage to enhance output voltage control. It boosts efficiency and regulation. Electric vehicle (EV) charging gains efficiency by applying a Variable Switching Frequency (VSF) and phase shifts.

This optimizes power delivery and reduces losses. Adjusting the switching frequency and phase shifts dynamically during charging reduces power losses and enhances energy transfer efficiency [59]. It doubles the output voltage ripple frequency and enables precise power-flow regulation.

The process flow of the dual-phase shift control strategy is illustrated in Fig.28. Three-phase shift control (TPS) is a versatile method for varying the output voltage of DC-DC converters. The SPS and DPS methods provide intermediate outcomes, whereas triple-phase-shifted (TPS) modulation offers advanced features, such as precise voltage regulation, improved efficiencies, and superior transient response. TPS modulation also eliminates dual-DC side flow back currents in isolated dual-active bridge (DAB) converters [61], [62], [63]. Furthermore, research has focused on developing mathematical models and closed-loop control configurations for DAB converters driven by cooperative triple-phase-shifted modulation (CTPS), and analyzing the impact of scattered resistive elements on the converter performance. These studies have led to optimized control strategies and improved transient behavior. In summary, phase-shift control techniques vary in complexity and performance, with TPS being the most advanced option [69], [70], [71].

The regulation of the power flow and output voltage in converters involves diverse techniques. One such approach is the single-phase shift (SPS), which maintains a set phase shift between the input voltage and the inductor current. Although simple, the SPS lacks precision. Dual-phase shift (DPS) enhances the output voltage control and efficiency by using two switch sets with a time delay. For most controls, the three-phase shift (TPS) employs three-phase shifts in the input voltage, finely adjusting the output voltage. The TPS, although intricate, offers superior control and efficiency. These techniques are vital in bidirectional converters for EVs, ensuring effective power flow and voltage control between the battery and grid. The choice of technique

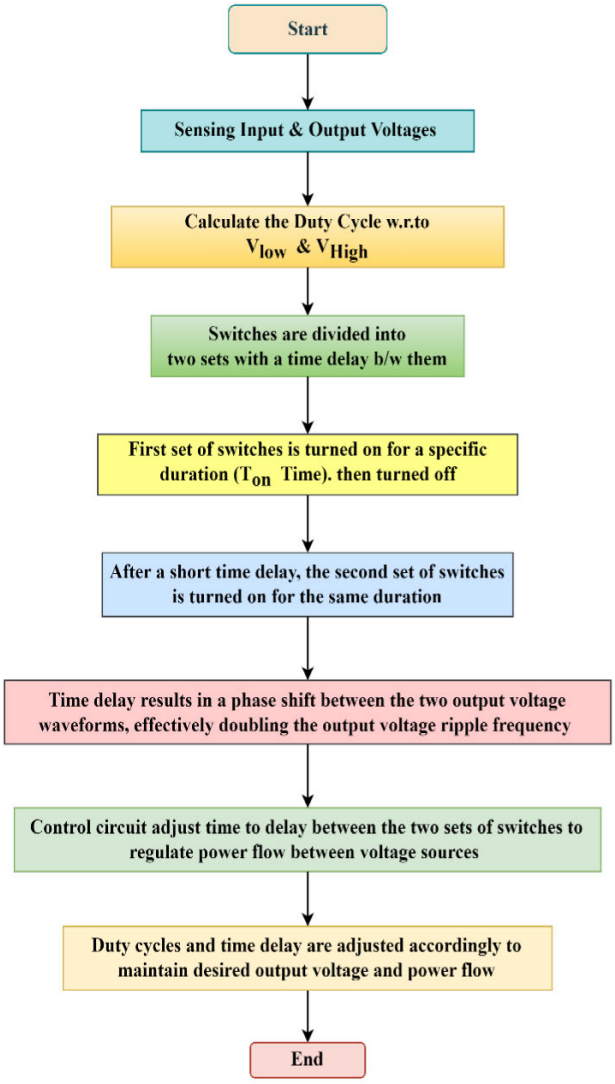

FIGURE 28. Process flow chart dual phase shift control.

depends on the control requirements, efficiency goals, and the converter difficulty. The adaptive super-twisting sliding mode control (ASTSMC) approach for improving the

TABLE 4. Comparison table for control technique and BDC for EV charger.

Control Techniques	Bidirectional DC Converters	Comparison
Hysteresis Control	Basic Converters, Push-pull, Half Bridge, Full Bridge, Dual Active Bridge, Multi-Level, 3L NPC, Cascaded H-Bridge, Multi-port DAB	Easy to implement, but may cause high switching losses and harmonic distortion. May not be suitable for high-power applications due to poor dynamic outcome.
Sliding-mode Control	Basic Converters, Forward, Push-pull, Half Bridge, Full Bridge, Dual Active Bridge, Multi-Level, 3L NPC, Cascaded H-Bridge, Multi-port DAB	It offers robust outcome and good tracking accuracy, but can result in chattering and high switching frequency.
PI Controller	Basic Converters, Forward, Push-pull, Half Bridge, Full Bridge, Dual Active Bridge, Multi-Level, 3L NPC, Cascaded H-Bridge, Multi-port DAB	Simple and effective, but may not provide optimal outcomes in terms of dynamic response and tracking accuracy.
Fuzzy Logic Control	Basic Converters, Forward, Push-pull, Half Bridge, Full Bridge, Dual Active Bridge, Multi-Level, 3L NPC, Cascaded H-Bridge, Multi-port DAB	It offers good outcome in the presence of uncertainties and nonlinearities, but may require many rules and high computational complexity.
Model Predictive Control	Basic Converters, SEPIC, Zeta, Flyback, Forward, Push-pull, Half Bridge, Full Bridge, Dual Active Bridge, Multi-Level, 3L NPC, Cascaded H-Bridge, Multi-port DAB	Provides good tracking accuracy and dynamic response, but requires a high computational effort and may not be suitable for high-speed applications due to its sampling time.
Neural Network Control	Basic Converters, Forward, Push-pull, Half Bridge, Full Bridge, Dual Active Bridge, Multi-Level, 3L NPC, Cascaded H-Bridge, Multi-port DAB	Offers good outcome in the presence of uncertainties and nonlinearities, but may require a large number of training samples and high computational complexity.
Space Vector Modulation Control	Half Bridge, Full Bridge, Dual Active Bridge	Provides excellent harmonic outcomes and low switching losses, but requires high computational complexity and may not be suitable for high-speed applications due to its sampling time.
Direct Torque Control	3L NPC, Cascaded H-Bridge	Provides excellent outcomes in torque control and dynamic response, but may require high computational complexity and may not be suitable for low-speed applications.
Dynamic Evolution Control	Basic Converters, Forward, Push-pull, Half Bridge, Full Bridge, Dual Active Bridge, Multi-Level, 3L NPC, Cascaded H-Bridge, Multi-port DAB	Provides good tracking accuracy and robustness in the presence of uncertainties and disturbances, but may require high computational complexity and tuning effort.
Phase Shift Control	Push-pull	Provides good harmonic outcomes and low switching losses, but may require precise control of the phase shift and may not be suitable for high-power applications due to its limited scalability.

efficiency of a dual active bridge (DAB) converter using extended phase shift (EPS) modulation. It introduces an online optimization method to generate phase shift ratios and optimizes backflow power and inductor current stress simultaneously. Furthermore, a variable gain-based STSMC scheme is proposed to enhance converter performance under various disturbances, demonstrated through simulation and experiments, outperforming conventional STSMC methods [116]. The integration of Dual Active Bridge (DAB) converters and Partial Power Converters (PPCs) to optimize efficiency. The study identifies a high-frequency DAB-based PPC configuration for efficiency enhancement and employs an extended-phase-shift-based control strategy to achieve zero-voltage switching (ZVS) and minimize current stress. The research also addresses non-ideal factors like output capacitors and utilizes magnetizing inductors to expand the ZVS range. Experimental results, using a 1 kW, 500 kHz prototype with GaN devices, validate the theoretical analysis, confirming the feasibility and effectiveness of the proposed approach for high-frequency power converters [117].

VI. SURVEY REVIEW OUTCOMES

A. SUITABILITY AND EFFICIENCY OF BDC'S FOR ELECTRIC VEHICLES

Table 4 assesses the suitability of various bidirectional DC-DC converter configurations for electric vehicles (EVs) based on their efficiency, tentative cost range, and key characteristics. Notably, converters like the Buck-Boost, Cuk, SEPIC, Zeta, Flyback, Forward, and Push-Pull converters exhibit limited power handling capabilities, making them unsuitable for high-power EV applications. In contrast, converters such as the Half Bridge and Full Bridge

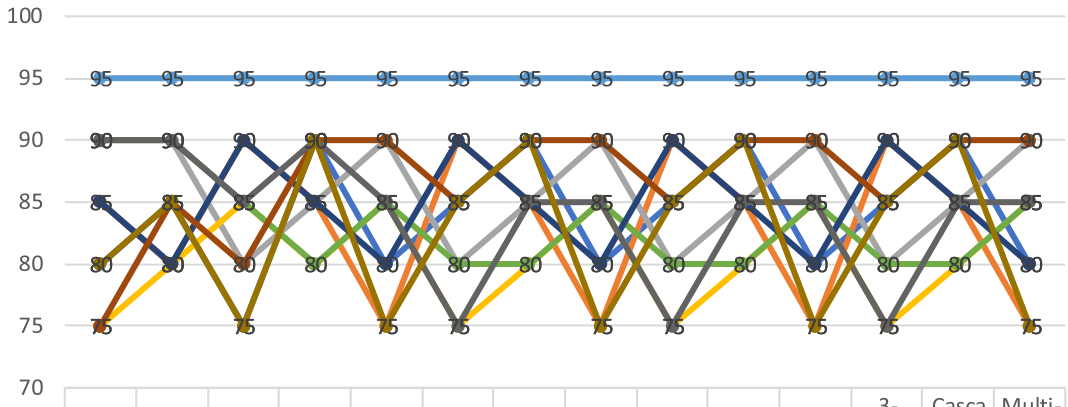

	Buck-Boost Converter	Cuk Converter	SEPIC Converter	Zeta Converter	Flyback Converter	Forward Converter	Push-pull Converter	Half Bridge Converter	Full Bridge Converter	Dual Active Bridge	Multi Level Converter	3-Level NPC Converter	Cascaded H-Bridge Converter	Multi-port DAB Converter
Hysteresis	80	85	75	90	80	85	90	80	85	90	80	85	90	80
Sliding-mode	85	80	90	85	75	90	85	75	90	85	75	90	85	75
PI Controller	90	90	80	85	90	80	85	90	80	85	90	80	85	90
Fuzzy Logic	75	80	85	80	85	75	80	85	75	80	85	75	80	85
Model Predictive	95	95	95	95	95	95	95	95	95	95	95	95	95	95
Neural Network	90	90	85	80	85	80	80	85	80	80	85	80	80	85
SVM Control	85	80	90	85	80	90	85	80	90	85	80	90	85	80
Direct Torque	75	85	80	90	90	85	90	90	85	90	90	85	90	90
Dynamic Evolution	90	90	85	90	85	75	85	85	75	85	85	75	85	85
Phase Shift	80	85	75	90	75	85	90	75	85	90	75	85	90	75

FIGURE 29. Control strategy & BDC converter's VS. efficiency chart.

offer medium-power handling capacities, potentially meeting the demands of medium-power EVs. Furthermore, the Dual Active Bridge Converter, Multi-Level Converter, 3-Level NPC Converter, Cascaded H-Bridge Converter, and Multi-Port DAB Converter demonstrate suitability for high-power EVs, given their robust power handling capabilities and high efficiency. Efficiency and cost considerations play a role in determining suitability, with converters like the Flyback displaying lower efficiency and cost-effectiveness, making them less suitable for high-power EVs. Conversely, the Multi-Port DAB Converter, while exhibiting higher costs, justifies its suitability through its exceptional efficiency and versatility for high-power EV applications.

In summary, the choice of a bidirectional DC-DC converter for an EV depends on power requirements, efficiency targets, and budget constraints, with certain converters offering more favorable attributes for high-power EVs than others.

B. CONTROL STRATEGY AND BDC CONVERTER VS EFFICIENCY CHART

Figure 29 serves as a pivotal visualization in our research, illustrating the intricate interplay between outcome efficiency and control method efficiency across various bidirectional DC converters. We examined 14 converters, as highlighted in our comprehensive analysis, encompassing converters ranging from the Buck-Boost and Cuk to the Dual Active Bridge and Multi-Port DAB. The plotted data in the figure encompasses the efficiency metrics derived from both MATLAB Simulation Results and Literature Survey aspects. This holistic approach allowed us to comprehensively evaluate each converter-control method combination in terms of outcome quality and energy efficiency.

For instance, the figure highlights that converter like the Buck-Boost and Cuk, while achieving reasonable control method efficiency, may struggle to deliver high outcome efficiency, particularly in high-power applications. Conversely, converters like the Multi-Port DAB exhibit remarkable outcome efficiency coupled with commendable control method efficiency, showcasing their potential for achieving optimal performance in terms of both energy efficiency and outcome quality. In essence, this figure empowers academics and practitioners with invaluable insights into the intricate tradeoffs and synergies between converter types and control methods, ultimately aiding in the selection of the most

TABLE 5. Summary of bidirectional DC converter's.

Converter Type	Summary	Advantages	Disadvantages
Buck-Boost Converter	- Voltage Stress: Vin- Voltage Range: Low to medium voltage- Efficiency: High efficiency (>90%)- No. of Switches: 2- No. of Diodes: 2- No. of Capacitors: 1 to 2- Duty Cycle Formula: Vout/Vin = 1/(1-D)- Features & Application: DC-DC power supplies, battery chargers, LED drivers	- Wide input voltage range- Simplicity and versatility in voltage regulation- High efficiency- Compact design- Suitable for portable and low-power applications	- Limited voltage range adaptation- Voltage stress on diodes and switches- Output current ripple
Cuk Converter	- Voltage Stress: Vin- Voltage Range: Low voltage- Efficiency: High efficiency (>90%)- No. of Switches: 2- No. of Diodes: 2- No. of Capacitors: 2- Duty Cycle Formula: Vout/Vin = -D/(1-D)- Features & Application: DC-DC power supplies, battery chargers	- Inverting output capability- Voltage step-up and step-down capability- High efficiency- Low output ripple- Suitable for battery-powered devices	- Complex control and design- Voltage stress on diodes and switches- High output ripple voltage
SEPIC Converter	- Voltage Stress: Vin- Voltage Range: Low to medium voltage- Efficiency: High efficiency (>90%)- No. of Switches: 2- No. of Diodes: 2- No. of Capacitors: 2- Duty Cycle Formula: Vout/Vin = 1+D- Features & Application: DC-DC power supplies, LED drivers	- Non-inverting output capability- Voltage step-up and step-down capability- High efficiency- Input and output isolation- Low output ripple voltage	- Complex control and design- Voltage stress on diodes and switches- High output ripple voltage
Zeta Converter	- Voltage Stress: Vin- Voltage Range: Low to medium voltage- Efficiency: High efficiency (>90%)- No. of Switches: 2- No. of Diodes: 2- No. of Capacitors: 1 to 2- Duty Cycle Formula: Vout/Vin = 1/(1-D)- Features & Application: DC-DC power supplies, LED drivers	- Voltage step-down capability- High efficiency- Low output ripple voltage- Compact design- Suitable for low-power applications	- Limited voltage range adaptation- Complex control and design- Voltage stress on diodes and switches
Flyback Converter	- Voltage Stress: Vout & Vin- Voltage Range: Low to medium voltage- Efficiency: High efficiency (>90%)- No. of Switches: 1 to 2- No. of Diodes: 1 to 2- No. of Capacitors: 1 to 2- Duty Cycle Formula: Vout/Vin = Np/Ns- Features & Application: AC-DC power supplies, low-power applications	- Isolated output capability- Voltage step-up and step-down capability- Suitable for multiple output designs- High efficiency- Wide input voltage range	- Complex transformer design- Output current and voltage ripple- Limited power handling capability
Forward Converter	- Voltage Stress: Vout & Vin- Voltage Range: Low to high voltage- Efficiency: High efficiency (>90%)- No. of Switches: 1 to 2- No. of Diodes: 1 to 2- No. of Capacitors: 1 to 2- Duty Cycle Formula: Vout/Vin = 1/(1-D)- Features & Application: AC-DC power supplies, motor drives	- Voltage step-up and step-down capability- High efficiency- Low output ripple voltage- Suitable for high-power applications- Wide input voltage range	- Complex control and design- Voltage stress on diodes and switches- Limited output voltage regulation range
Push-Pull Converter	- Voltage Stress: Vin- Voltage Range: Low to medium voltage- Efficiency: High efficiency (>95%)- No. of Switches: 2- No. of Diodes: 2- No. of Capacitors: 1- Duty Cycle Formula: It depends on the load- Features & Application: Power supplies, motor drives, lighting systems	- High efficiency- Reduced output voltage ripple- Simple control- Suitable for medium-power applications- Low electromagnetic interference (EMI)	- Limited output voltage range- Complex transformer design (for high power)- Limited voltage step-up capability

TABLE 5. *(Continued.)* **Summary of bidirectional DC converter's.**

Half Bridge Converter	- Voltage Stress: Vin- Voltage Range: Low to medium voltage- Efficiency: High efficiency (>95%)- No. of Switches: 2- No. of Diodes: 4- No. of Capacitors: 1- Duty Cycle Formula: It depends on the load- Features & Application: Power supplies, motor drives, lighting systems	- High efficiency- Suitable for medium to high-power applications- Low EMI- Reduced output voltage ripple- Improved thermal management	- Limited output voltage range- Complex transformer design (for high power)- Higher component count and cost
Full Bridge Converter	- Voltage Stress: Vout & Vin- Voltage Range: Low to medium voltage- Efficiency: High efficiency (>95%)- No. of Switches: 4- No. of Diodes: 8- No. of Capacitors: 2- Duty Cycle Formula: It depends on the load- Features & Application: Power supplies, motor drives, lighting systems	- High efficiency- Suitable for high-power applications- Low EMI- Reduced output voltage ripple- Improved thermal management	- Limited output voltage range- Complex transformer design (for high power)- Higher component count and cost
DAB Converter	- Voltage Stress: Vout- Voltage Range: Low to high voltage and current- Efficiency: High efficiency (>95%)- No. of Switches: 4- No. of Diodes: 8- No. of Capacitors: 2- Depends on the load- Features & Application: Renewable energy systems, motor drives	- High efficiency- Suitable for high-power applications- Bidirectional power flow- Enhanced control capabilities- Low harmonic distortion	- Complex control and design- Voltage stress on diodes and switches- Limited voltage range adaptation
Multi-Level Converter	- Voltage Stress: Depends on the topology and number of levels- Voltage Range: High voltage and power- Efficiency: High efficiency (>95%)- Based on the specific Level- Based on the specific Level- Based on the specific Level- Based on the specific Level- Features & Application: Renewable energy systems, motor drives, HVDC systems, etc.	- High efficiency- Reduced harmonic distortion- Suitable for high-voltage and high-power applications- Enhanced voltage quality control	- Complex control and design- Higher component count- Increased cost and complexity
3 L - NPC Converter	- Voltage Stress: Vout & Vin- Voltage Range: Medium voltage- Efficiency: High efficiency (>95%)- No. of Switches: 2N- No. of Diodes: 3(N-1)- No. of Capacitors: 3(N-1)- Based on the specific Level- Industrial applications, renewable energy systems	- High efficiency- Low harmonic distortion- Suitable for medium-voltage applications- Improved voltage quality control	- Complex control and design- Higher component count- Increased cost and complexity
Cascaded H-Bridge Converter	- Voltage Stress: Depends on the topology and number of levels- Voltage Range: High voltage and power- Efficiency: High efficiency (>95%)- N(N-1)- 2N+2- 2N+2- Based on the specific Level- Renewable energy systems, motor drives, HVDC systems, etc.	- High efficiency- Reduced harmonic distortion- Suitable for high-voltage and high-power applications- Enhanced voltage quality control	- Complex control and design- Higher component count- Increased cost and complexity
Multiport DAB Converter	- Voltage Stress: Depends on the topology and number of levels- Voltage Range: Low to medium voltage- Efficiency: High efficiency (>95%)- 2N- 2N- 2N- Based on the specific Level- Renewable energy systems, motor drives, HVDC systems, etc.	- High efficiency- Bidirectional power flow- Enhanced control capabilities- Low harmonic distortion- Suitable for multi-port applications	- Complex control and design- Voltage stress on diodes and switches- Limited voltage range adaptation

promising combinations to enhance the performance and energy efficiency of bidirectional DC converters for electric vehicle applications. Table 4 highlights the extensive range of bidirectional DC converters, where control techniques vary in complexity and application. Through extensive formal research and practical experimentation, the nuanced strengths and limitations of each control strategy have been identified. For instance, hysteresis control, despite its simplicity, faces challenges in high-power scenarios due to issues such as switching losses and harmonic distortion. Similarly, sliding-mode control, known for its robustness and precision, may introduce undesired chattering and elevated switching frequencies. PI controllers, admired for their straightforwardness and effectiveness, may occasionally fall short of delivering a desired dynamic response and accuracy. Meanwhile, fuzzy logic control excels in managing

uncertainties, but it struggles with computational complexities and a surfeit of rules. Model predictive control impresses with its tracking prowess and dynamic response capabilities; however, its substantial computational requirement may render it less suitable for high-speed applications.

Furthermore, a plethora of alternative techniques such as neural network control, space vector modulation, direct torque control, dynamic evolution control, and phase shift control offer bespoke advantages and limitations. These techniques serve as versatile tools carefully adapted to specific converter types and application requirements. This comprehensive overview caters to the discerning needs of both researchers and practitioners, providing them with invaluable insights to select the optimal control strategy for their bidirectional DC converters. The plotted data in the figure encompasses the efficiency metrics derived from both MATLAB Simulation Results and Literature Survey aspects.

Table 5 provides a concise overview of various power converter types, highlighting their key parameters, including voltage stress on diodes and switches, voltage range, efficiency, and applications. Each converter type comes with distinct advantages and disadvantages, influencing their suitability for specific applications. From the versatile Buck-Boost Converter suitable for battery chargers and LED drivers to the high-power capabilities of Full Bridge and Cascaded H-Bridge Converters, the table offers valuable insights into power conversion solutions. Additionally, advanced multi-level converters and multi-port DAB converters offer enhanced control and efficiency for renewable energy systems and HVDC applications. This comprehensive summary serves as a reference for selecting the most appropriate converter technology based on specific needs and constraints. Using a survey, this study offers a comprehensive grasp of the control methods and converter types that are applied in bidirectional DC converters for applications involving electric vehicles using a survey. They act as visual assistance in assessing and comparing the performance and applicability of various control techniques and converter configurations, which helps in the selection of solutions that are most appropriate for system requirements.

VII. CONCLUSION

The conclusion of this review paper shows a significant achievement in the field of bidirectional direct-current converters and their applications in electric vehicles (EVs). Our exhaustive analysis and comparative study have successfully identified optimal converter topologies and corresponding control strategies for enhancing EV performance, efficiency, range, and cost-effectiveness. Notably, the strengths and limitations of various control methods, such as hysteresis, sliding-mode, PI, fuzzy logic, and model predictive control were explored for researchers and practitioners. Furthermore, the findings have led to recommendations for specific converter types, including full-bridge, dual active bridge, and multi-port DAB converters, demonstrating their efficiency and power-handling capabilities in EV charging systems.

Incorporating advanced techniques like direct torque control and dynamic evolution control can further elevate EV charging system performance. By offering a comprehensive overview of the current state of research, discoveries, and potential areas for future advancement in advanced electric mobility, this review paper serves as a valuable resource for driving innovation in this rapidly evolving domain. With the insights provided, EV industry could make informed choices in converter and control method selection, paving the way for a greener, more efficient, and sustainable future of electric mobility.

REFERENCES

[1] M. S. Bhaskar, V. K. Ramachandaramurthy, S. Padmanaban, F. Blaabjerg, D. M. Ionel, M. Mitolo, and D. Almakhles, "Survey of DC–DC non-isolated topologies for unidirectional power flow in fuel cell vehicles," *IEEE Access*, vol. 8, pp. 178130–178166, 2020, doi: 10.1109/ACCESS.2020.3027041.

[2] M. Forouzesh, Y. P. Siwakoti, S. A. Gorji, F. Blaabjerg, and B. Lehman, "Step-up DC–DC converters: A comprehensive review of voltage-boosting techniques, topologies, and applications," *IEEE Trans. Power Electron.*, vol. 32, no. 12, pp. 9143–9178, Dec. 2017, doi: 10.1109/TPEL.2017.2652318.

[3] L. Cheng, P. Acuna, R. P. Aguilera, J. Jiang, S. Wei, J. E. Fletcher, and D. D. C. Lu, "Model predictive control for DC–DC boost converters with reduced-prediction horizon and constant switching frequency," *IEEE Trans. Power Electron.*, vol. 33, no. 10, pp. 9064–9075, Oct. 2018, doi: 10.1109/TPEL.2017.2785255.

[4] S. A. Gorji, H. G. Sahebi, M. Ektesabi, and A. B. Rad, "Topologies and control schemes of bidirectional DC–DC power converters: An overview," *IEEE Access*, vol. 7, pp. 117997–118019, 2019, doi: 10.1109/ACCESS.2019.2937239.

[5] B. Moon, H. Y. Jung, S. H. Kim, and S.-H. Lee, "A modified topology of two-switch buck–boost converter," *IEEE Access*, vol. 5, pp. 17772–17780, 2017, doi: 10.1109/ACCESS.2017.2749418.

[6] K. Prag, M. Woolway, and T. Celik, "Data-driven model predictive control of DC-to-DC buck–boost converter," *IEEE Access*, vol. 9, pp. 101902–101915, 2021, doi: 10.1109/ACCESS.2021.3098169.

[7] M. Duan, D. Sun, J. Duan, L. Sun, and Y. Liu, "Interleaved modulation scheme with optimized phase shifting for double-switch buck–boost converter," *IEEE Access*, vol. 9, pp. 55422–55435, 2021, doi: 10.1109/ACCESS.2021.3071314.

[8] H.-I. Joo and S.-K. Han, "Lossless snubber cell for a soft-switched bidirectional buck–boost converter," *IEEE Access*, vol. 8, pp. 165708–165719, 2020, doi: 10.1109/ACCESS.2020.3022397.

[9] K. M. Smedley and S. Cuk, "Dynamics of one-cycle controlled Cuk converters," *IEEE Trans. Power Electron.*, vol. 10, no. 6, pp. 634–639, Nov. 1995, doi: 10.1109/63.471282.

[10] D. Maksimovic and S. Cuk, "Switching converters with wide DC conversion range," *IEEE Trans. Power Electron.*, vol. 6, no. 1, pp. 151–157, Jan. 1991, doi: 10.1109/63.65013.

[11] A. Anand and B. Singh, "Modified dual output cuk converter-fed switched reluctance motor drive with power factor correction," *IEEE Trans. Power Electron.*, vol. 34, no. 1, pp. 624–635, Jan. 2019, doi: 10.1109/TPEL.2018.2827048.

[12] K.-B. Park, G.-W. Moon, and M.-J. Youn, "Nonisolated high step-up boost converter integrated with Sepic converter," *IEEE Trans. Power Electron.*, vol. 25, no. 9, pp. 2266–2275, Sep. 2010, doi: 10.1109/TPEL.2010.2046650.

[13] Y. P. Siwakoti, A. Mostaan, A. Abdelhakim, P. Davari, M. N. Soltani, M. N. H. Khan, L. Li, and F. Blaabjerg, "High-voltage gain quasi-SEPIC DC–DC converter," *IEEE J. Emerg. Sel. Topics Power Electron.*, vol. 7, no. 2, pp. 1243–1257, Jun. 2019, doi: 10.1109/JESTPE.2018.2859425.

[14] S. A. Ansari and J. S. Moghani, "A novel high voltage gain noncoupled inductor SEPIC converter," *IEEE Trans. Ind. Electron.*, vol. 66, no. 9, pp. 7099–7108, Sep. 2019, doi: 10.1109/TIE.2018.2878127.

[15] P. K. Maroti, S. Padmanaban, J. B. Holm-Nielsen, M. S. Bhaskar, M. Meraj, and A. Iqbal, "A new structure of high voltage gain SEPIC converter for renewable energy applications," *IEEE Access*, vol. 7, pp. 89857–89868, 2019, doi: 10.1109/ACCESS.2019.2925564.

[16] D. Murthy-Bellur and M. K. Kazimierczuk, "Isolated two-transistor zeta converter with reduced transistor voltage stress," *IEEE Trans. Circuits Syst. II, Exp. Briefs*, vol. 58, no. 1, pp. 41–45, Jan. 2011, doi: 10.1109/TCSII.2010.2092829.

[17] B.-R. Lin and F.-Y. Hsieh, "Soft-switching zeta-flyback converter with a buck–boost type of active clamp," *IEEE Trans. Ind. Electron.*, vol. 54, no. 5, pp. 2813–2822, Oct. 2007, doi: 10.1109/TIE.2007.901366.

[18] M. S. Bhaskar, N. Gupta, S. Selvam, D. J. Almakhles, P. Sanjeevikumar, J. S. M. Ali, and S. Umashankar, "A new hybrid zeta-boost converter with active quad switched inductor for high voltage gain," *IEEE Access*, vol. 9, pp. 20022–20034, 2021, doi: 10.1109/ACCESS.2021.3054393.

[19] R. Kushwaha and B. Singh, "Bridgeless isolated Zeta–Luo converter-based EV charger with PF preregulation," *IEEE Trans. Ind. Appl.*, vol. 57, no. 1, pp. 628–636, Jan. 2021, doi: 10.1109/TIA.2020.3036019.

[20] M. R. Banaei and H. A. F. Bonab, "A high efficiency nonisolated buck–boost converter based on ZETA converter," *IEEE Trans. Ind. Electron.*, vol. 67, no. 3, pp. 1991–1998, Mar. 2020, doi: 10.1109/TIE.2019.2902785.

[21] R. Kumar and B. Singh, "BLDC motor-driven solar PV array-fed water pumping system employing zeta converter," *IEEE Trans. Ind. Appl.*, vol. 52, no. 3, pp. 2315–2322, May 2016, doi: 10.1109/TIA.2016.2522943.

[22] F. Zhang and Y. Yan, "Novel forward-flyback hybrid bidirectional DC–DC converter," *IEEE Trans. Ind. Electron.*, vol. 56, no. 5, pp. 1578–1584, May 2009, doi: 10.1109/TIE.2008.2009561.

[23] D. A. Ruiz-Caballero and I. Barbi, "A new flyback-current-fed push–pull DC–DC converter," *IEEE Trans. Power Electron.*, vol. 14, no. 6, pp. 1056–1064, Nov. 1999, doi: 10.1109/63.803399.

[24] W. Li, L. Fan, Y. Zhao, X. He, D. Xu, and B. Wu, "High-step-up and high-efficiency fuel-cell power-generation system with active-clamp flyback-forward converter," *IEEE Trans. Ind. Electron.*, vol. 59, no. 1, pp. 599–610, Jan. 2012, doi: 10.1109/TIE.2011.2130499.

[25] D. D. Vracar and P. V. Pejovic, "Active-clamp flyback converter as auxiliary power-supply of an 800V inductive-charging system for electric vehicles," *IEEE Access*, vol. 10, pp. 38254–38271, 2022, doi: 10.1109/ACCESS.2022.3165059.

[26] D. D. Vracar, "Quasi-resonant flyback converter as auxiliary power-supply of an 800V inductive-charging system for electric vehicles," *IEEE Access*, vol. 10, pp. 109609–109625, 2022, doi: 10.1109/ACCESS.2022.3214526.

[27] C. Wang, S. Xu, S. Lu, and W. Sun, "A low-cost constant current control method for DCM and CCM in digitally controlled primary-side regulation flyback converter," *IEEE J. Emerg. Sel. Topics Power Electron.*, vol. 6, no. 3, pp. 1483–1494, Sep. 2018, doi: 10.1109/JESTPE.2017.2779136.

[28] K.-B. Park, G.-W. Moon, and M.-J. Youn, "Two-switch active-clamp forward converter with one clamp diode and delayed turnoff gate signal," *IEEE Trans. Ind. Electron.*, vol. 58, no. 10, pp. 4768–4772, Oct. 2011, doi: 10.1109/TIE.2011.2107710.

[29] J. Ge, Z. Zhao, L. Yuan, and T. Lu, "Energy feed-forward and direct feed-forward control for solid-state transformer," *IEEE Trans. Power Electron.*, vol. 30, no. 8, pp. 4042–4047, Aug. 2015, doi: 10.1109/TPEL.2014.2382613.

[30] R. R. Khorasani, E. Adib, and H. Farzanehfard, "ZVT resonant core reset forward converter with a simple auxiliary circuit," *IEEE Trans. Ind. Electron.*, vol. 65, no. 1, pp. 242–250, Jan. 2018, doi: 10.1109/TIE.2017.2716871.

[31] H. Wu and Y. Xing, "Families of forward converters suitable for wide input voltage range applications," *IEEE Trans. Power Electron.*, vol. 29, no. 11, pp. 6006–6017, Nov. 2014, doi: 10.1109/TPEL.2014.2298617.

[32] G.-J. Son, F.-S. Kang, and S.-J. Park, "Grid connection using a structure that combines a buck converter and a push–pull converter to reduce the low-frequency current ripple of the fuel-cell," *IEEE Access*, vol. 10, pp. 95804–95823, 2022, doi: 10.1109/ACCESS.2022.3204989.

[33] N. Weitz, S. Utzelmann, S. Ditze, and M. März, "A resonant push–pull DC–DC converter with an intrinsic current source behavior for radio frequency power conversion," *IEEE Trans. Power Electron.*, vol. 37, no. 6, pp. 7001–7012, Jun. 2022, doi: 10.1109/TPEL.2022.3142431.

[34] A. Ali and Y. Liao, "Optimized control for modified push–pull dual active bridge converter to achieve wide ZVS range and low current stress," *IEEE Access*, vol. 9, pp. 140258–140267, 2021, doi: 10.1109/ACCESS.2021.3117873.

[35] T.-F. Wu, J.-C. Hung, J.-T. Tsai, C.-T. Tsai, and Y.-M. Chen, "An active-clamp push–pull converter for battery sourcing applications," *IEEE Trans. Ind. Appl.*, vol. 44, no. 1, pp. 196–204, Jan. 2008, doi: 10.1109/TIA.2007.912748.

[36] D. R. Nayanasiri, G. H. B. Foo, D. M. Vilathgamuwa, and D. L. Maskell, "A switching control strategy for single- and dual-inductor current-fed push–pull converters," *IEEE Trans. Power Electron.*, vol. 30, no. 7, pp. 3761–3771, Jul. 2015, doi: 10.1109/TPEL.2014.2348800.

[37] J.-W. Lim, J. Hassan, and M. Kim, "Bidirectional soft switching push–pull resonant converter over wide range of battery voltages," *IEEE Trans. Power Electron.*, vol. 36, no. 11, pp. 12251–12267, Nov. 2021, doi: 10.1109/TPEL.2021.3078413.

[38] C. Zhang, P. Li, Z. Kan, X. Chai, and X. Guo, "Integrated half-bridge CLLC bidirectional converter for energy storage systems," *IEEE Trans. Ind. Electron.*, vol. 65, no. 5, pp. 3879–3889, May 2018, doi: 10.1109/TIE.2017.2758741.

[39] S. Chakraborty and S. Chattopadhyay, "Fully ZVS, minimum RMS current operation of the dual-active half-bridge converter using closed-loop three-degree-of-freedom control," *IEEE Trans. Power Electron.*, vol. 33, no. 12, pp. 10188–10199, Dec. 2018, doi: 10.1109/TPEL.2018.2811640.

[40] S. Chakraborty and S. Chattopadhyay, "Minimum-RMS-current operation of asymmetric dual active half-bridge converters with and without ZVS," *IEEE Trans. Power Electron.*, vol. 32, no. 7, pp. 5132–5145, Jul. 2017, doi: 10.1109/TPEL.2016.2613874.

[41] A. K. Rathore and U. R. Prasanna, "Analysis, design, and experimental results of novel snubberless bidirectional naturally clamped ZCS/ZVS current-fed half-bridge DC/DC converter for fuel cell vehicles," *IEEE Trans. Ind. Electron.*, vol. 60, no. 10, pp. 4482–4491, Oct. 2013, doi: 10.1109/TIE.2012.2213563.

[42] Z. Zhang, O. C. Thomsen, and M. A. E. Andersen, "Optimal design of a push–pull-forward half-bridge (PPFHB) bidirectional DC–DC converter with variable input voltage," *IEEE Trans. Ind. Electron.*, vol. 59, no. 7, pp. 2761–2771, Jul. 2012, doi: 10.1109/TIE.2011.2134051.

[43] F. Z. Peng, H. Li, G.-J. Su, and J. S. Lawler, "A new ZVS bidirectional DC–DC converter for fuel cell and battery application," *IEEE Trans. Power Electron.*, vol. 19, no. 1, pp. 54–65, Jan. 2004, doi: 10.1109/TPEL.2003.820550.

[44] Y. Shen, W. Zhao, Z. Chen, and C. Cai, "Full-bridge LLC resonant converter with series-parallel connected transformers for electric vehicle on-board charger," *IEEE Access*, vol. 6, pp. 13490–13500, 2018, doi: 10.1109/ACCESS.2018.2811760.

[45] O. Ibrahim, N. Z. Yahaya, N. Saad, and K. Y. Ahmed, "Development of observer state output feedback for phase-shifted full bridge DC–DC converter control," *IEEE Access*, vol. 5, pp. 18143–18154, 2017, doi: 10.1109/ACCESS.2017.2745417.

[46] J. Chen, C. Yang, S. Tang, and J. Zou, "A high power interleaved parallel topology full-bridge LLC converter for off-board charger," *IEEE Access*, vol. 9, pp. 157790–157799, 2021, doi: 10.1109/ACCESS.2021.3130051.

[47] T.-F. Wu, J.-G. Yang, C.-L. Kuo, and Y.-C. Wu, "Soft-switching bidirectional isolated full-bridge converter with active and passive snubbers," *IEEE Trans. Ind. Electron.*, vol. 61, no. 3, pp. 1368–1376, Mar. 2014, doi: 10.1109/TIE.2013.2262746.

[48] M. C. Mira, Z. Zhang, A. Knott, and M. A. E. Andersen, "Analysis, design, modeling, and control of an interleaved-boost full-bridge three-port converter for hybrid renewable energy systems," *IEEE Trans. Power Electron.*, vol. 32, no. 2, pp. 1138–1155, Feb. 2017, doi: 10.1109/TPEL.2016.2549015.

[49] M. Gao, D. Wang, Y. Li, and T. Yuan, "Fixed frequency pulse-width modulation based integrated sliding mode controller for phase-shifted full-bridge converters," *IEEE Access*, vol. 6, pp. 2181–2192, 2018, doi: 10.1109/ACCESS.2017.2782225.

[50] L. Shu, W. Chen, and Z. Song, "Prediction method of DC bias in DC–DC dual-active-bridge converter," *CPSS Trans. Power Electron. Appl.*, vol. 4, no. 2, pp. 152–162, Jun. 2019, doi: 10.24295/CPSSTPEA.2019.00015.

[51] M. J. Heller, F. Krismer, and J. W. Kolar, "Duty-cycle dependent phase shift modulation of dual three-phase active bridge four-port AC–DC/DC–AC converter eliminating low frequency power pulsations," *IEEE Open J. Power Electron.*, vol. 3, pp. 705–722, 2022, doi: 10.1109/OJPEL.2022.3213274.

[52] H. Akagi, S.-I. Kinouchi, and Y. Miyazaki, "Bidirectional isolated dual-active-bridge (DAB) DC–DC converters using 1.2-kV 400-A SiC-MOSFET dual modules," *CPSS Trans. Power Electron. Appl.*, vol. 1, no. 1, pp. 33–40, Dec. 2016, doi: 10.24295/CPSSTPEA.2016.00004.

[53] Y. Shi, R. Li, Y. Xue, and H. Li, "Optimized operation of current-fed dual active bridge DC–DC converter for PV applications," *IEEE Trans. Ind. Electron.*, vol. 62, no. 11, pp. 6986–6995, Nov. 2015, doi: 10.1109/TIE.2015.2432093.

[54] S. M. Akbar, A. Hasan, A. J. Watson, and P. Wheeler, "Model predictive control with triple phase shift modulation for a dual active bridge DC–DC converter," *IEEE Access*, vol. 9, pp. 98603–98614, 2021, doi: 10.1109/ACCESS.2021.3095553.

[55] B. Zhao, Q. Song, W. Liu, and Y. Sun, "Overview of dual-active-bridge isolated bidirectional DC–DC converter for high-frequency-link power-conversion system," *IEEE Trans. Power Electron.*, vol. 29, no. 8, pp. 4091–4106, Aug. 2014, doi: 10.1109/TPEL.2013.2289913.

[56] S. Shao, H. Chen, X. Wu, J. Zhang, and K. Sheng, "Circulating current and ZVS-on of a dual active bridge DC–DC converter: A review," *IEEE Access*, vol. 7, pp. 50561–50572, 2019, doi: 10.1109/ACCESS.2019.2911009.

[57] J. Wu, D. Liu, Y. Wang, H. Zhao, and Z. Chen, "A hybrid-bridge-based dual active bridge converter with reduced device count," *IEEE Open J. Power Electron.*, vol. 3, pp. 930–941, 2022, doi: 10.1109/OJPEL.2022.3224376.

[58] Y. Shi and H. Li, "Isolated modular multilevel DC–DC converter with DC fault current control capability based on current-fed dual active bridge for MVDC application," *IEEE Trans. Power Electron.*, vol. 33, no. 3, pp. 2145–2161, Mar. 2018, doi: 10.1109/TPEL.2017.2695575.

[59] Q. Tian and K. Bai, "Widen the zero-voltage-switching range and secure grid power quality for an ev charger using variable-switching-frequency single-dual-phase-shift control," *Chin. J. Electr. Eng.*, vol. 4, no. 1, pp. 11–19, Mar. 2018, doi: 10.23919/CJEE.2018.8327366.

[60] L. Jorge, H. Concepcion, M. A. Arjona, M. Lesedi, and C. Ambrish, "Performance evaluation of an active neutral-point-clamped multilevel converter for active filtering in G2V-V2G and V2H applications," *IEEE Access*, vol. 10, pp. 41607–41621, 2022, doi: 10.1109/ACCESS.2022.3167694.

[61] Y. Dai, S. Luo, and Z. Li, "Direct power based control strategy for DAB DC–DC converter with cooperative triple phase shifted modulation," *IEEE Access*, vol. 9, pp. 147791–147800, 2021, doi: 10.1109/ACCESS.2021.3122954.

[62] Z. Farooq, T. Zaman, M. A. Khan, Nasimullah, S. M. Muyeen, and A. Ibeas, "Artificial neural network based adaptive control of single phase dual active bridge with finite time disturbance compensation," *IEEE Access*, vol. 7, pp. 112229–112239, 2019, doi: 10.1109/ACCESS.2019.2934253.

[63] J. Yin, J. Lu, H. Jiang, Y. Liu, and J. Peng, "Modified phase-shift scheme for optimal transient response of dual-active-bridge DC/DC converters considering the resistive impact," *IEEE Access*, vol. 9, pp. 87706–87714, 2021, doi: 10.1109/ACCESS.2021.3088839.

[64] L. Martinez-Salamero, J. Calvente, R. Giral, A. Poveda, and E. Fossas, "Analysis of a bidirectional coupled-inductor cuk converter operating in sliding mode," *IEEE Trans. Circuits Syst. I, Fundam. Theory Appl.*, vol. 45, no. 4, pp. 355–363, Apr. 1998, doi: 10.1109/81.669058.

[65] A. S. Samosir and A. H. M. Yatim, "Implementation of dynamic evolution control of bidirectional DC–DC converter for interfacing ultracapacitor energy storage to fuel-cell system," *IEEE Trans. Ind. Electron.*, vol. 57, no. 10, pp. 3468–3473, Oct. 2010, doi: 10.1109/TIE.2009.2039458.

[66] A. Pirooz and R. Noroozian, "Model predictive control of classic bidirectional DC–DC converter for battery applications," in *Proc. 7th Power Electron. Drive Syst. Technol. Conf. (PEDSTC)*, Tehran, Iran, Feb. 2016, pp. 517–522, doi: 10.1109/PEDSTC.2016.7556914.

[67] M. Ebad and B.-M. Song, "Accurate model predictive control of bidirectional DC–DC converters for DC distributed power systems," in *Proc. IEEE Power Energy Soc. Gen. Meeting*, San Diego, CA, USA, Jul. 2012, pp. 1–8, doi: 10.1109/PESGM.2012.6345659.

[68] E. T. Maddalena, M. W. F. Specq, V. L. Wisniewski, and C. N. Jones, "Embedded PWM predictive control of DC–DC power converters via piecewise-affine neural networks," *IEEE Open J. Ind. Electron. Soc.*, vol. 2, pp. 199–206, 2021, doi: 10.1109/OJIES.2021.3058411.

[69] H. Bai, Z. Nie, and C. C. Mi, "Experimental comparison of traditional phase-shift, dual-phase-shift, and model-based control of isolated bidirectional DC–DC converters," *IEEE Trans. Power Electron.*, vol. 25, no. 6, pp. 1444–1449, Jun. 2010, doi: 10.1109/TPEL.2009.2039648.

[70] J. Huang, Y. Wang, Z. Li, and W. Lei, "Unified triple-phase-shift control to minimize current stress and achieve full soft-switching of isolated bidirectional DC–DC converter," *IEEE Trans. Ind. Electron.*, vol. 63, no. 7, pp. 4169–4179, Jul. 2016, doi: 10.1109/TIE.2016.2543182.

[71] K. Wu, C. W. de Silva, and W. G. Dunford, "Stability analysis of isolated bidirectional dual active full-bridge DC–DC converter with triple phase-shift control," *IEEE Trans. Power Electron.*, vol. 27, no. 4, pp. 2007–2017, Apr. 2012, doi: 10.1109/TPEL.2011.2167243.

[72] J. Liu, M. Zhao, G. Li, and J. Chen, "Multiple linear regression prediction and wavelet neural network based intelligent online tuning control method," *IEEE Access*, vol. 8, pp. 160684–160696, 2020, doi: 10.1109/ACCESS.2020.3020980.

[73] J. Park, H. Kim, K. Hwang, and S. Lim, "Deep reinforcement learning based dynamic proportional-integral (PI) gain auto-tuning method for a robot driver system," *IEEE Access*, vol. 10, pp. 31043–31057, 2022, doi: 10.1109/ACCESS.2022.3159785.

[74] M. H. Qais, H. M. Hasanien, and S. Alghuwainem, "A grey wolf optimizer for optimum parameters of multiple PI controllers of a grid-connected PMSG driven by variable speed wind turbine," *IEEE Access*, vol. 6, pp. 44120–44128, 2018, doi: 10.1109/ACCESS.2018.P2864303.

[75] K. Y. Ahmed, N. Z. B. Yahaya, V. S. Asirvadam, N. Saad, R. Kannan, and O. Ibrahim, "Development of power electronic distribution transformer based on adaptive PI controller," *IEEE Access*, vol. 6, pp. 44970–44980, 2018, doi: 10.1109/ACCESS.2018.2861420.

[76] C. Yanarates and Z. Zhou, "Design and cascade PI controller-based robust model reference adaptive control of DC–DC boost converter," *IEEE Access*, vol. 10, pp. 44909–44922, 2022, doi: 10.1109/ACCESS.2022.3169591.

[77] C. Aguilar-Ibanez, J. Moreno-Valenzuela, O. García-Alarcón, M. Martinez-Lopez, J. Á. Acosta, and M. S. Suarez-Castanon, "PI-type controllers and $\Sigma - \Delta$ modulation for saturated DC–DC buck power converters," *IEEE Access*, vol. 9, pp. 20346–20357, 2021, doi: 10.1109/ACCESS.2021.3054600.

[78] G. Gupta and M. Sreejeth, "Study and analysis of field oriented control of brushless DC motor drive using hysteresis current control technique," in *Proc. 2nd Asian Conf. Innov. Technol. (ASIANCON)*, Ravet, India, Aug. 2022, pp. 1–5, doi: 10.1109/ASIANCON55314.2022.9909355.

[79] Y.-S. Hwang, J.-J. Chen, J.-X. Xu, H.-S. Yang, C.-H. Lai, and Y. Ku, "An improved fast-transient-response low-transient-voltage boost converter with pseudo-current hysteresis-controlled techniques," *IEEE Access*, vol. 9, pp. 127270–127277, 2021, doi: 10.1109/ACCESS.2021.3112065.

[80] S. K. Annam, R. K. Pongiannan, and N. Yadaiah, "A hysteresis space vector PWM for PV tied Z-source NPC-MLI with DC-link neutral point balancing," *IEEE Access*, vol. 9, pp. 54420–54434, 2021, doi: 10.1109/ACCESS.2021.3068335.

[81] S. Lee, Y.-C. Jeung, and D.-C. Lee, "Voltage balancing control of IPOS modular dual active bridge DC/DC converters based on hierarchical sliding mode control," *IEEE Access*, vol. 7, pp. 9989–9997, 2019, doi: 10.1109/ACCESS.2018.2889345.

[82] M. I. Ghiasi, M. A. Golkar, and A. Hajizadeh, "Lyapunov based-distributed fuzzy-sliding mode control for building integrated-DC microgrid with plug-in electric vehicle," *IEEE Access*, vol. 5, pp. 7746–7752, 2017, doi: 10.1109/ACCESS.2017.2689807.

[83] M. A. Qureshi, I. Ahmad, and M. F. Munir, "Double integral sliding mode control of continuous gain four quadrant quasi-Z-source converter," *IEEE Access*, vol. 6, pp. 77785–77795, 2018, doi: 10.1109/ACCESS.2018.2884092.

[84] Y. Li, X. Ruan, L. Zhang, and Y.-K. Lo, "Multipower-level hysteresis control for the class E DC–DC converters," *IEEE Trans. Power Electron.*, vol. 35, no. 5, pp. 5279–5289, May 2020, doi: 10.1109/TPEL.2019.2940043.

[85] S. C. C. Huerta, P. Alou, J. Á. Oliver, O. Garcia, J. A. Cobos, and A. M. Abou-Alfotouh, "Nonlinear control for DC–DC converters based on hysteresis of the C_{OUT} current with a frequency loop to operate at constant frequency," *IEEE Trans. Ind. Electron.*, vol. 58, no. 3, pp. 1036–1043, Mar. 2011, doi: 10.1109/TIE.2010.2049707.

[86] A. Schild, J. Lunze, J. Krupar, and W. Schwarz, "Design of generalized hysteresis controllers for DC–DC switching power converters," *IEEE Trans. Power Electron.*, vol. 24, no. 1, pp. 138–146, Jan. 2009, doi: 10.1109/TPEL.2008.2009176.

[87] A. Lekic and D. M. Stipanovic, "Hysteresis switching control of the Ćuk converter operating in discontinuous conduction modes," *IEEE Trans. Circuits Syst. II, Exp. Briefs*, vol. 64, no. 9, pp. 1077–1081, Sep. 2017, doi: 10.1109/TCSII.2016.2631510.

[88] G. Sha, Q. Duan, W. Sheng, C. Ma, C. Zhao, Y. Zhang, and J. Tian, "Research on multi-port DC–DC converter based on modular multilevel converter and cascaded H bridges for MVDC applications," *IEEE Access*, vol. 9, pp. 95006–95022, 2021, doi: 10.1109/ACCESS.2021.3072161.

[89] S. Onodera, M. Sato, and M. Uno, "Multi-port converter integrating bidirectional converters and induction heating inverter for electric vehicles," in *Proc. 46th Annu. Conf. IEEE Ind. Electron. Soc.*, Singapore, Oct. 2020, pp. 1383–1388, doi: 10.1109/IECON43393.2020.9255120.

[90] S. Kurm and V. Agarwal, "Interfacing standalone loads with renewable energy source and hybrid energy storage system using a dual active bridge based multi-port converter," *IEEE J. Emerg. Sel. Topics Power Electron.*, vol. 10, no. 4, pp. 4738–4748, Aug. 2022, doi: 10.1109/JESTPE.2021.3118462.

[91] D. Sha, G. Xu, and Y. Xu, "Utility direct interfaced charger/discharger employing unified voltage balance control for cascaded H-bridge units and decentralized control for CF-DAB modules," *IEEE Trans. Ind. Electron.*, vol. 64, no. 10, pp. 7831–7841, Oct. 2017, doi: 10.1109/TIE.2017.2696511.

[92] Y. Yu, G. Konstantinou, B. Hredzak, and V. G. Agelidis, "Power balance of cascaded H-bridge multilevel converters for large-scale photovoltaic integration," *IEEE Trans. Power Electron.*, vol. 31, no. 1, pp. 292–303, Jan. 2016, doi: 10.1109/TPEL.2015.2406315.

[93] H. Akagi and R. Kitada, "Control and design of a modular multilevel cascade BTB system using bidirectional isolated DC/DC converters," *IEEE Trans. Power Electron.*, vol. 26, no. 9, pp. 2457–2464, Sep. 2011, doi: 10.1109/TPEL.2011.2107752.

[94] K. Wang, R. Zhu, C. Wei, F. Liu, X. Wu, and M. Liserre, "Cascaded multilevel converter topology for large-scale photovoltaic system with balanced operation," *IEEE Trans. Ind. Electron.*, vol. 66, no. 10, pp. 7694–7705, Oct. 2019, doi: 10.1109/TIE.2018.2885739.

[95] Z. Du, B. Ozpineci, L. M. Tolbert, and J. N. Chiasson, "DC–AC cascaded H-bridge multilevel boost inverter with no inductors for electric/hybrid electric vehicle applications," *IEEE Trans. Ind. Appl.*, vol. 45, no. 3, pp. 963–970, May/Jun. 2009, doi: 10.1109/TIA.2009.2018978.

[96] Y. Yu, G. Konstantinou, B. Hredzak, and V. G. Agelidis, "Operation of cascaded H-bridge multilevel converters for large-scale photovoltaic power plants under bridge failures," *IEEE Trans. Ind. Electron.*, vol. 62, no. 11, pp. 7228–7236, Nov. 2015, doi: 10.1109/TIE.2015.2434995.

[97] S. A. Saleh, E. Ozkop, and A. Rubaai, "Testing the frame-angle-based direct torque control for 3ϕ induction motor drives," *IEEE Trans. Ind. Appl.*, vol. 57, no. 3, pp. 2918–2930, May 2021, doi: 10.1109/TIA.2021.3057351.

[98] P. Maciejewski and G. Iwanski, "Study on direct torque control methods of a doubly fed induction machine working as a stand-alone DC voltage generator," *IEEE Trans. Energy Convers.*, vol. 36, no. 2, pp. 853–862, Jun. 2021, doi: 10.1109/TEC.2020.3012589.

[99] M. H. Holakooie, G. Iwanski, and T. Miazga, "Five-dimensional switching-table-based direct torque control of six-phase drives," *IEEE Trans. Power Electron.*, vol. 37, no. 12, pp. 15260–15271, Dec. 2022, doi: 10.1109/TPEL.2022.3189876.

[100] S. Y. Yip, H. S. Che, C. P. Tan, and W. T. Chong, "A lookup table model predictive direct torque control of permanent-magnet synchronous generator based on Vienna rectifier," *IEEE J. Emerg. Sel. Topics Power Electron.*, vol. 8, no. 2, pp. 1208–1222, Jun. 2020, doi: 10.1109/JESTPE.2019.2900917.

[101] K. K. Prabhakar, C. Upendra Reddy, P. Kumar, and A. K. Singh, "A new reference flux linkage selection technique for efficiency improvement of direct torque controlled IM drive," *IEEE J. Emerg. Sel. Topics Power Electron.*, vol. 8, no. 4, pp. 3751–3762, Dec. 2020, doi: 10.1109/JESTPE.2020.2979235.

[102] X. Chen and M. Kazerani, "Space vector modulation control of an AC–DC–AC converter with a front-end diode rectifier and reduced DC-link capacitor," *IEEE Trans. Power Electron.*, vol. 21, no. 5, pp. 1470–1478, Sep. 2006, doi: 10.1109/TPEL.2006.880236.

[103] S. B. Monge, S. Somavilla, J. Bordonau, and D. Boroyevich, "Capacitor voltage balance for the neutral-point-clamped converter using the virtual space vector concept with optimized spectral performance," *IEEE Trans. Power Electron.*, vol. 22, no. 4, pp. 1128–1135, Jul. 2007, doi: 10.1109/TPEL.2007.900547.

[104] X. Li, F. Wu, G. Yang, H. Liu, and T. Meng, "Dual-period-decoupled space vector phase-shifted modulation for DAB-based three-phase single-stage AC–DC converter," *IEEE Trans. Power Electron.*, vol. 35, no. 6, pp. 6447–6457, Jun. 2020, doi: 10.1109/TPEL.2019.2950059.

[105] Y. Liu, S. Liu, C. Wang, J. Jiang, J. Li, and S. Ye, "An improved space vector modulation with capacitor voltage control for T-type five-level nested neutral point piloted converter," *IEEE Trans. Power Electron.*, vol. 36, no. 5, pp. 5262–5277, May 2021, doi: 10.1109/TPEL.2020.3025976.

[106] S. Busquets-Monge, J. D. Ortega, J. Bordonau, J. A. Beristain, and J. Rocabert, "Closed-loop control of a three-phase neutral-point-clamped inverter using an optimized virtual-vector-based pulsewidth modulation," *IEEE Trans. Ind. Electron.*, vol. 55, no. 5, pp. 2061–2071, May 2008, doi: 10.1109/TIE.2008.918646.

[107] M. A. Hannan, Z. A. Ghani, M. M. Hoque, P. J. Ker, A. Hussain, and A. Mohamed, "Fuzzy logic inverter controller in photovoltaic applications: Issues and recommendations," *IEEE Access*, vol. 7, pp. 24934–24955, 2019, doi: 10.1109/ACCESS.2019.2899610.

[108] F.-J. Lin, K.-H. Tan, W.-C. Luo, and G.-D. Xiao, "Improved LVRT performance of PV power plant using recurrent wavelet fuzzy neural network control for weak grid conditions," *IEEE Access*, vol. 8, pp. 69346–69358, 2020, doi: 10.1109/ACCESS.2020.2984803.

[109] C. S. Chin, J. Xiao, A. M. Y. M. Ghias, M. Venkateshkumar, and D. U. Sauer, "Customizable battery power system for marine and offshore applications: Trends, configurations, and challenges," *IEEE Electrific. Mag.*, vol. 7, no. 4, pp. 46–55, Dec. 2019.

[110] G. A. Reddy, S. A. Lakshmanan, M. Venkateshkumar, M. N. Kamlesh, and L. Batni, "Design and analysis of cascaded H bridge converter with ANN based SPWM technique for EV applications," in *Proc. IEEE 19th India Council Int. Conf. (INDICON)*, Kochi, India, Nov. 2022, pp. 1–7, doi: 10.1109/INDICON56171.2022.10040107.

[111] S. A. Lakshmanan and M. Venkateshkumar, "Analysis and design of lead-lag controller and fuzzy logic controller for boost converter applicable to RES," in *Proc. Int. Conf. Power, Energy, Control Transmiss. Syst. (ICPECTS)*, Chennai, India, Dec. 2020, pp. 1–6, doi: 10.1109/ICPECTS49113.2020.9337004.

[112] R. B. Thota and K. R. M. V. Chandrakala, "Modeling and attenuation of conducted EMI in DC–DC converters using hybrid filter," in *Proc. Int. Interdiscipl. Conf. Math., Eng. Sci. (MESIICON)*, Durgapur, India, Nov. 2022, pp. 1–6, doi: 10.1109/MESIICON55227.2022.10093533.

[113] A. S. Daniel and K. R. M. V. Chandrakala, "Design of an isolated onboard plug-in electric vehicle charger," in *Proc. 7th Int. Conf. Electr. Energy Syst. (ICEES)*, Chennai, India, Feb. 2021, pp. 147–149, doi: 10.1109/ICEES51510.2021.9383717.

[114] P. S. Babu, S. Subhash, and K. Ilango, "SOC estimation of Li-ion battery using hybrid artificial neural network and adaptive neuro-fuzzy inference system," in *Intelligent Solutions for Smart Grids and Smart Cities* (Lecture Notes in Electrical Engineering), vol. 1022, P. Siano, S. Williamson, and S. Beevi, Eds. Singapore: Springer, 2023.

[115] R. Ghosh, K. Dasgupta, and S. P. Ghoshal, "Analysis of a hysteresis current control DC–DC buck converter suitable for wide range of operating conditions," in *Proc. Int. Conf. Comput., Electr. Commun. Eng. (ICCECE)*, Kolkata, India, Jan. 2023, pp. 1–5, doi: 10.1109/ICCECE51049.2023.10085385.

[116] F. Bagheri, N. Guler, H. Komurcugil, and S. Bayhan, "An adaptive sliding mode control for a dual active bridge converter with extended phase shift modulation," *IEEE Access*, vol. 11, pp. 91260–91274, 2023, doi: 10.1109/ACCESS.2023.3264013.

[117] S. Gao, Y. Zhang, Y. Wang, J. Liu, and D. Xu, "An optimal control strategy for the DAB-based partial power converter based on extended-phase-shift control," *IEEE Open J. Power Electron.*, vol. 4, pp. 817–827, 2023, doi: 10.1109/OJPEL.2023.3319488.

[118] S. Kofler, E. Luchini, A. Schirrer, M. Fallmann, O. König, M. Kozek, C. Hametner, and S. Jakubek, "Agent-based decentralized model predictive control for plants with multiple identical actuators," *IEEE Trans. Control Syst. Technol.*, vol. 31, no. 2, pp. 841–855, Mar. 2023, doi: 10.1109/TCST.2022.3207354.

[119] H. Shu, X. Li, Y. Liu, and R. Wang, "Model predictive control with disturbance observer for marine diesel engine speed control," *IEEE Access*, vol. 11, pp. 49300–49318, 2023, doi: 10.1109/ACCESS.2023.3270286.

[120] S. Singirikonda, Y. P. Obulesu, R. Kannan, K. J. Reddy, G. K. Kumar, W. Alhakami, A. Baz, and H. Alhakami, "Adaptive control-based isolated bi-directional converter for G2V & V2G charging with integration of the renewable energy source," *Energy Rep.*, vol. 8, pp. 11416–11428, Nov. 2022.

[121] Y. Liang and S. Lin, "Research on bi-directional four-port converter of solar electric vehicle," *Energy Rep.*, vol. 9, pp. 271–278, May 2023.
[122] Y. Lee and A. Castellazzi, "High-temperature integrated SiC MOSFET bi-directional switch in power-overlay technology," *Microelectron. Rel.*, vol. 151, Dec. 2023, Art. no. 115223.
[123] Md. R. Haque, K. M. A. Salam, and M. A. Razzak, "A modified PI-controller based high current density DC–DC converter for EV charging applications," *IEEE Access*, vol. 11, pp. 27246–27266, 2023, doi: 10.1109/ACCESS.2023.3258181.

PATTAN MUTHUKUMAR received the bachelor's degree in electrical and electronics engineering from the Dhanalakshmi Srinivasan College of Engineering and Technology, Chennai, and the master's degree in power systems from AMET University, Chennai. He is currently pursuing the Ph.D. degree with Amrita Vishwa Vidyapeetham, Chennai Campus, India, where he is delving deep into the realm of smart electric vehicle systems. This academic pursuit follows a robust foundation. He also brought five years of industrial experience to the table, having started his journey as a Research an Development Engineer. He contributed his expertise in various areas, including power electronics drives, UPS, and Servo Stabilizer technology, and even the intricate world of elevators and escalators. He is an Embedded Software Engineer in the dynamic domain of automotive systems. His dedication to academic and professional growth reflects his pursuit of excellence. His ongoing research on smart electric vehicle systems showcases his commitment to innovation and cutting-edge technology. Drawing from his diverse experiences, he aims to bridge theoretical insights into practical applications. He envisions a future where electric vehicles play a pivotal role in sustainable transportation, and he is on a mission to contribute significantly to the advancement of electric vehicle systems through his research.

MOHAN VENKATESHKUMAR (Member, IEEE) is currently an Assistant Professor (SL Grade) with the Department of Electrical and Electronics Engineering, Amrita School of Engineering, Amrita Vishwa Vidyapeetham, Coimbatore Campus. With more than 15 years of teaching and research experience, he specializes in power systems engineering. He has conducted significant research in the field of design and control of artificial intelligence-based hybrid renewable energy sources for both on-grid and off-grid applications, as well as electric vehicles. He has published more than 60 research papers in international journals and conferences and serves as a technical committee member for more than 40 international journals and conferences. He has authored three books/chapters with Elsevier and Intech open publications. In addition, he is a member of IEEE P825 and P2030 research working groups in USA. He received the Young Scientist Award from the government of Tamil Nadu. In addition, he has been recognized for his outstanding contributions to the field by receiving the MATLAB Outstanding Contribution Award for three consecutive years, from 2015 to 2017. He holds the position of the Vice Chair of the IEEE Power and Energy Society and the IEEE Education Society IEEE Madras Section. He is an Associate Editor of IEEE Access journal, which has an impact factor of 4.09.

CHENG SIONG CHIN (Senior Member, IEEE) received the B.Eng. degree (Hons.) in mechanical and aerospace engineering from Nanyang Technological University (NTU), in 2000, the M.Sc. degree (Hons.) in advanced control and systems engineering from The University of Manchester, in 2001, and the Ph.D. degree in applied control engineering from the Robotics Research Centre, NTU, in 2008.

He was a Lecturer in mechatronics engineering with Temasek Polytechnic. Before moving into academia, he worked in the consumer electronics industry for a few years. He is currently a Chair Professor of intelligent systems modeling and simulation with Newcastle University in Singapore. He currently holds three U.S. patents in electronics test systems and components. His research interests include systems design, simulation, and predictive analytics. He is the author/coauthor of more than 170 peer-reviewed papers in journals and conference proceedings. He is an Associate Editor of IEEE Access, *Applied Artificial Intelligence*, and IEEE Transportation Electrification Community (TEC) eNewsletter. He has served as the general chair and a keynote speaker at various international conferences.